

PREDICTION OF PROPERTIES AND  
MODELING FIRE BEHAVIOR OF POLYETHYLENE  
USING CONE CALORIMETER

By

ROSHAN J. PATEL

Bachelor of Chemical Engineering

The Maharaja Sayajirao University of Baroda

Gujarat, India

2011

Submitted to the Faculty of the  
Graduate College of the  
Oklahoma State University  
in partial fulfillment of  
the requirements for  
the Degree of  
MASTER OF SCIENCE  
December, 2014

PREDICTION OF PROPERTIES AND  
MODELING FIRE BEHAVIOR OF POLYETHYLENE  
USING CONE CALORIMETER

Thesis Approved:

Dr. Qingsheng Wang

---

Thesis Adviser

Dr. Sundararajan Madihally

---

Dr. Clint Aichele

---

## ACKNOWLEDGEMENTS

I would like to take this opportunity to convey my sincere regards to my academic and thesis advisor Prof. Dr. Qingsheng Wang for his continuous support, encouragement and trust in my abilities. I would further extend my thanks to Dr. Sundararajan Madihally and Dr. Clint Aichele for their support and suggestions which served as good directions to explore throughout my research.

Further I would extend my deepest appreciation to Dr. Ting Ma. It was him who made it possible for me to perform experiments safely & effectively by training me on calibration and test procedures of Cone Calorimeter. I am also thankful to Dr. Bryan Hoskins and Mr. Luinstra Floyd for their continuous support with my experimental work.

I would like to thank all my group members Fazle Rabbi and Zhen Wang for their help. Being a multi-disciplinary research project, the co-operation & support of the Chemical Engineering and Engineering Technology staff was remarkable.

I am grateful to Dr. N. V. Bhate, my parents and Mr. Harshad Amin for their motivation and support.

To conclude I would thank all the faculty members in School of Chemical Engineering and Department of Fire Protection & Safety and entire student community for making my association with Oklahoma State University a memorable one, which I would cherish for the time to come.

Name: ROSHAN J. PATEL

Date of Degree: DECEMBER, 2014

Title of Study: PREDICTION OF PROPERTIES AND MODELING FIRE BEHAVIOR  
OF POLYETHYLENE USING CONE CALORIMETER

Major Field: CHEMICAL ENGINEERING

Abstract:

Fire behavior of pure polyethylene has been investigated by performing thermal analysis using a standard cone calorimeter. Specifications of polyethylene samples were  $100 \pm 1$  mm long,  $100 \pm 1$  mm wide and 5 mm thick, with mass of  $25.0 \pm 0.1$  gm. Sample surface area exposed to the external heat flux was limited to 94 mm in length, 94 mm in width due to use of edge lip sample holder frame. The values of external heat flux used were ranging from 40 – 55 kW/m<sup>2</sup> with an incremental step of 5 kW·m<sup>-2</sup>. Three set of experiments were performed for each value of external heat flux. The results obtained were recorded and fitted to a set of mathematical equations to determine the thermal inertia, critical heat flux and the peak heat release rate. Study shows that thermal inertia value obtained from experimental data was  $0.86 \text{ kJ}^2 \cdot \text{m}^{-4} \cdot \text{K}^{-2} \cdot \text{s}^{-1}$  and from well-known correlations was  $0.83 \text{ kJ}^2 \cdot \text{m}^{-4} \cdot \text{K}^{-2} \cdot \text{s}^{-1}$  with a difference of 3.49 %. The factors to relate the observed critical heat flux with the actual critical heat flux were determined as 0.77 and 0.64. The peak heat release rate for each test was determined using the model equation based on oxygen depletion index and concentrations of gaseous species such as oxygen, carbon monoxide, carbon dioxide and water. The values observed experimentally and the ones calculated had a standard deviation of  $\pm 4.56$  %. Thus, this thesis serves as basis for transformation of qualitative understanding of polyethylene fire behavior into systematic quantification which can be generalized for other polymers and their composites.

## TABLE OF CONTENTS

Chapter	Page
I. INTRODUCTION.....	1
II. REVIEW OF LITERATURE.....	8
III. CONE CALORIMETER .....	12
IV. EXPERIMENTAL WORK .....	20
V. DATA ANALYSIS AND MODELING.....	30
VI. CONCLUSION AND FUTURE WORK.....	48
NOMENCLATURE .....	52
REFERENCES .....	53
APPENDICES .....	59

## LIST OF TABLES

Table	Page
Table 1 Characterization of Polyethylene (PE) sample .....	20
Table 2 Ignition time and flame out time observations .....	26
Table 3 Timeline of different regimes for polyethylene thermal degradation (first set).....	29
Table 4 Thermal inertia of polyethylene.....	36
Table 5 Concentrations of gas components in ambient air and exhaust gas (first set) .....	42
Table 6 Concentrations of gas components in ambient air and exhaust gas (second set).....	42
Table 7 Concentrations of gas components in ambient air and exhaust gas (third set) .....	42
Table 8 Peak heat release rate ( $40 \text{ kW}\cdot\text{m}^{-2}$ ).....	46
Table 9 Peak heat release rate ( $45 \text{ kW}\cdot\text{m}^{-2}$ ).....	46
Table 10 Peak heat release rate ( $50 \text{ kW}\cdot\text{m}^{-2}$ ).....	46
Table 11 Peak heat release rate ( $55 \text{ kW}\cdot\text{m}^{-2}$ ).....	47
Table 12 United States fire statistics.....	59
Table 13 United States structure fire statistics.....	61

## LIST OF FIGURES

Figure	Page
Figure 1 World plastic materials demand .....	7
Figure 2 Schematic arrangement of cone calorimeter .....	13
Figure 3 Zoomed view of test specimen and cone .....	13
Figure 4 Cone calorimeter assembly in Fire Protection and Safety Technology Lab.....	22
Figure 5 Timeline of cone calorimeter test .....	26
Figure 6 Heat release rate profile .....	27
Figure 7 Oxygen concentration profile in exhaust duct .....	28
Figure 8 Carbon monoxide concentration profile in exhaust duct.....	28
Figure 9 Carbon dioxide concentration profile in exhaust duct.....	29
Figure 10 Determination of thermal inertia for Polyethylene (PE).....	34
Figure 11 Extrapolated thermal inertia model for critical heat flux determination .....	37
Figure 12 Model profiles for critical heat flux determination.....	39

## CHAPTER I

### INTRODUCTION

Looking into the history of major events that enhanced the quality of human lives across the planet, one common fact that will definitely catch our eye would be the infrastructure availability. Since the time of industrial revolution which triggered the mass production of goods and consumer items until today and in the times to come, availability of infrastructure has played and will continue to play the decisive role. Indeed it's a well-developed and integrated process wherein a variety of industries, manufacturing firms and production houses are cohesively associated to produce the desired product. It has been a trend to optimize and integrate the processes. A variety of manufacturing industries have relied on conventional raw materials of construction for over two centuries since, the early days of industrial revolution back in ~1760. In the quest of optimizing the manufacturing cost and time there were two prevailing approaches which were employed, one is to improve the process itself and the second one is to have a cheaper, easy to process raw material which is available in abundance or has an unconstrained supply. Over the course of time with the evolution of oil industry came along the petrochemical industry. Among the products of petrochemical industry the one product branch which gained a rapid and high popularity across the globe was polymers. Owing due to their physical and chemical properties polymers were readily accepted as a preferred raw material in the manufacturing industry and other downstream consumer products industries.



Among the factors that favored polymers over the conventional construction and manufacturing raw materials comprised of their resemblance in the desired set of mechanical & chemical properties and easy processing. As the technology is advancing, new classes of polymers and their composites are being developed to specifically meet the desired set of properties for a particular application. A level of expertise has been attained in polymer synthesis that polymers with specific compositions are being manufactured to meet the desired property requirements. As of today, polymers have become an essential part of electrical, construction, automobile, textile, packaging, and military industry. The net worth of global polymer industry as estimated in 2011 was \$ 454 billion. The future trend of for the polymer industry is predicted to be governed by the growing economies, which is projected to take it to \$ 567 billion by 2017 [1].

With the constantly improvising trend of polymers replacing conventional materials there are certain aspects which need to be addressed pertaining to the risk associated with extensive use of polymers. Majority of the polymers are derived from hydrocarbons. As a result most of them share a hydrocarbon backbone on which different functional groups are attached to yield the desired properties. Thus in spite of having a multitude of applications, polymers poses a potential fire hazard because of their basic construction blocks being hydrocarbon molecules. Some of the thermoplastic polymers which are widely used consist of polyethylene (PE), polypropylene (PP), polymethylmethacrylate (PMMA), polystyrene (PS), polyvinylchloride (PVC) and polyethylene terephthalate (PET) which carry hydrocarbon backbone. So they all can serve as a potential fuel given the ignition source, the supply of oxygen and sustained chain reactions.

The fire statistics from the National Fire Protection Association (NFPA) [2] over the years, demonstrate the magnitude of the issue would be self-evident. During the year of 2013 there were 487,500 reported structure fires resulting into 2,855 civilian fatalities, 14,075 civilian injuries and property loss worth \$9.5 billion. Also, during the year of 2012 there were 480,500

recorded structure fires resulting in to 2,470 civilian fatalities, 14,700 injuries and \$9.8 billion property loss [2]. Thus it becomes an issue which needs to be addressed with undivided attention.

Efforts are ongoing to develop fire retardant polymers and their composites to have an enhanced fire retardant behavior to reduce the fire risk and mitigate associated consequences. Process of polymer degradation comprise of series of steps starting with physical degradation under effect of an external heat source where in polymer loses its mechanical strength and starts to become soft. Next stage is of chemical degradation wherein the low energy bonds of the polymer molecules break converting a large polymer molecule into monomer molecules. Then comes the pyrolysis stage in which polymer decomposes to produce gaseous products which mix with air and eventually serves as a fuel source in case of any ignition source. Once ignited the combustion reaction goes on until entire polymer is burnt.

Addition of filler molecules into virgin polymer is one of the current techniques being used to enhance fire behavior of polymers. Production technology for polymers adopted worldwide allow doping such additives right during polymerization process making it convenient to maintain the uniform distribution of filler particles and at the same time to yield the desired set of properties. Flame retardant additives can be classified into three basic categories based on their constituents; minerals, organohalogen compounds and organophosphorus compounds. Aluminum hydroxide, magnesium hydroxide and hydromagnesite are some of the examples of widely used mineral type flame retardants. They serve as the additive flame retardant which do not get attached with polymer molecules chemically. Whereas organohalogens and organophosphorus type of flame retardants form weak chemical bonds with the polymer molecules. Chlorinated paraffins, tetrabromobisphenol A and hexabromocyclododecane are commonly used organohalogen type of flame retardants. Triphenyl phosphate, bisphenol A diphenyl phosphate and dimethyl methylphosphonate are the examples of widely used organophosphorus type of flame retardants [3]. These flame retardants can work both in the condensed phase and in the

vapor phase. But, the fact that conventional flame retardants have limited application because of their health and environmental concerns; is providing the driving force for new research in flame retardant nanocomposites. Flame retardant nanofillers like clays [4], carbon nanotubes [5, 6], and metal oxide nanoparticles [7] when added in to the polymer act in the condensed phase by forming a film in the condensed polymer. This limits the availability of vapor generated from polymer which serves as fuel to the fire, at the same time constraining the supply of oxygen to the polymer and shielding condensed polymer against the flame heat flux. The two basic contributing effects that have been identified which make the nanocomposite materials highly efficient are physical barrier effect and catalytic charring effect [8]. During the combustion process of polymer nanocomposites, the nanofillers migrate through the condensed polymer and reach the surface to form a thermally stable ceramic like surface layer which serves as barrier. This layer restricts the supply of pyrolysis gases to the flame and supply of oxygen from flame to the polymer on the other side of layer. This behavior observed from nanofillers is termed as physical barrier effect. Also, the physical barrier effect help reduce the external heat flux which is applied on the polymer by reflecting a certain amount of the radiation [8]. Various theories have been proposed describing mechanism of nanofillers' action. Some of them are as follows:

1. Gasification of polymers and subsequently gradual precipitation of nanoparticles on the surface [9]
2. Migration or convection of nanoparticles to the surface [10]
3. Nanoconfinement, wherein nanofillers exert spatial constraints on a polymer and its degradation [11]

In the catalytic charring effect, the nanofillers induce partial charring by forming newer more stable bonds as the original polymer bonds deteriorate under the effect of external heat and hence modify the degradation pattern of the polymer [12, 13]. The nanofillers which exhibit the physical barrier effect does slow down the rate of heat release during the process of polymer

combustion. This reduces the value of peak heat release rate; but the total amount of heat released remains the same as that for the pure virgin polymer. This implies that the total area under the curve for a heat release rate profile for pure polymer and for polymer with nanofillers will be same, only the peak heat release rate value for polymer with nanofillers would be lower than pure polymer. Whereas with nanofillers which result in catalytic char formation, total amount of heat released also reduces. This is due the fact that formation of char reduces supply of carbon to the flame by retaining it within condensed phase. Both the phenomenon described so far have their distinct significance towards improving polymer fire behavior; however in most of the cases nanofillers resulting into physical barrier effect or catalytic charring effect are not effective by themselves to reduce the total heat release. Hence the situation calls for the study of synergistic effect of nanofillers with these two effects.

Researchers have been studying the effect of fire retardant nano-materials on the polymer fire behavior [14, 15] using a variety of experimental [16, 17] and theoretical analysis like thermogravimetry, cone calorimetry, differential scanning calorimetry, limited oxygen index, UL-94 and morphological studies like X-ray diffraction. But most of the data reported in the literature is qualitative [18, 19]. For the knowledge to be useful and find its application it needs to be quantitative in nature. Hence, the primary objective of this research work is to quantify the fire behavior of polymer nano-composites considering the synergistic effect of physical barrier effect and catalytic charring effect.

Efforts are ongoing to study and predict the fire behavior of the polymers. Luche et al. [20] have studied the fire behavior of black polymethylmethacrylate (PMMA) and demonstrated its property characterization. Similarly thermal analysis has been performed and fire behavior been investigated for polystyrene (PS), polyethylene terephthalate (PET), polypropylene (PP) and polyvinyl chloride (PVC) by Shi et al. [21]. Fire behaviors of polycarbonates (PC) and polyvinyl chloride (PVC) have been investigated by Stoliarov et al. [22]. They have demonstrated the

relation among cone calorimeter results with model equations using a computational framework called ThermaKin [23, 24]. Lautenberger et al. [25] have worked on the generalized pyrolysis model for combustible solids using Gpyro model for polymethyl methacrylate (PMMA) and polyurethane foam. Most of the research has yielded a general idea about how a polymer degrades under pyrolysis conditions, what are the different stages involved and what are the external factors governing the process. Thus a sound qualitative interpretation has been developed with an insight that the fire behavior can be modeled and hence quantified. As such pyrolysis models have been reviewed by Colomba Di Blasi [26], Takashi Kashiwagi [27], A. C. Fernandez-Pello [28] and others [29-31], though the application of these models have not crossed the lab environment. Current research work is an effort to bridge this gap and create a platform for quantitative comparison of polymer fire behavior.

The first step in this direction is to synthesize the polymer nanocomposites to achieve the flame retardancy of polymers through the physical barrier effect and catalytic charring effect independently as well as synergistically. Subsequently study the kinetics and mechanics of thermal degradation of polymer nanocomposites and the individual effects of physical barriers, catalytic charring and combination of both the effects. The last stage of the research is to quantify the synergistic effect of the two categories of nanofillers by performing thermal analysis using cone calorimeter. As such the research project is a collaborative effort among School of Chemical Engineering and Department of Fire Protection & Safety Technology at Oklahoma State University and Marry Kay O'Connor Process Safety Center of Texas A&M University. The scope split is well defined among the collaborators. Texas A&M University is working on synthesis of polymer nanocomposites and their morphological analysis. Oklahoma State University, i.e. our research group will be working on the thermal analysis and modeling of the fire behavior of polymer nanocomposites.

To get started with the research objective of performing thermal analysis using cone calorimeter, it was decided to start performing experiments with pure polymers, study their fire behavior and fit them to a set of model equations. One of the objective of current research project is to obtain a quantitative understanding of fire behavior. A validated set of model equations that describe polymer fire behavior can play elemental role in prediction of the fire behavior and hence in quantification. Polyethylene has been chosen as the pure polymer to carry out thermal analysis using cone calorimeter.

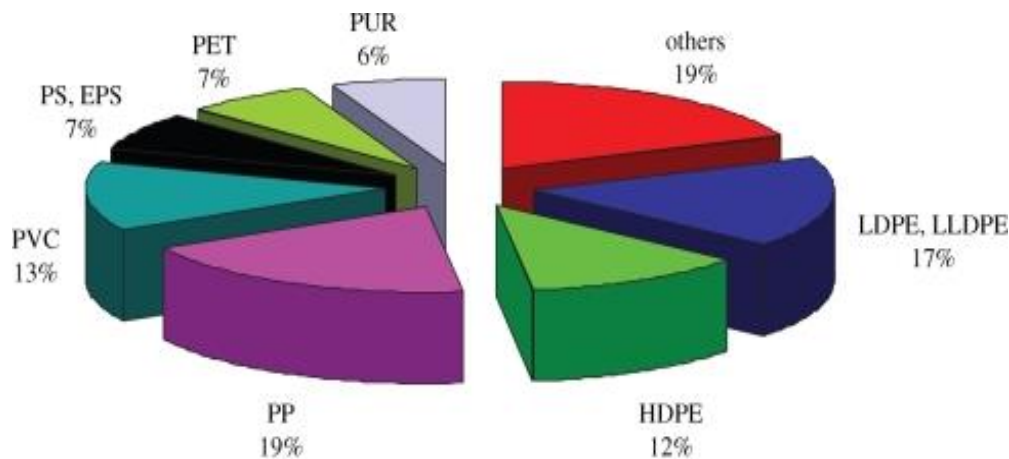


Figure 1 World plastic materials demand

Polyethylene [32] is one of the most commonly used polymers today along with polypropylene, polystyrene, polyvinylchloride and polymethylmethacrylate. Figure 1 represents the global demand of plastic in the year of 2006 [32].

The objective of this thesis is to study the thermal analysis and understand the fire behavior of polyethylene. This has been achieved by validating the set of model equations which can describe the fire behavior of polyethylene. This would help in creating a reliable and tested approach to quantify the polymer fire behavior and eventually for polymer nanocomposites. Thus this thesis would serve the purpose to create a proven basis to quantify the polymer fire behavior.

## CHAPTER II

### REVIEW OF THE LITERATURE

The inspiration for the current research work is derived from fact that there is a limited understanding of the quantitative effects of nanocomposite fire retardants on the polymer fire behavior. With the constantly increasing share of polymers in today's construction and other industries, as discussed in the Chapter I, it is of prime importance that the issue of fire cases created due to polymers is addressed. There were a total of 1,240,000 fires reported in United States during the year 2013, out of which 478,500 were identified as structure fires which accounts for a hopping amount of ~39 % of the total reported fires with an increase of ~1.5 % since 2012. Further it also lead to 2855 civilian fatalities, 14,075 civilian injuries and a property damage worth of \$ 9.5 billion as reported in the National Fire Protection Association (NFPA) report "Fire Loss in United States during 2013" [2]. Please find the more details about United States fire history in Appendix A and B. Most of the deaths reported were due to inhalation of toxic fumes generated as a result of fire. Polymers and their derivatives find increased share of application owing due to their excellent mechanical and chemical properties and have replaced the conventional materials of construction such as metals, wood, natural rubber and ceramics. Thus presence of polymers can be found almost everywhere surrounding us may it be building, housing, vehicles, electronics or other consumer goods. Hence, it becomes important to study the fire behavior of polymer thoroughly to be able to design an effective fire retardant material.

Nanocomposites have been successful in enhancing the fire behavior of the polymers. Studies have been ongoing with various nanoparticles being used as fillers to create a polymer nanocomposite to investigate their fire behaviors. Some of the most commonly used nanofillers are zirconium phosphate, ammonium polyphosphate, antimony oxide, benzyl phosphate, benzyl sulfonate, calcium iron undecenoate, montmorillonite, mixture of decabromodiphenylether and antimony trioxide, bis(2-ethylhexyl)phosphate, molybdenum sulfide, hexa decyl allyl dimethyl ammonium chloride, tricresylphosphate, trixylylphosphate and resorcinoldiphosphate [33].

As discussed in the Chapter I, polymer nanocomposites exhibit two distinct mechanisms, physical barrier effect and catalytic charring effect which contribute toward enhancing the fire retardancy. Cinausero et al. [34] studied the synergistic effects using a combination of nano-sized hydrophobic oxides and ammonium polyphosphate as flame retardant filler. The study demonstrated that the formation of a specific silicon metaphosphate crystalline phase which stimulated charring and formation of an efficient insulating layer. As a result of this phenomenon a notable decrease in the peak heat release rate and smoke opacity was observed.

A system of silicotungstic acid which acted as catalyst to promote the charring in polypropylene as the base polymer was studied by Qu et al. [12]. Liu et al. [35] showed that synergistic interaction among the clay and phosphomolybdates where the later act as catalyst to promote charring using the base polymer as styrene-acrylonitrile. A combined system of nano metal oxides  $\text{TiO}_2$  &  $\text{Al}_2\text{O}_3$  along with char forming phosphonated flame retardant was studied on the base system of polymethylmethacrylate by Laachachi et al. [18, 36-38].

Zhang et al. [39] have conducted experimental and numerical studies on the effect of nanoparticles on pyrolysis of polyamide-6 nanocomposite in cone calorimeter. They have focused on gasification of polymer and precipitation of nanoparticles, migration of nanoparticles towards the surface and nanoconfinement. Experiments demonstrated that even a small amount



(~2.5 % wt.) of nanoparticles can reduce the mass loss rate and thus the heat release rate due formation surface layer of nanoparticles.

While trying to study the synergistic effect of polymer nanocomposites on the fire behavior with the objective of current work being to contribute toward quantification and modeling of polymer fire behavior, a couple of well-known model equations that can be used to model polymer fire behavior have been studied. This approach can definitely help in predicting the fire behavior of polymer nanocomposites with a set of validated models. There have been models proposed to predict the heat release rate and mass loss rate, to determine the thermal thickness of the sample, to determine the thermal inertia of polymer samples, to determine the actual critical heat flux for the sample and others.

Hopkins Jr. [40] have predicted the ignition time and burning rate of thermoplastics such as nylon 6, polyethylene and polypropylene using cone calorimeter. A protocol for thermal analysis of thermoplastics has been presented in this work which allows prediction of ignition time and the burning rate. Models developed by Quintiere and Rhodes were employed to derive the properties of polymers to determine the ignition time and transient burning rates from the cone calorimeter data. The predicted values of thermal inertia for nylon 6, polyethylene, polypropylene and PMMA are 0.874, 1.834, 2.15 and 2.12  $\text{kJ}^2 \cdot \text{m}^{-4} \cdot \text{K}^{-2} \cdot \text{s}^{-1}$  respectively.

Mouritz et al. [41] have studied the mass loss rate, heat release rate, carbon monoxide yield, carbon dioxide yield and ignition time for various polymers and their composites such as polyester, epoxy resin, aramid fibers, vinyl ester, polyethylene fibers and vinyl ester using cone calorimeter data based on oxygen consumption.

Tsai et al. [42] have performed the experimental and numerical study of autoignition and pilot ignition of PMMA plates using a cone calorimeter. They have conducted experiments with PMMA plates at various radiative heat fluxes while measuring the surface temperatures and have

numerically proposed a two-dimensional axisymmetric model to simulate the burning process of polymer. Some of the facts they came up with were that the autoignition process is not only pyrolysis dependent but also reaction dependent at low values of heat fluxes. They also proved that gas phase reaction has significant effect on the autoignition time of the polymer. Whereas the piloted ignition process is controlled by the pyrolysis process.

Stoliarov et al. [43] have studied the burning rates of non-charring polymers and have evaluated the feasibility of one-dimensional numerical pyrolysis model to predict the transient energy transport and chemical reactions occurring during cone calorimeter test in a one-dimensional specimen. Polymers that have been used in the study are PMMA, high-impact polystyrene and high density polyethylene.

Out of above mentioned models, the current work has validated the models to predict the thermal inertia, actual critical heat flux and to determine the peak heat release rate using a pure non-charring polyethylene as the sample.

## CHAPTER III

### CONE CALORIMETER

#### 3.1 Introduction

Cone calorimeter is a sophisticated and a significant bench scale instrument used in thermal analysis and fire testing. Cone calorimeter was first announced in 1982 which started the modern era of fire testing. Evolution of cone calorimeter lies in the requirements of a bench scale heat release rate measuring device which can operate with minimum errors and laboratory scale environment. Eventually recognition of oxygen consumption principle to determine heat release rate resulted into cone calorimeter [44]. Cone calorimeter has been accepted by the International Organization for Standardization (ISO 5660-1) for measuring heat release rate of a sample. It has been observed and recorded in the literature that approximately ~13.1 MJ of heat is liberated per unit kg of oxygen consumed in the combustion reaction. Thus based on the observed consumption of oxygen the amount of heat released for a sample under consideration can be determined. Figures 2 [45] and 3 show the schematic arrangement of a cone calorimeter. As shown in figure 2 following are the major parts of a cone calorimeter apparatus:

- a. Load Cell
- b. Cone Heater
- c. Exhaust Duct
- d. Gas Analyzer Panel
- e. Control Panel

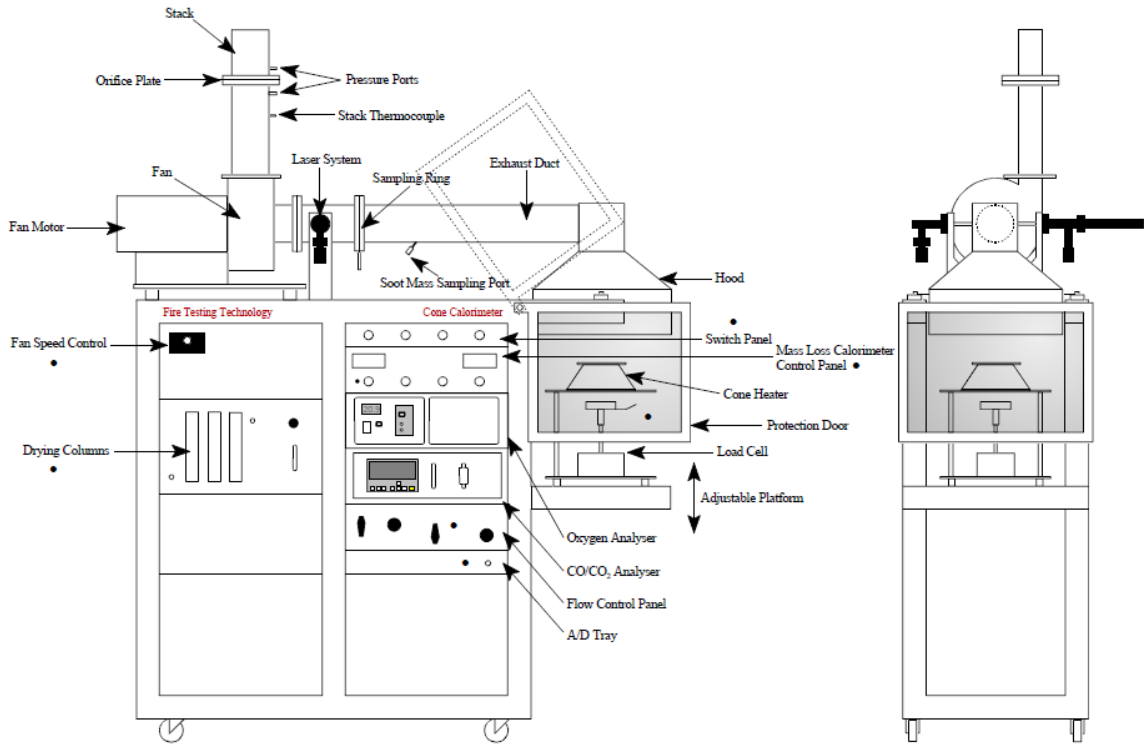


Figure 2 Schematic arrangement of cone calorimeter

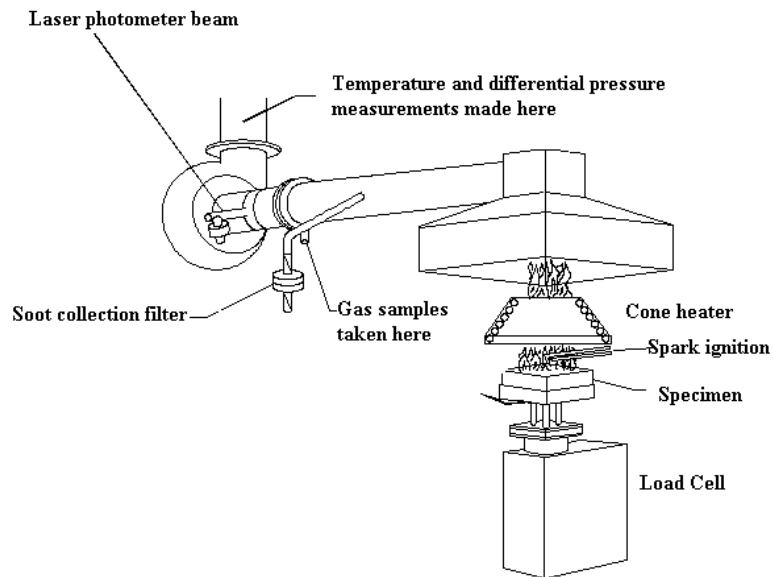


Figure 3 Zoomed view of test specimen and cone

Load cell is the place where the sample to be tested is mounted in horizontal position. It is situated right under the cone heater, which contains the heater coil to supply a predetermined amount of heat flux. The load cell is equipped with a weigh balance which helps observe the mass loss rate of the sample as a function of time during the test. The separation between the specimen holder and the cone heater should be maintained as 25mm. The instrument facilitates two type of tests, one with piloted ignition and without pilot ignition. It has an inbuilt electric ignition switch which can help trigger the sample ignition if it is desired that ignition should start at a fix time before sample attains its autoignition temperature. The other type of test is in which the sample is allowed to attain its autoignition temperature and then ignite without using of external spark as ignition source. It is equipped with a heat flux gauge which helps in setting the temperature of cone heater so as to generate desired value of heat flux.

Right above the cone heater there is an exhaust hood followed by duct. Exhaust duct facilitates removal of all the fumes / vapor generated prior to ignition and the smoke produced during combustion. It is equipped with an exhaust fan, two differential pressure ports across an orifice plate to maintain constant differential pressure across the duct which makes sure there is always a negative gradient to prevent accumulation of any fumes or smoke in the laboratory. It also contains a sampling ring for the gas analyzers such as oxygen, carbon monoxide and carbon dioxide which constantly draws a gas sample and route it to gas analyzer chamber. Gas analyzer chamber monitor the concentration of these gaseous species in the exhaust gas as a function of time over the test duration. To prevent the soot and other solid particles from entering the gas analyzer chamber, the sample gas is filtered using a series of filters. Precaution is taken to remove any water vapor using the adsorption column filter packed with hygroscopic adsorbent generally being soda lime, ascarite or silica gel / drierite. In this case, drierite have been used. Further the entrained water vapor is removed in the cold trap which freezes the carried over moisture to allow

a dried solid free gas sample to enter the gas analyzer chamber. Thus the accurate functioning of gas analyzers is ensured.

### 3.2 Calibration

Before a test can be performed, cone calorimeter requires calibration. As discussed in section 3.1, each element of the cone calorimeter needs to be calibrated at the beginning. The gas analyzers used with the equipment use laser beams to detect the gas molecule and operate at very high temperatures. Thus, most of the manufacturers suggest that the gas analyzers be kept on all the time, as it takes a couple of hours for these lasers to attain the operational temperature. Before starting the instrument one needs to make sure that Balston filter and the secondary Hepa Vent are clean and the adsorber column is filled with fully active adsorbent (drierite). Also, one needs to make sure that the drain valve on the cold trap line is closed.

First thing to calibrate is the exhaust duct flow rate. Make sure that the exhaust fan of cone calorimeter and the main room extraction systems are off to record the initial differential pressure reading across the orifice plate in exhaust duct. This differential pressure will correspond to zero flow. After taking these precautions and recording the zero point for flow one can start the exhaust duct fan and set the flow rate through exhaust duct to a constant value of  $24 \text{ L}\cdot\text{s}^{-1}$  by varying the speed of the fan. Subsequently start the main room extraction system.

Next thing to be calibrated is smoke system. One needs to place a “smoke zero blank” between the laser and the compensating photodiode. At this point of time there is no smoke in the duct and corresponding reading is recorded as zero point. Repeat the steps after removing “smoke zero blank” to get the normalized ratios for photodiodes. Next on the list is the most important calibrations of gas analyzers. For this sample gas pump is started first. Then pure nitrogen is employed to set the zero points for each gas analyzer. This is achieved by routing pure nitrogen gas through the analyzer and recording the electric potential generated by the analyzers as

corresponding zero points. After this, turn off the nitrogen gas and operate the system on the air to set the span value for oxygen, i.e. maximum concentration of oxygen expected in the exhaust duct. Once span value for oxygen is attained, air is turn off and calibration gas is routed through the system which has a known concentration of CO and CO<sub>2</sub> which is sufficient enough to cover the maximum concentration of each species that can be achieved in the exhaust gas. Once span values for the CO and CO<sub>2</sub> are set, calibration gas is turned off.

With this basic calibration attained comes the calibration of the heat release system. Turn on the power to cone heater and ignition switch. For this a methane gas stream is used. Place the methane gas burner under the cone. Open the shutters which separate the cone and gas burner underneath. Start the methane gas flow and ignite the gas with electric spark generator. As the flame appears, cone measures the value for the flame heat flux. Now by adjusting the flow rate of methane gas with the help of a manual ball valve the desired value for flame heat flux is achieved. Generally the preferred value is 5 kW·m<sup>2</sup>. Once it is attained, the system is allowed to stabilize for 180 sec (3 min) and it calculates a parameter called orifice flow constant, “C-factor”. Since the value for heat of combustion of methane is known and the gas analyzers are calibrated, system can determine the C-factor. Typically the values for C-factor range between 0.040 – 0.046. Then turn off the methane gas valve.

Next is calibration of the load cell. Turn on the power of load cell. Scale of the load cell is first aligned with the software tool. Place the empty sample holder on the load cell. Select tare option on the load cell control panel. Select the corresponding electric potential to this point as the zero weight.

The last step required before the test can be performed is to set the desired heat flux for cone heater. Place the heat flux meter under the cone heater. Make sure you have the flow of cooling water through the system which serves as a coolant for the heat flux gauge and prevents it

from getting damaged from the heat. Set a particular temperature for cone heater and observe the heat flux as detected by the heat flux meter. While performing this make sure you do not touch the black top surface of the flux meter as it affects its ability to detect the heat flux adversely. Also, make sure that the separation between the flux meter and bottom of cone heater is maintained as 25 mm. This concludes the calibration process. Appendix F contains detailed procedures for calibration, sample preparation and performing tests.

### 3.3 Experimental

Once calibration is complete, prepare the samples for test. For consistency in the test data it is highly advisable that same steps are followed while preparing the samples. The accuracy of results depends on the reproducibility of exactly the same samples which are identical in weight, thickness and are uniformly distributed. The typical sample size that is employed is 100 x 100 mm. If you are using a sample holder which has an edge lip, then the exposed surface area typically becomes 94 x 94 mm<sup>2</sup>. Magnitudes of thickness can vary from 4 mm to 15 mm, with typical thickness being used as 5 mm. Generally tests are performed on the identical sample specimen for different values of external heat fluxes. This helps us study how the sample behaves under the effect of varying heat flux. Following are the typical information that can be obtained from a cone calorimeter test:

- a. Heat release rate profile
- b. Mass loss rate profile
- c. Oxygen concentration profile in exhaust gas
- d. Carbon monoxide concentration profile in exhaust gas
- e. Carbon dioxide concentration profile in exhaust gas
- f. Smoke generation rate profile
- g. Exhaust duct volumetric flow rate as a function of time



All these data help us in interpreting and analyzing the sample fire behavior which can be classified as under:

- a. Fire growth modeling
- b. Simulating real scale fire behavior
- c. Ranking of products on basis of their fire performance
- d. Pass/fail test for newly developed materials / composites

### 3.4 Shutdown procedure

To initialize the shutdown process, set the cone temperature as 0°C using the temperature control manifold. Wait until the manifold display the value 250°C. Once a temperature of 250°C or less is attained then turn off the exhaust duct fan and main room extraction. Subsequently turn off the sample pump, cold trap, load cell, ignition, cone, and power buttons. Ensure that you leave the gas analyzer lasers on.

### 3.5 Safety precautions

Following are some of the safety precautions to be observed while performing the experiments with cone calorimeter:

- Use proper personal protective equipment such as protective glasses, rubber gloves while handling the adsorbent material, wear closed toe shoes (preferably safety shoes) and heat resistive gloves while handling the sample holder.
- Ensure there is cooling water flow through the heat flux gauge.
- Check whether the room extraction and exhaust duct fan both are operating while performing the tests. If anyone of them is not operational immediately abort the tests and shutdown the equipment as it may lead to accumulation of fumes and smoke in the laboratory.

- Maintain a vertical separation of 25 mm between bottom of the cone heater and heat flux meter, methane gas burner or top surface of sample holder, depending on the type of activity being performed.
- Ensure that the doors of the room are latched all the time as the lab corridors are equipped with smoke detectors which may lead to false alarms.
- Make sure you leave gas analyzers and smoke detector buttons on.
- Ensure you open the cold trap drain valve so as to allow the condensed moisture to be drained after shutdown.

## CHAPTER IV

### EXPERIMENTAL WORK

#### 4.1 Material specimen

Material used for this study is white non-charring Polyethylene (PE), supplied by SIGMA-ALDRICH®, manufactured under the trade name of 427799 – Polyethylene [46]. Being a laboratory grade polymer, it is reasonable to make an assumption that sample contain trace levels or negligible quantities of chlorine and sulfur as impurities. Its molecular weight and molecular weight distribution were obtained using Gel Permeation Chromatography (GPC) [46]. PE tested in this work was in form of small granules. Polyethylene and its co-polymers are being used in various applications such as construction industry as separators, support structures, pipes, moisture containment layers and others. These application employ a polymer with density  $920 - 930 \text{ kg}\cdot\text{m}^{-3}$ , which corresponds to the molecular weight of more than 25000 gm/gmol. Thus, polyethylene with molecular weight of 35000 gm/gmol was selected for current work, which has the molecular weight in same order of magnitude. Table 1 shows the number average molecular weight ( $M_n$ ), molecular weight ( $M_w$ ), molecular weight distribution ( $I_p$ ) and polymerization degree ( $n$ ) of test polymer.

Table 1 Characterization of Polyethylene (PE) sample

$M_n$	$M_w$	$I_p = M_w/M_n$	$n$
7700	35000	4.5	275

Molecular weight distribution ( $I_p$ ) value being 4.5 indicated that PE is a poly-molecular compound. From this, the degree of polymerization ( $n$ ) of polyethylene sample is determined to be of the order of 275.

#### 4.2. Sample preparation

As the polyethylene sample was in granule form, it was precisely weighed into 4 equal samples of 25 gm each with an accuracy of  $\pm 0.1$  gm. The temporary sample holder was created using aluminum foil. The sample was evenly spread through the sample holder having dimensions 100 x 100 mm. Use of edge lip sample holder frame reduces the sample surface area exposed to the external heat flux. As mentioned in section 3.2, an area of 94 x 94 mm<sup>2</sup> is available as the exposed surface area. The thickness of the sample for all the tests was maintained uniformly as 5 mm.

#### 4.3 Calibration parameters

The equipment employed for current work is supplied by Fire Testing Technology Limited. Figure 4 shows the actual cone calorimeter assembly in Fire Protection and Safety Technology lab. Before initiating the test, calibration procedures were followed thoroughly and safety precautions adhered to. Following were some of the important calibration parameters of cone calorimeter for the tests:

- a. Ambient pressure = 97.688 kPa
- b. Ambient temperature = 24°C
- c. Relative humidity = 63%
- d. Exhaust duct volumetric flow rate =  $24 \pm 3 \text{ L}\cdot\text{s}^{-1} = 0.024 \pm 0.003 \text{ m}^3\cdot\text{s}^{-1}$
- e. Baseline oxygen concentration = 20.95% (v/v)
- f. Baseline carbon dioxide concentration = 0.067% (v/v)
- g. External heat flux from cone heater (three sets of test) = 40 – 45 – 50 – 55 kW·m<sup>-2</sup>

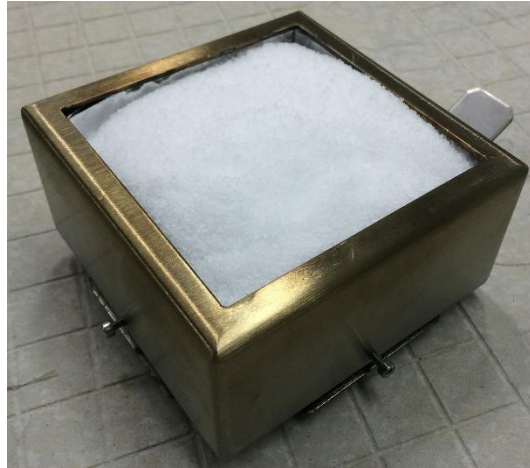
h. Surface area exposed to the external heat flux =  $88.36 \text{ cm}^2$



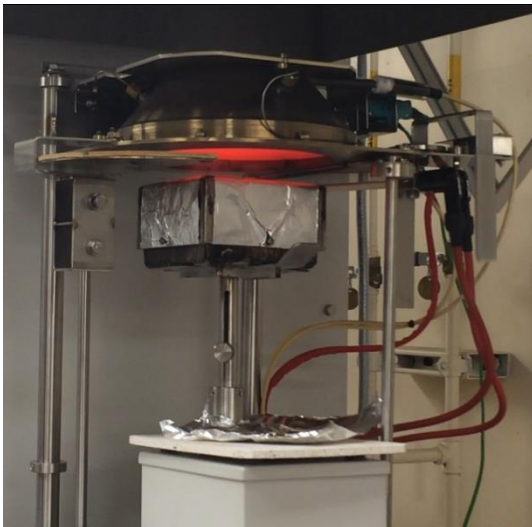
Figure 4 Cone calorimeter assembly in Fire Protection and Safety Technology Lab

Thermal analysis of four identical samples at different external heat fluxes ranging from  $40$  to  $55 \text{ kW}\cdot\text{m}^{-2}$  in step of  $5 \text{ kW}\cdot\text{m}^{-2}$  were conducted without the aid of electric spark ignition, allowing sample to attain its autoignition temperature each time. As per standard practice recommended by Fire Testing Laboratory Limited, the exhaust fan speed in the cone calorimeter was adjusted so as to maintain the volumetric flow rate at a constant value of  $0.024 \pm 0.003 \text{ m}^3\cdot\text{s}^{-1}$ . Three such sets of experiments were conducted for each value of heat flux.

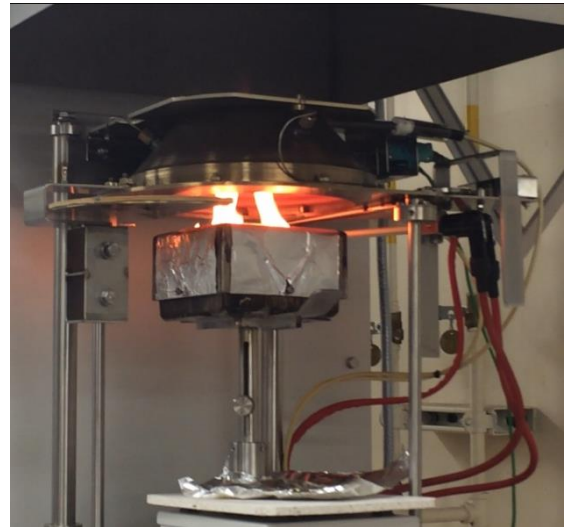
Following figure 5 exhibit timeline of test spanning from sample preparation and instances captured during the test conducted at  $40 \text{ kW}\cdot\text{m}^{-2}$ . Also, one can see the final residue obtained at the end of the test.



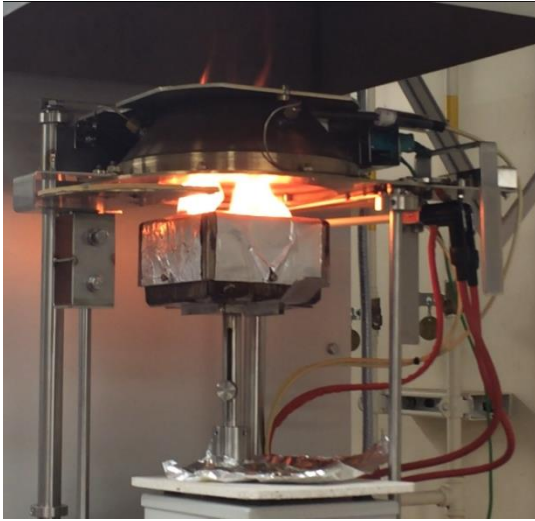
(a)  $t = 0$  sec



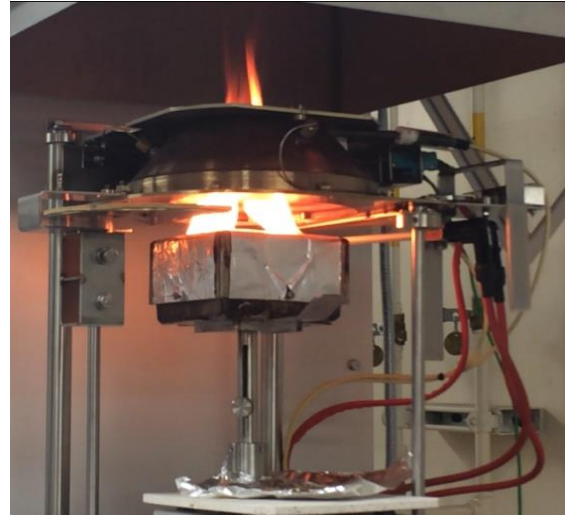
(b)  $t = 30$  sec



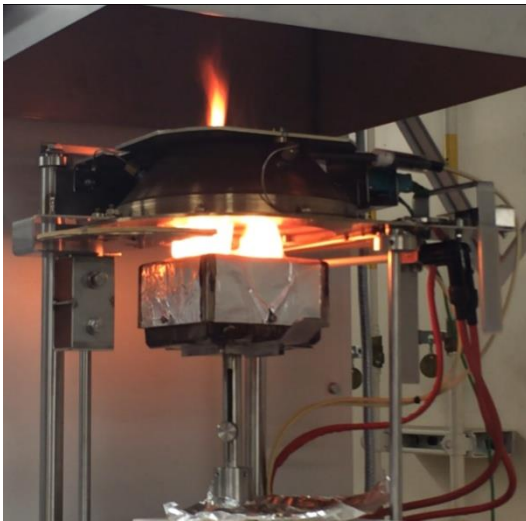
(c)  $t = 70$  sec



(d)  $t = 90 \text{ sec}$



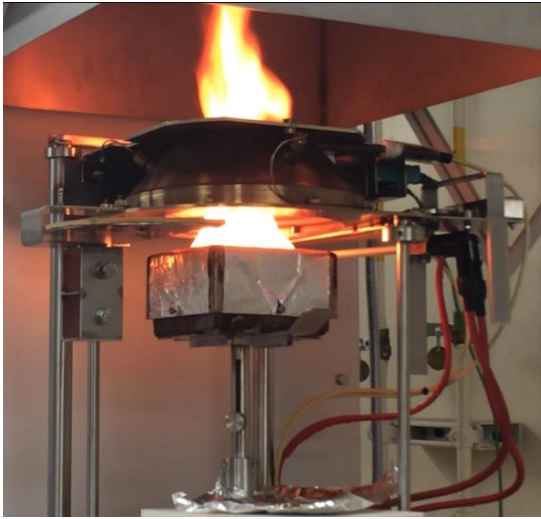
(e)  $t = 105 \text{ sec}$



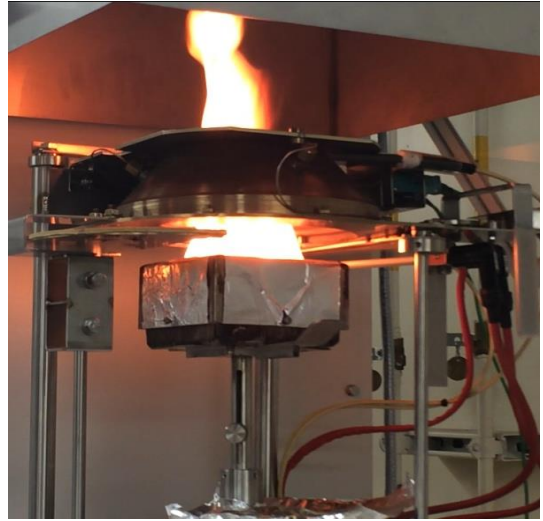
(f)  $t = 120 \text{ sec}$



(g)  $t = 135 \text{ sec}$



(h)  $t = 150$  sec



(i)  $t = 165$  sec



(j)  $t = 180$  sec



(k)  $t = 250$  sec





(l) end of test residue



(m) end of test residue

Figure 5 Timeline of cone calorimeter test

#### 4.4 Data collection

Various events were recorded during the timeline of each test such as start of test, ignition time, flame out time and end of test time. Here, start of tests corresponds to the instance when sample is first exposed to external heat flux. Ignition time corresponds to the instance when sample starts burning. Flame out time corresponds to the instance when the flame is almost about to extinguish. And test stop time corresponds to the instance when the external heat flux is stopped. Table 2 shows the observations for ignition time and flame out time for each test.

Table 2 Ignition time and flame out time observations

<b>Test No.</b>	<b>External heat flux (kW·m<sup>-2</sup>)</b>	<b>Experimental average ignition time (sec)</b>	<b>Experimental average time to flame out (sec)</b>
1	40	72.3	421.3
2	45	63.3	327.0
3	50	48.3	321.7
4	55	35.3	248.7

Cone calorimeter, based on the recorded data and its software tools generates some of the useful profiles as a function of time. The best ones and the ones useful in current research work are heat release rate profile (HRR), oxygen concentration profile in the exhaust gas, carbon monoxide concentration profile in the exhaust gas and carbon dioxide concentration profile in the exhaust gas. These data is very helpful in understanding the fire behavior of polymer sample as it is available as continuous function of time, i.e. instantaneous values of each of the parameter can be determined over the entire duration of test. Figures 6 - 9 represent the heat release rate, oxygen concentration profile, carbon monoxide concentration and carbon dioxide concentration profiles in the exhaust gas respectively (for first set of tests).

One of the best features of cone calorimeter is that it allows generation of profiles for individual tests and it also facilitates merging data for a couple of tests, making comparison easy. This feature is very useful when it comes to comparison of data among different test runs with different values of heat fluxes.

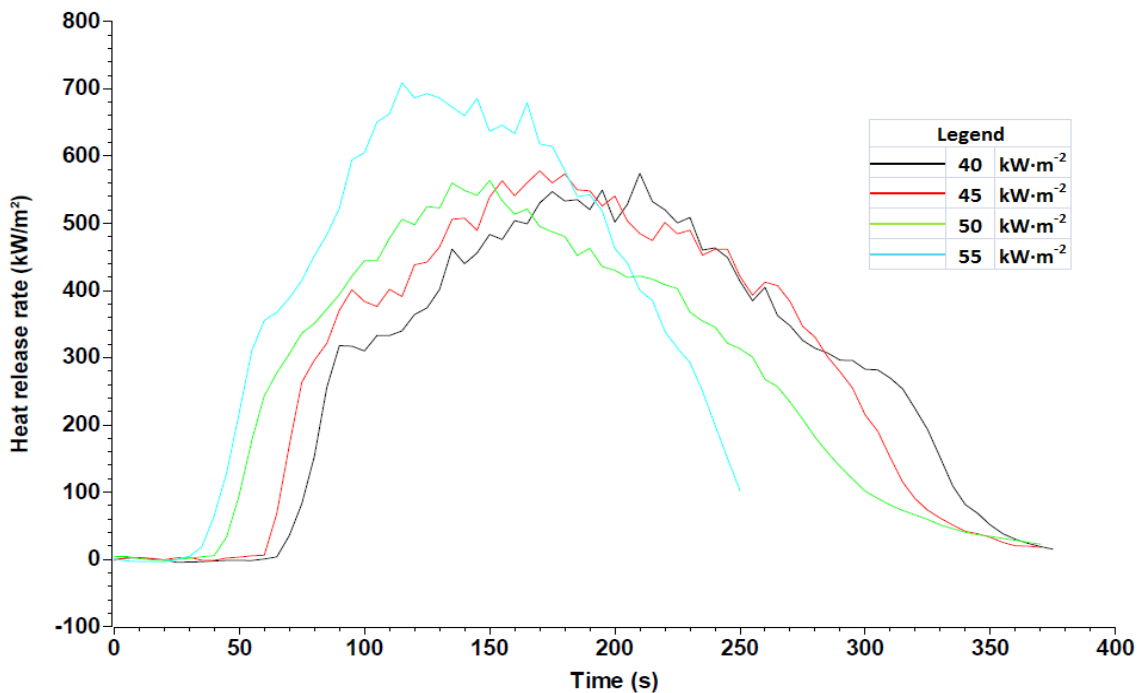


Figure 6 Heat release rate profile

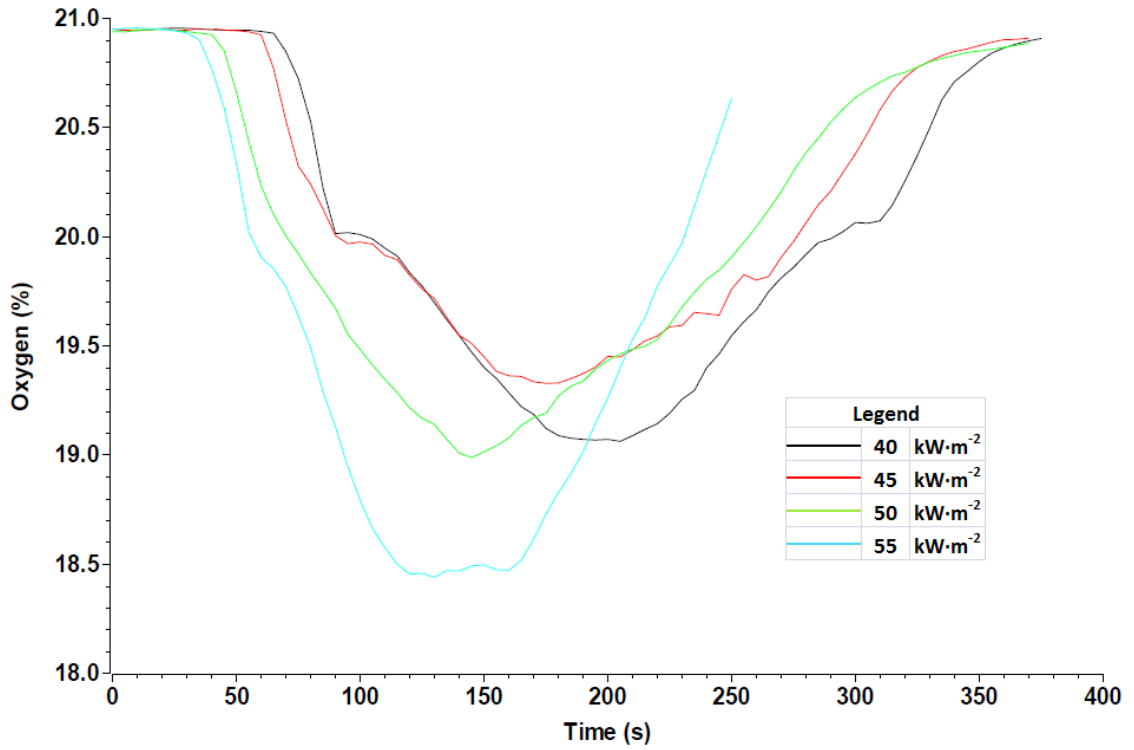


Figure 7 Oxygen concentration profile in exhaust duct

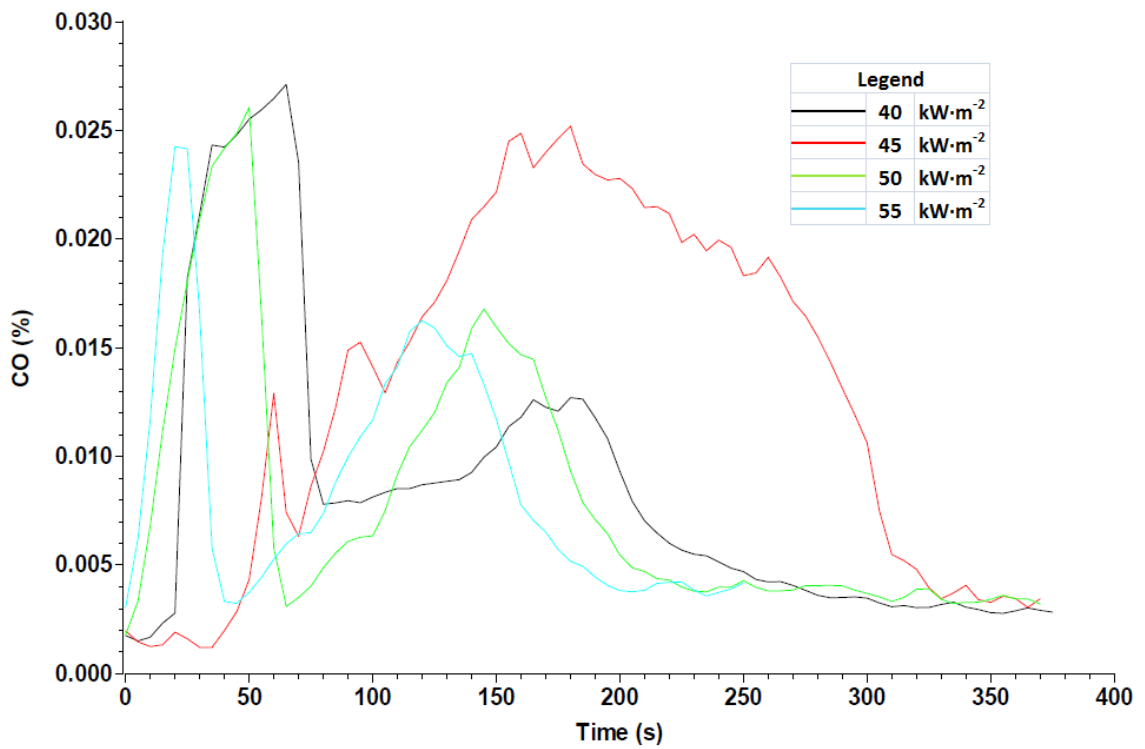


Figure 8 Carbon monoxide concentration profile in exhaust duct

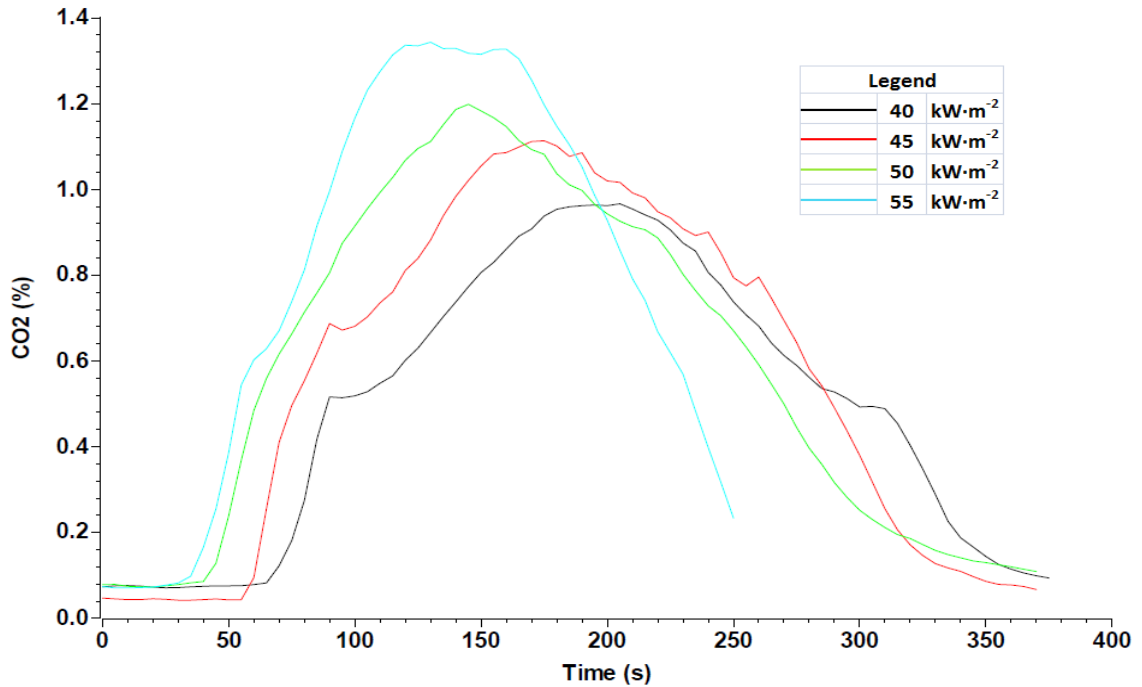


Figure 9 Carbon dioxide concentration profile in exhaust duct

From figure 6 it can be observed that the thermal degradation of PE can be divided in to four distinct regimes which are physical degradation, ignition & flame development, flame stabilization and flame out, based on the slope of heat release rate profile. These regimes are in alignments with the thermogravimetry analysis of PE. Table 3 represents those regimes as function of time.

Table 3 Timeline of different regimes for polyethylene thermal degradation (first set)

Heat Flux (kW·m <sup>-2</sup> )	Time Zone (sec)			
	1 <sup>st</sup> Stage	2 <sup>nd</sup> Stage	3 <sup>rd</sup> Stage	4 <sup>th</sup> Stage
40	69-135	136-215	215-345	>345
45	60-115	116-210	211-355	>355
50	44-115	116-225	225-300	>300
55	35-100	101-175	175-250	>250

Please refer to the Appendix C, D and E for more information about each test. They contain the combined reports for all tests of three trials, comparing the fire behavior of polyethylene.

## CHAPTER V

### DATA ANALYSIS AND MODELING

#### 5.1 Requirement of mathematical models

With the main aim of current research being able to quantify the fire behavior of polymers, the use of model equations get the first preference. It is always desirable to have an equation or a set of equations that can best fit the available data. As discussed in Chapter IV, substantial experimental data is available for polyethylene, which is intended to provide quantitative insight. Further once a validated set of model equations is available, dependence on the experimental analysis can be reduced. This is due to the fact that polymer fire behavior can be predicted using these equations. The main purpose to use the model equations is to be able to compare the improvement in the fire behavior among different polymers and their composites. In this chapter, a couple of model equations have been discussed that can prove to be elemental in quantification of polymer fire behavior.

#### 5.2 Model for external heat flux

As discussed in Chapter III, while performing the thermal analysis of polyethylene samples under autoignition condition [21] using cone calorimeter, the only heat source available is cone heater. Also, there is no direct physical contact among the cone heater and the test specimen. Thus, it can be concluded that the only means by which heat transfer occurs are convection and radiation. Based on this hypothesis, using the first principles of heat transfer, Rhodes et al. [47-49] came up with following relations which relates external heat flux and the

ignition time with the basic properties of polymer.

$$\dot{q} = \varepsilon \dot{q}_{ext} - [h_c(T_{ig} - T_0) + \varepsilon \sigma T_{ig}^4] \quad \text{Eq 1}$$

$$t_{ig} = \frac{2}{3} k \rho C_p \left( \frac{T_{ig} - T_0}{\dot{q}} \right)^2 \quad \text{Eq 2}$$

Here,  $\dot{q}$  ( $\text{kW} \cdot \text{m}^{-2}$ ) is the heat flux at the specimen surface.  $\dot{q}_{ext}$  ( $\text{kW} \cdot \text{m}^{-2}$ ) is the set value of external heat flux being supplied by cone heater which remains constant through each test.  $t_{ig}$  (sec) is the ignition time recorded during each test.  $\varepsilon$  is the emissivity of PE which has a constant value of  $\sim 0.92$ .  $k$  ( $\text{kW} \cdot \text{m}^{-1} \cdot \text{K}^{-1}$ ) is the thermal conductivity,  $\rho$  ( $\text{kg} \cdot \text{m}^{-3}$ ) is density and  $C_p$  ( $\text{kJ} \cdot \text{kg}^{-1} \cdot \text{K}^{-1}$ ) is specific heat of PE. Product of all three properties together is called thermal inertia.  $T_{ig}$  (K) and  $T_0$  (K) are the absolute ignition temperature and absolute ambient temperature.  $h_c$  ( $\text{kW} \cdot \text{m}^{-2} \cdot \text{K}^{-1}$ ) is the convective heat transfer coefficient among polymer surface and surrounding.  $\sigma$  is Stefan Boltzmann constant which is  $5.6704 \times 10^{-8} \text{ W} \cdot \text{m}^{-2} \cdot \text{K}^{-4}$ .

It has been assumed that heat transfer takes place only in vertical direction from the cone across the polyethylene thickness, one dimensional unsteady heat conduction equation applies during the preheating period. This is the time duration of the test when sample is exposed to the cone heat flux, but is not ignited. Assuming constant properties, following governing equation was proposed by Quintiere [50].

$$\frac{\partial T}{\partial t} = \alpha \frac{\partial^2 T}{\partial y^2} \quad \text{Eq 3}$$

Here, T is temperature (K), t is time (sec) and y is sample thickness (mm). and  $\alpha$  is thermal diffusivity ( $\text{m}^2 \cdot \text{s}^{-1}$ ) which is defined as

$$\alpha = \frac{k}{\rho C_p}$$

Considering initial temperature to be constant and same as ambient temperature,

$$T = T_0 \text{ at } t = 0$$

Now, considering the convective heat transfer at specimen surface ( $y = 0$ ) and radiative losses,

$$-k \left. \frac{\partial T}{\partial y} \right|_{y=0} = \dot{q} \equiv \varepsilon \dot{q}_{ext} - h_c(T - T_0) - \varepsilon \sigma T^4 \quad \text{Eq 4}$$

An approximate integral solution for the partial differential equation 3 is applied. Thus, integrating equation 3 between surface position ( $y = 0$ ) and certain penetration depth ( $y = \delta$ ),

$$T = T_0$$

$$\left. \frac{\partial T}{\partial y} \right|_{y=\delta} = 0 \quad \text{Eq 5}$$

A quadratic profile is then assumed for temperature (T) such that boundary conditions mentioned in equations 4 and 5 are satisfied.

$$T - T_0 = \frac{\dot{q}\delta}{2k} \left(1 - \frac{y}{\delta}\right)^2 \quad \text{Eq 6}$$

Applying above boundary condition to equation 3 and integrating between  $y = 0$  to  $y = \delta$ ,

$$\frac{d}{dt}(\dot{q}\delta^2) = 6\alpha\dot{q} \quad \text{Eq 7}$$

Assuming  $\dot{q}$  to be constant, which is a reasonable assumption considering the large external heat flux  $\dot{q}_{ext}$ , equation 7 can be reduced to,

$$\delta \cong \sqrt{6\alpha t_{ig}} \quad \text{Eq 8}$$

Substituting the equation 8 into equation 6 at  $y = 0$ , yields,

$$T_{ig} - T_0 = \frac{\dot{q}\delta}{2k} = \frac{\dot{q}}{2k} \sqrt{6\alpha t_{ig}} \quad \text{Eq 9}$$

Solving equation 9 for  $t_{ig}$ , gives equation 2,

$$t_{ig} = \frac{2}{3} k\rho C_P \left( \frac{T_{ig} - T_0}{\dot{q}} \right)^2 \quad \text{Eq 2}$$

Also, the critical heat flux for ignition  $\dot{q}_{crt}$  can be determined by extrapolating the ignition data for  $(t_{ig})^{-0.5}$  to zero. At this intercept,

$$\dot{q}_{ext} = \frac{1}{\varepsilon} [h_c(T_{ig} - T_0) + \varepsilon\sigma T_{ig}^4] \equiv \dot{q}_{crt} \quad \text{Eq 1}$$

Here, equation 1 represents the external heat flux in terms of convective and radiative heat transfer. Whereas equation 2 relates the ignition time with polymer properties like thermal inertia, external heat flux and the difference between ambient temperature and autoignition temperature. Here, thermal inertia of a substance is defined as the product of thermal conductivity, specific heat and density. Now, on combining the equations 1 and 2, equation 10 is obtained as under:

$$t_{ig} = \frac{\frac{2}{3} k\rho C_P (T_{ig} - T_0)^2}{\left[ \varepsilon \dot{q}_{ext} - [h_c(T_{ig} - T_0) + \varepsilon\sigma T_{ig}^4] \right]^2}$$

$$\frac{1}{\sqrt{t_{ig}}} = \left[ \frac{\varepsilon}{\sqrt{\frac{2}{3} k\rho C_P (T_{ig} - T_0)}} \right] \dot{q}_{ext} - \left[ \frac{h_c(T_{ig} - T_0) + \varepsilon\sigma T_{ig}^4}{\sqrt{\frac{2}{3} k\rho C_P (T_{ig} - T_0)}} \right] \quad \text{Eq 10}$$

Comparing equation 10 with the general equation of straight line yields,

$$Slope = \frac{\varepsilon}{\sqrt{\frac{2}{3} k\rho C_P (T_{ig} - T_0)}} \quad \text{Eq 11}$$

$$y - axis \text{ Intercept} = - \frac{h_c(T_{ig} - T_0) + \varepsilon\sigma T_{ig}^4}{\sqrt{\frac{2}{3} k\rho C_P (T_{ig} - T_0)}} \quad \text{Eq 12}$$



What this implies is graph of  $\frac{1}{\sqrt{t_{ig}}}$  vs.  $\dot{q}_{ext}$  would result in a straight line. Slope can be determined for the obtained straight line. Now using equation 11, with known values of the ambient & autoignition temperatures, emissivity and observed value of slope, the thermal inertia for polyethylene can be determined. Figure 10 represents the plot for equation 10 which is  $\left(\frac{1}{\sqrt{t_{ig}}} \text{ vs. } \dot{q}_{ext}\right)$ .

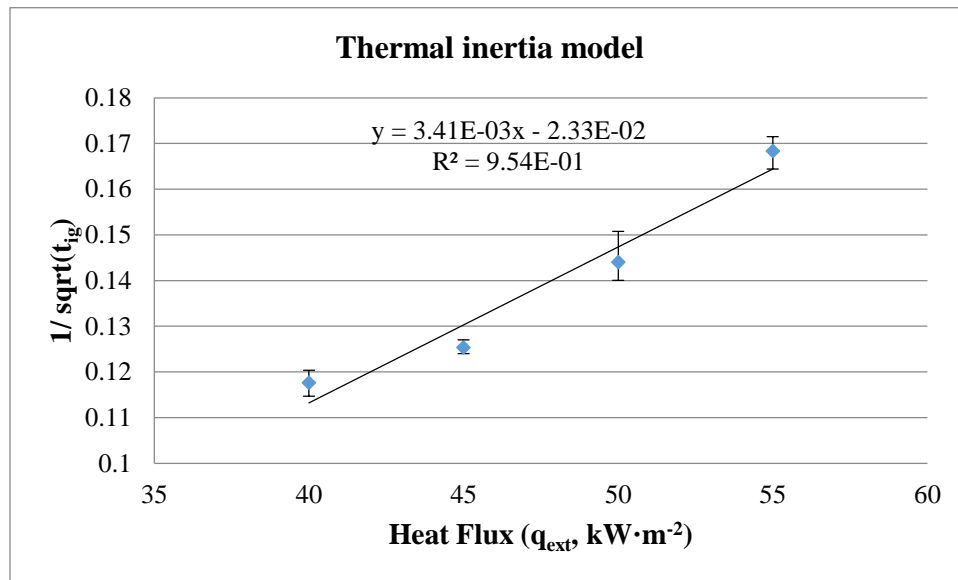


Figure 10 Determination of thermal inertia for Polyethylene (PE)

Above plot represent the data with error bars observed in the ignition time for the three sets of experiments performed for four distinct values of heat flux. From figure 10 the value of slope obtained is  $3.41 \times 10^{-3}$ . With autoignition temperature of polyethylene being 653 K, emissivity as  $\sim 0.92$  and ambient temperature of 297 K assumed to be constant, thermal inertia for polyethylene sample was determined as  $0.86 \text{ kJ}^2 \cdot \text{m}^{-4} \cdot \text{K}^{-2} \cdot \text{s}^{-1}$ . Also, Hopkins Jr. [40] has recorded the slope value for polyethylene to be  $3.23 \times 10^{-3}$ , which is in accordance with the observed value of slope  $3.41 \times 10^{-3}$ .

Now to be able to prove that the equation 10 can represent the polymer fire behavior it needs to be validated using the calculated value of thermal inertia for polyethylene. For this proven correlations for property estimation of polyethylene as a function of temperature were employed. Equation 13 represents the correlation to determine density of polyethylene as a function of temperature [51].

$$\rho = 0.8674 - 6.313 \times 10^{-4}T + 0.367 \times 10^{-6}T^2 - 0.055 \times 10^{-8}T^3 \quad \text{Eq 13}$$

To be able to estimate the realistic thermal inertia of polyethylene, average value of density over the entire temperature range starting from ambient room temperature to the autoignition temperature of polyethylene was used with equation 13. For this, the values of density were estimated at each temperature starting from room temperature (297 K) up to its autoignition temperature (653 K) in the step of 5 K. Average of the density value was then determined and considered towards the estimation of thermal inertia. The average value of density obtained is  $750.71 \text{ kg}\cdot\text{m}^{-3}$ .

Further equation 14 represents the correlation to estimate the specific heat of polyethylene [52].

$$C_p(T) = C_p(298)[1 + 1.3 \times 10^{-3}(T - 298)] \quad \text{Eq 14}$$

In equation 14 the value of  $C_p$  at 298 K is considered to be  $2.26 \text{ kJ}\cdot\text{kg}^{-1}\cdot\text{K}^{-1}$ , as determined experimentally. Then similar to the approach used for average density estimation, values of specific heat are estimated at each temperature starting from ambient (297 K) to autoignition (653 K) temperature in the step of 5 K. The average value of specific heat obtained is  $2.77 \text{ kJ}\cdot\text{kg}^{-1}\cdot\text{K}^{-1}$ .

To predict the thermal conductivity, the graphical representation of thermal conductivity of polyethylene as a function of temperature is used [53]. The value of thermal conductivity observed from the correlation is  $4 \times 10^{-4} \text{ kW}\cdot\text{m}^{-1}\cdot\text{K}^{-1}$ .

Multiplying all three average values thermal inertia of polyethylene can be obtained as  $0.83 \text{ kJ}^2\cdot\text{m}^{-4}\cdot\text{K}^{-2}\cdot\text{s}^{-1}$ . Table 4 represents the collective values used in determination of thermal inertia for polyethylene. Error of 3.49 % was observed among the experimental and calculated thermal inertia.

Table 4 Thermal inertia of polyethylene

Experimental Thermal Inertia $\text{kJ}^2\cdot\text{m}^{-4}\cdot\text{K}^{-2}\cdot\text{s}^{-1}$	Calculated thermal Inertia $\text{kJ}^2\cdot\text{m}^{-4}\cdot\text{K}^{-2}\cdot\text{s}^{-1}$			Error %
	Density [51] $\text{kg}\cdot\text{m}^{-3}$	Specific Heat [52] $\text{kJ}\cdot\text{kg}^{-1}\cdot\text{K}^{-1}$	Thermal conductivity [53] $\text{kW}\cdot\text{m}^{-1}\cdot\text{K}^{-1}$	
0.86	750.71	2.77	$4.0 \times 10^{-4}$	3.49
	0.83			

### 5.3 Critical heat flux

From figure 11 it can be observed that the intercept on x-axis is  $\sim 7 \text{ kW}\cdot\text{m}^{-2}$ . This value corresponds to be critical heat flux (CHF). CHF is defined as the value which represents the minimum amount of external heat flux required for the polyethylene (i.e. polymer sample) to ignite without the aid of external spark.

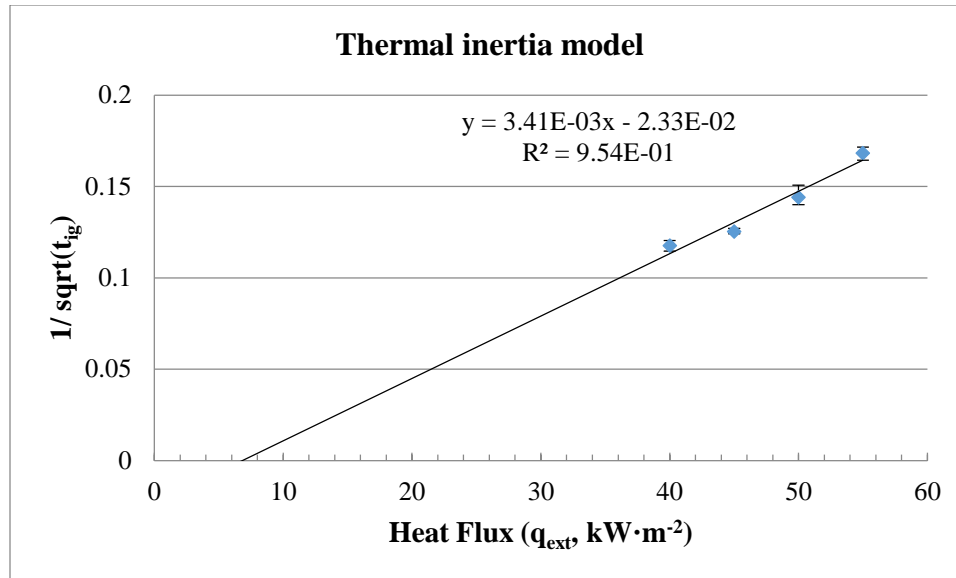


Figure 11 Extrapolated thermal inertia model for critical heat flux determination

The significance of critical heat flux is that to ignite a sample, a minimum value of external heat flux is required which should be greater than the critical heat flux.

$$CHF = -\frac{y_{intercept}}{slope} \quad \text{Eq 15}$$

Critical heat flux estimated from equation 15 is  $6.81 \text{ kW}\cdot\text{m}^{-2}$  ( $\sim 7 \text{ KW}\cdot\text{m}^{-2}$ ). The estimated value of critical heat flux from figure 11 is on lower side than the values observed experimentally. Experiments have revealed that the actual values for critical heat flux for polyethylene is higher than  $7 \text{ kW}\cdot\text{m}^{-2}$ . To be able to predict the factor which can relate the predicted value with experimental value, another mathematical model equation has been employed. There are many correlations available in literature that claim to best predict the critical heat flux factor. This thesis discuss the most proven and cited correlation developed by Quintiere [54]. It is an integral model derived based on following assumptions:

- a. Polymer sample ignites only when its surface temperature attains a critical value of autoignition temperature
- b. Solid polymer sample act as an inert until ignition
- c. Solid is infinitely thick (to justify the boundary conditions of one side of polymer being at ambient temperature and other being exposed to external heat flux)

Above mentioned assumptions are also valid in our experimental system. Thus, the use of integral model proposed by Quintiere [54] is justified for our system under consideration.

$$\frac{1}{\sqrt{\tau_{ig}}} = \left[ \frac{2(2-\beta_{ig})(1-\beta_{ig})}{\pi} \right]^{1/2} \frac{1}{\beta_{ig}} \quad \text{Eq 16}$$

Equation 16 represents the final form of integral model which relates dimensionless time ( $\tau_{ig}$ ) with the ratio of convective gain and radiative loss with external heat flux ( $\beta_{ig}$ ). Both the quantities are dimensionless and are defined as in equations 17 and 18.

$$\tau_{ig} = \frac{\dot{q}_{ext}^2 t_{ig}}{(T_{ig}-T_0)^2 k \rho C_P} \quad \text{Eq 17}$$

$$\beta_{ig} \equiv \frac{\sigma(T_s^4 - T_0^4) + h_c(T_s - T_0)}{\dot{q}_{ext}} \quad \text{Eq 18}$$

$$\beta_{ig} \equiv \frac{\dot{q}_{crt}}{\dot{q}_{ext}} \quad \text{Eq 19}$$

A complete derivation has been reported by Quintiere [54] using finite element integral analysis. Dimensionless groups for ignition time and external heat flux are used to model the critical heat flux as they have already been used in previous works.

Further to compare the factor obtained from integral model of Quintiere [54], a couple of other equations developed by Delichatsios et al. [55] were also considered. In fact the model equations proposed by Delichatsios are special cases of the original integral model of Quintiere. Delichatsios et al. have classified the original integral model equation into two equations based on the values of external heat flux being high heat flux and low heat flux. Each value of external

heat flux corresponds to a specific value of  $\beta_{ig}$ . Thus, based on the values of  $\beta_{ig}$ , Equations 20 and 21 represent the model equations proposed by Delichatsios, wherein equation 20 represents the high external heat flux and equation 21 represent the low heat flux scenario respectively.

$$\frac{1}{\sqrt{\tau_{ig}}} = \frac{2}{\sqrt{\pi}} \left( \frac{1}{\beta_{ig}} - 0.64 \right); \frac{1}{\beta_{ig}} > 3 \quad \text{Eq 20}$$

$$\frac{1}{\sqrt{\tau_{ig}}} = \sqrt{\pi} \left( \frac{1}{\beta_{ig}} - 1 \right); \frac{1}{\beta_{ig}} < 1.1 \quad \text{Eq 21}$$

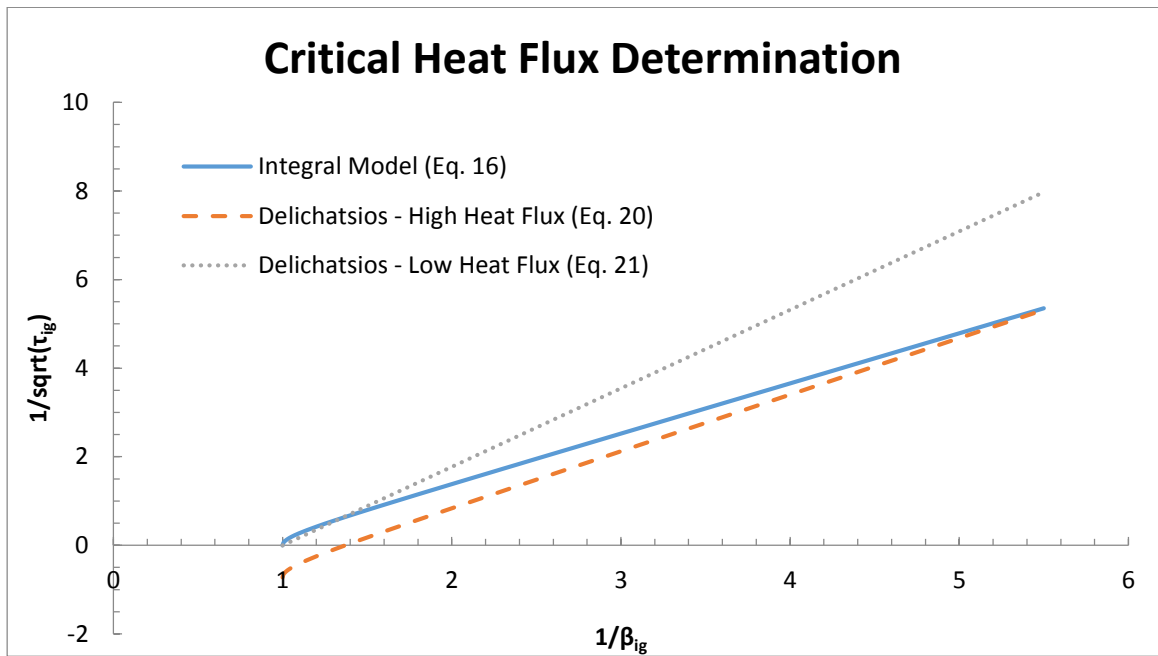


Figure 12 Model profiles for critical heat flux determination

Now plotting the points of  $\frac{1}{\sqrt{\tau_{ig}}}$  vs.  $\frac{1}{\beta_{ig}}$  based on equations 16, 20 and 21, profiles can be obtained as shown in figure 12.

From the integral model solution for equation 16, on choosing three distinct values for high heat flux, corresponding values of  $\frac{1}{\sqrt{\tau_{ig}}}$  and  $\frac{1}{\beta_{ig}}$  obtained are as follows:

$$\frac{1}{\sqrt{\tau_{ig}}} = 1.38 \text{ when } \frac{1}{\beta_{ig}} = 2.0$$

$$\frac{1}{\sqrt{\tau_{ig}}} = 3.09 \text{ when } \frac{1}{\beta_{ig}} = 3.5$$

$$\frac{1}{\sqrt{\tau_{ig}}} = 4.78 \text{ when } \frac{1}{\beta_{ig}} = 5.0$$

At high heat fluxes,  $\beta_{ig} \rightarrow 0$ , so equation 16 can be rewritten as

$$\frac{1}{\sqrt{\tau_{ig}}} = \frac{2}{\sqrt{\pi}} \left( \frac{1}{\beta_{ig}} \right) \quad \text{Eq 22}$$

Further the difference between the exact solution and the extrapolated solution is  $(1/\beta_{ig} - 1/\beta_{ig,intercept})$ . Thus equation 15 can be written as

$$\frac{1}{\sqrt{\tau_{ig}}} = \frac{2}{\sqrt{\pi}} \left( \frac{1}{\beta_{ig}} - \frac{1}{\beta_{ig,intercept}} \right) \quad \text{Eq 23}$$

Substituting the values for  $\frac{1}{\sqrt{\tau_{ig}}}$  and  $\frac{1}{\beta_{ig}}$  the respective values for  $\frac{1}{\beta_{ig,intercept}}$  determined are 0.78, 0.76 and 0.76. Average of three values obtained is 0.77. Plug this value along with the value for the X-axis intercept value obtained from figure 11, in equation 19 to get the actual critical heat flux for polyethylene.

$$\dot{q}_{crt} = \frac{\dot{q}_{int}}{0.77} \quad \text{Eq 24}$$

Similarly, Delichatsios et al. proposed the factor value to be 0.64 based on their high heat flux model described in equation 20.

The values of critical heat flux determined are  $\sim 9.09 \text{ kW}\cdot\text{m}^{-2}$  for Quintiere model and  $\sim 10.93 \text{ kW}\cdot\text{m}^{-2}$  for Delichatsios model. Though there is wide range of reported values of critical heat flux for polyethylene available in literature ranging between  $10 - 25 \text{ kW}\cdot\text{m}^{-2}$  [40].

#### 5.4 Model for heat release rate

For a fire to occur four basic things required are the fuel source, sufficient oxygen supply, an ignition source and sustained chain reactions. Whereas for a fire to propagate, a potential source for heat emission is required to sustain the flame in absence of continuous ignition source. Thus, heat release rate become one of the important aspects to be considered while studying the fire retardancy of polymers. The rate of heat release ultimately controls the spread of fire, generation of noxious gases and smoke. The value of peak heat release rate is the decisive factor in the fire behavior of a polymer or polymer composite. Higher the value of peak heat release rate, more vigorous and rapid will be the spread of fire. Thus it is of prime importance to predict this phenomenon to understand their fire behavior fully [56, 57]. Heat release rate have been determined based on the concentrations of various gaseous species in the ambient air as well as in the exhaust gas such as O<sub>2</sub>, CO, CO<sub>2</sub> and H<sub>2</sub>O as they comprise of more than 99% (v/v) of the gases. The calculation procedure is based on the oxygen depletion factor [58, 59] derived from the consumption rate of oxygen over the course of test. Equation 18 represents the oxygen depletion factor ( $\phi$ ) as per ISO 5660 standard [60, 61]. Oxygen depletion factor is calculated based on the change in mole fraction of gaseous species such as oxygen, carbon monoxide and carbon dioxide in the ambient air and exhaust gas.

$$\phi = \frac{X_{O_2}^0(1-X_{CO}-X_{CO_2})-X_{O_2}(1-X_{CO_2}^0)}{X_{O_2}^0(1-X_{O_2}-X_{CO_2}-X_{CO})} \quad \text{Eq 25}$$

Here,  $X_i^0$  is the initial mole fraction of gaseous species  $i$  in exhaust duct before the test has started and  $X_i$  is the mole fraction of the gaseous species  $i$  in the exhaust duct over the duration of test. Here subscript  $i$  is O<sub>2</sub>, CO, CO<sub>2</sub> and H<sub>2</sub>O.

Tables 5 – 7 contain the observed concentrations (mole fractions) of the gas species during the battery of the tests conducted for each values of external heat flux.



Table 5 Concentrations of gas components in ambient air and exhaust gas (first set)

Heat Flux (kW·m <sup>-2</sup> )	$X_{O_2}^0$	$X_{CO_2}^0$	$X_{H_2O}^0$	$X_{O_2}$	$X_{CO_2}$	$X_{CO}$	$X_{H_2O}$
40	0.2095	7.33 x 10 <sup>-4</sup>	0.0186	0.1908	9.60 x 10 <sup>-3</sup>	7.00 x 10 <sup>-5</sup>	0.0365
45	0.2095	4.46 x 10 <sup>-4</sup>	0.006	0.1934	1.11 x 10 <sup>-2</sup>	2.36 x 10 <sup>-4</sup>	0.0329
50	0.2095	7.18 x 10 <sup>-4</sup>	0.0189	0.19	1.18 x 10 <sup>-2</sup>	1.60 x 10 <sup>-4</sup>	0.0414
55	0.2095	7.29 x 10 <sup>-4</sup>	0.0186	0.185	1.34 x 10 <sup>-2</sup>	1.32 x 10 <sup>-4</sup>	0.0439

Table 6 Concentrations of gas components in ambient air and exhaust gas (second set)

Heat Flux (kW·m <sup>-2</sup> )	$X_{O_2}^0$	$X_{CO_2}^0$	$X_{H_2O}^0$	$X_{O_2}$	$X_{CO_2}$	$X_{CO}$	$X_{H_2O}$
40	0.2095	4.36 x 10 <sup>-4</sup>	0.0066	0.1956	9.70 x 10 <sup>-3</sup>	1.8 x 10 <sup>-4</sup>	0.0255
45	0.2095	4.68 x 10 <sup>-4</sup>	0.006	0.1886	1.43 x 10 <sup>-2</sup>	3.1 x 10 <sup>-4</sup>	0.0343
50	0.2095	4.56 x 10 <sup>-4</sup>	0.006	0.189	1.40 x 10 <sup>-2</sup>	3.0 x 10 <sup>-4</sup>	0.0377
55	0.2095	4.65 x 10 <sup>-4</sup>	0.006	0.177	2.20 x 10 <sup>-2</sup>	5.2 x 10 <sup>-4</sup>	0.0501

Table 7 Concentrations of gas components in ambient air and exhaust gas (third set)

Heat Flux (kW·m <sup>-2</sup> )	$X_{O_2}^0$	$X_{CO_2}^0$	$X_{H_2O}^0$	$X_{O_2}$	$X_{CO_2}$	$X_{CO}$	$X_{H_2O}$
40	0.2095	4.33 x 10 <sup>-4</sup>	0.0066	0.1958	9.40 x 10 <sup>-3</sup>	1.87 x 10 <sup>-4</sup>	0.0249
45	0.2095	4.57 x 10 <sup>-4</sup>	0.006	0.186	1.58 x 10 <sup>-2</sup>	3.5 x 10 <sup>-4</sup>	0.0374
50	0.2095	4.61 x 10 <sup>-4</sup>	0.006	0.1906	1.30 x 10 <sup>-2</sup>	2.65 x 10 <sup>-4</sup>	0.0316
55	0.2095	4.67 x 10 <sup>-4</sup>	0.006	0.1785	2.14 x 10 <sup>-2</sup>	4.8 x 10 <sup>-4</sup>	0.0488

For external heat flux of  $40 \text{ kW} \cdot \text{m}^{-2}$  the recorded values were,

$$X_{O_2}^0 = 0.2095$$

$$X_{CO_2}^0 = 7.33 \times 10^{-4}$$

$$X_{O_2} = 0.1908$$

$$X_{CO_2} = 9.60 \times 10^{-3}$$

$$X_{CO} = 7.00 \times 10^{-5}$$

Substitution of above mentioned values in the equation 25 yields,

$$\varphi = \frac{0.2095(1 - 7.00 \times 10^{-5} - 9.60 \times 10^{-3}) - 0.1908(1 - 7.33 \times 10^{-4})}{0.2095(1 - 0.1908 - 9.60 \times 10^{-3} - 7.00 \times 10^{-5})}$$

Thus, the value of oxygen depletion factor ( $\varphi$ ) is 0.1004. Similarly the other values for oxygen depletion factor ( $\varphi$ ) are calculated for the external heat flux values of 45, 50 and  $55 \text{ kW} \cdot \text{m}^{-2}$  respectively.

From the experiments performed for heat fluxes ranging from  $40 - 55 \text{ kW} \cdot \text{m}^{-2}$ , the peak heat release rate has been determined for each case using calculated oxygen depletion factor ( $\varphi$ ) and equations 26 & 27 [58, 59, 62-64].

$$HRR = \frac{1}{A} \left\{ E\varphi - (E_{CO} - E) \frac{1-\varphi}{2} \frac{X_{CO}}{X_{O_2}} \right\} \frac{M_{O_2}}{M_{Air}} \dot{m}_{Air} (1 - X_{H_2O}^0 - X_{CO_2}^0) X_{O_2}^0 \quad \text{Eq. 26}$$

$$\frac{\dot{m}_{Air}}{M_{Air}} = \frac{(1 - X_{H_2O})(1 - X_{O_2} - X_{CO_2} - X_{CO})}{(1 - X_{H_2O}^0)(1 - X_{O_2}^0 - X_{CO_2}^0)} \frac{\dot{m}_e}{M_e} \quad \text{Eq. 27}$$

To determine the peak heat release rate, concentration values for the gaseous fractions corresponding to the time of peak heat release were used as mentioned in tables 5 - 7. These concentrations are corresponding to the time zone representing maximum heat release rate in the

experimental profiles. Heat release rate profiles and exhaust gas concentrations for oxygen, carbon monoxide and carbon dioxide can be found in figures 6 - 9 respectively. In equation 19 the value for net heat release per unit mass of oxygen consumed (E) is taken to be 13.1 MJ/kg of O<sub>2</sub>; heat release per unit mass of oxygen consumed to produce CO (E<sub>CO</sub>) is taken as 17.6 MJ/kg of O<sub>2</sub>. Further A = 88.36 cm<sup>2</sup> is the area of the polymer sample exposed to the external heat flux from cone calorimeter, molecular weight of oxygen (M<sub>O<sub>2</sub></sub>) = 32 gm/gmol, molecular weight of air (M<sub>Air</sub>) = 28.8 gm/gmol, mass flow rate of air ( $\dot{m}_{Air}$ ) is determined using equation 27, X<sub>i</sub><sup>0</sup> is the initial mole fraction of gaseous species *i* in exhaust duct before the test has started and X<sub>i</sub> is the mole fraction of the gaseous species *i* in the exhaust duct over the duration of test. Further to simplify the calculations a reasonable assumption has been made that the gas flowing through the exhaust duct is same in composition to the air, as there are only small change in concentrations of gaseous species. Thus, concluding that the molecular weight of exhaust gas is same as that of ambient air (~28.8 gm/gmol). Tables 8 - 11 represent comparison among observed and calculated values of peak heat release rates along with % errors, which is acceptable as per the literature data available.

Following are the steps to determine peak heat release rate for the test with external heat flux of 40 kW·m<sup>-2</sup>. First of all, the mass flow rate of air ( $\dot{m}_{Air}$ ) is to be determined as per equation 27. Substitution of all input variables yields,

$$\frac{\dot{m}_{Air}}{28.8} = \frac{(1 - 0.0365)(1 - 0.1908 - 9.60 \times 10^{-3} - 7.00 \times 10^{-5}) 1.76 \times 10^{-2}}{(1 - 0.0186)(1 - 0.2095 - 7.33 \times 10^{-4}) (\sim 28.8)}$$

In above expression, the mass flow rate of exhaust gas ( $\dot{m}_e$ ) has been calculated from the known value of volumetric flow rate of exhaust gas which was set to be 24 L·s<sup>-1</sup> (~0.024 m<sup>3</sup>·s<sup>-1</sup>) and assumption that exhaust gas behaves like an ideal gas. Thus using the ideal gas equation the density of exhaust gas can be calculated and then multiply calculated density with the volumetric flow rate to determine the mass flow rate of exhaust gas.

$$\rho = \frac{PM}{RT} \quad \text{Eq 28}$$

$$\rho = \frac{(101.325) * (\sim 28.8)}{(8.314) \left( \frac{653 + 297}{2} \right)} = 0.739 \frac{kg}{m^3} = 7.39 \times 10^{-4} \frac{kg}{lit}$$

Here, to get the average density of the exhaust gas, average temperature (475 K) has been considered starting from the ambient room temperature up to the autoignition temperature of polyethylene. The other values used are pressure (P) as 101.325 kPa, molecular weight of exhaust gas as ~28.8 kg/kmol and universal gas constant as 8.314 kPa·m<sup>3</sup>·kmol<sup>-1</sup>·K<sup>-1</sup>. Thus, the density of the exhaust gas obtained is 7.39 x 10<sup>-4</sup> kg·lit<sup>-1</sup>. Multiplying the volumetric flow rate of exhaust gas with density, required mass flow rate of exhaust gas was obtained as 1.77 x 10<sup>-2</sup> kg·s<sup>-1</sup>.

Also, in experimental set up used was not facilitated with necessary instruments to observe and record the concentration of moisture in the exhaust gas. Though, lab was equipped with relative humidity measuring device whose reading was recoded at the beginning of each test. From the value of relative humidity, the % H<sub>2</sub>O in the ambient air was determined using its saturation vapor pressure at ambient temperature. Further to that, combustion reaction was considered to be the only source for concentration of H<sub>2</sub>O to change. Hence, based on the % change in concentration of carbon monoxide & carbon dioxide and the stoichiometric coefficients of combustion reactions % concentration of H<sub>2</sub>O in the exhaust gas stream was estimated. The value for  $X_{H_2O}$  for the test of 40 kW·m<sup>-2</sup> is 0.0365.

Having done this, the value of mass flow rate of air ( $\dot{m}_{Air}$ ) for the system was determined to be 0.0176 kg·s<sup>-1</sup>.

Peak heat release rate can now be determined using equation 25. Substitution of all the values in equation 25 yields,

$$\begin{aligned}
HRR = & \frac{1}{88.36 \times 10^{-4} m^2} \left[ \left( 13100 \frac{kJ}{kg O_2} \right) (0.0990) \right. \\
& \left. - \left( 17600 \frac{kJ}{kg O_2} - 13100 \frac{kJ}{kg O_2} \right) \left( \frac{1 - 0.0990}{2} \right) \frac{1.29 \times 10^{-4}}{0.1910} \right] \\
& \left( \frac{32 \frac{kg O_2}{kmol}}{28.8 \frac{kg Air}{kmol}} \right) \left( 0.0176 \frac{kg Air}{s} \right) (1 - 0.0186 - 6.95 \times 10^{-4}) (0.2095)
\end{aligned}$$

The value for peak heat release rate thus obtained is 598.46 kW·m<sup>-2</sup>. Similarly the peak heat release rates for other tests have been determined and are tabulated for distinct heat fluxes in tables 8-11.

Table 8 Peak heat release rate (40 kW·m<sup>-2</sup>)

Test	$\phi$	HRR <sub>exp</sub> (kW·m <sup>-2</sup> )	HRR <sub>calc</sub> (kW·m <sup>-2</sup> )	Error (%)
1	0.1004	573.71	598.46	4.31
2	0.0716	508.07	428.28	15.70
3	0.0707	500.69	423.49	15.42

Table 9 Peak heat release rate (45 kW·m<sup>-2</sup>)

Test	$\phi$	HRR <sub>exp</sub> (kW·m <sup>-2</sup> )	HRR <sub>calc</sub> (kW·m <sup>-2</sup> )	Error (%)
1	0.0829	577.32	492.53	14.68
2	0.1074	703.3	638.38	9.23
3	0.1208	724.54	717.05	1.03

Table 10 Peak heat release rate (50 kW·m<sup>-2</sup>)

Test	$\phi$	HRR <sub>exp</sub> (kW·m <sup>-2</sup> )	HRR <sub>calc</sub> (kW·m <sup>-2</sup> )	Error (%)
1	0.1025	563.04	606.19	7.66
2	0.1054	710.88	626.78	11.83
3	0.0972	649.35	578.85	10.85

Table 11 Peak heat release rate ( $55 \text{ kW}\cdot\text{m}^{-2}$ )

Test	$\phi$	$\text{HRR}_{\text{exp}} (\text{kW}\cdot\text{m}^{-2})$	$\text{HRR}_{\text{calc}} (\text{kW}\cdot\text{m}^{-2})$	Error (%)
1	0.1300	708.14	770.97	8.87
2	0.1662	1010.71	975.79	3.45
3	0.1582	1005.77	929.31	7.60

## 5.5 Results

From the battery of thermal analysis tests performed using cone calorimeter the fire behavior data for polyethylene was recorded over a practical range of external heat flux values ranging from  $40$  to  $55 \text{ kW}\cdot\text{m}^{-2}$ . Please refer to combined test reports attached in the Appendix C, D and E for further information on test results.

As discussed in Chapters IV and V, the thermal inertia of polyethylene determined based on experimental data was  $0.86 \text{ kJ}^2\cdot\text{m}^{-4}\cdot\text{K}^{-2}\cdot\text{s}^{-1}$  and the value calculated using property correlations derived from numerical estimation and additive group contribution approaches was  $0.83 \text{ kJ}^2\cdot\text{m}^{-4}\cdot\text{K}^{-2}\cdot\text{s}^{-1}$ . The difference among the two values of thermal inertia is  $3.49\%$  which is in line with the literature data available for polyethylene and other polymers.

Also, the estimated factor to determine the actual critical heat flux for polyethylene using mathematical models developed by Quintiere [54] and Delichatsios et al. [55] were found to be  $9.09$  and  $10.93 \text{ kW}\cdot\text{m}^{-2}$  respectively.

Lastly the peak heat release rate was quantified based on the oxygen depletion factor ( $\phi$ ) and external heat flux by determining the peak heat release rate for each test which are in good agreement with the experimental observations with a standard deviation of  $\pm 4.56\%$ . The calculated and observed data are recorded in tables 8 - 11.

## CHAPTER VI

### CONCLUSION AND FUTURE WORK

#### 6.1 Conclusion

From thermal analysis of polyethylene it can be concluded that increase in external heat flux results in increased peak heat release rate, early ignition and rapid thermal degradation. As the external heat flux increases it has been observed that oxygen consumption also increases validating the higher heat release rate. With increase in external heat flux the concentrations of carbon monoxide and carbon dioxide in the exhaust gas increases considerably. Based on the heat release rate profile, thermal degradation of polyethylene can be classified into four distinct regimes corresponding to physical degradation, ignition & flame development, flame stabilization and flame out.

With the proposed model equations being validated for the thermal inertia and peak heat release rate for polyethylene, it can be concluded that a strong platform has been created towards quantification of polymer fire behavior. This thesis serves as a basis that proposed model equations hold good for pure polymers and hence they can also be employed to investigate the fire behavior of polymer nanocomposites.

Thus, the current thesis serves the purpose to provide a quantitative insight to polyethylene fire behavior which would prove to be elemental in fulfilling the next objectives of the research project.

## 6.2 Future work

### 6.2.1 To study the thermal analysis of polymer nanocomposites

Model equations discussed in current work can be used to analyze the thermal analysis results obtained using cone calorimeter for newly designed polymer nanocomposites. This would allow a quantitative insight of properties and the extent to which polymer nanocomposites differ from pure polymer. This information could be of very useful as to help retain some of the desired properties of pure polymer while adding nanofillers into them.

### 6.2.2 To design a fire retardant polymer nanocomposite

An important future work would be to check if the model equations discussed in this thesis can be employed to predict the properties and fire behavior of polymer nanocomposites by interpolation. This would require three samples each with distinct % loading of nanofillers. Thermal analysis would have to be performed on the samples with maximum and minimum % loading of nanofillers. Autoignition time would be determined for each of the samples. Here, it has been assumed that polymer nanocomposites have known set of properties such as autoignition temperature and thermal inertia. If not properties of pure polymer could be used. Based on these data, autoignition time for the polymer nanocomposite with intermediate % loading of nanofillers could be estimated. This value would then be validated by performing the thermal analysis of the intermediate polymer nanocomposite.

### 6.2.3 To design sample holder

While performing experiments polyethylene samples were observed to swell and drip down from the edges of sample holder made from aluminum foil. Eventually use of 3 layers of aluminum foil helped overcome this challenge. But, there is a need to design a suitable sample holder which may contain the molten solid. This would help in producing effective test results



and also reduce the risk of spread of hot molten polymer and fire. Suitable materials for this application could be ceramic or metal.

### 6.3 Recommendations

Following are certain recommendations for conducting efficient thermal analysis tests using cone calorimeter:

- The weight of the sample being tested can be among 15 – 100 gm and its thickness can vary among 4 – 15 mm. Optimum weight for a polymer sample would be 25 – 30 gm with thickness of 5 – 10 mm.
- Though the sample dimensions are fixed by the standard, the choice of sample weight should be made such that the test lasts for at least 180 sec, with ideal test duration ranging from 240 – 600 sec.
- This is recommended to obtain the reliable data for the samples. If a small sample mass is chosen, it will get exhausted within couple of seconds and the data collected will comprise of spikes. It will not yield the desired profiles which actually represent various stages of sample degradation.
- On the other hand the selection of heat flux values should be made such that it allows the sample to last for above mentioned time range. Heat flux should not be too high making test duration less than 180 sec and also not too low that it takes much longer for sample to ignite.
- Choice of sample mass and heat flux values should be selected such that each test lasts long enough to yield the results which represent all stages of thermal degradation and their transition.
- It is recommended to have three or four layers of aluminum foil base to carry the polymer sample, as using a single layer results in polymer dripping, when it starts melting.

- On entering the lab, make sure that main exhaust duct of the lab is operational and all the gas cylinders including methane, calibration gas and nitrogen are turned off (i.e. both the pressure gauges indicate zero).
- Before starting the cone calorimeter, ensure that cold trap valve is closed, adsorber column is recharged with fresh drierite and make sure cooling water is circulating through the heat flux gauge.
- Always wear personal protective equipments while performing the experiments such as safety glasses, closed toe shoes and lab coat. Ensure that you wear cotton clothes the day you are performing the tests. Use heat resistive gloves available in lab to handle the sample holder while performing the tests.

## NOMENCLATURE

$\dot{q}_{ext}$	= external heat flux ( $\text{kW}\cdot\text{m}^{-2}$ )
$\dot{q}_{crt}$	= critical heat flux ( $\text{kW}\cdot\text{m}^{-2}$ )
$\dot{q}$	= external heat flux absorbed by sample ( $\text{kW}\cdot\text{m}^{-2}$ )
$\varepsilon$	= emissivity (dimensionless)
$h_c$	= convective heat transfer coefficient ( $\text{kW}\cdot\text{m}^{-2}\cdot\text{K}^{-1}$ )
$T_{ig}$	= ignition temperature (K)
$T_0$	= ambient (initial) temperature (K)
$\sigma$	= Stephan-Boltzmann constant ( $5.6704 \times 10^{-8} \text{ W}\cdot\text{m}^{-2}\cdot\text{K}^{-4}$ )
$t_{ig}$	= ignition time (sec)
$\tau_{ig}$	= dimensionless time (dimensionless)
$k$	= thermal conductivity ( $\text{kW}\cdot\text{m}^{-1}\cdot\text{K}^{-1}$ )
$\rho$	= density ( $\text{kg}\cdot\text{m}^{-3}$ )
$C_p$	= specific heat ( $\text{kJ}\cdot\text{kg}^{-1}\cdot\text{K}^{-1}$ )
$\alpha$	= thermal diffusivity ( $\text{m}^2\cdot\text{s}^{-1}$ )
$\beta_{ig}$	= ratio of convective gain and radiative loss with external heat flux (dimensionless)
$\varphi$	= oxygen depletion index (dimensionless)
$X_i^0$	= initial mole fraction of gaseous species $i$ in the exhaust duct before test commences, Here, $i = \text{O}_2, \text{CO}_2, \text{CO}, \text{H}_2\text{O}$
$X_i$	= mole fraction of gaseous species $i$ in the exhaust gas during the course of test Here, $i = \text{O}_2, \text{CO}_2, \text{CO}, \text{H}_2\text{O}$
$\dot{m}_i$	= mass flow rate of species $i$ , here $i = \text{Air}, \text{exhaust gas (e)}$
$M_i$	= molecular weight of gaseous species $i$ , here $i = \text{Air}, \text{O}_2, \text{exhaust gas (e)}$
$\delta$	= thermal penetration thickness (mm)
$R$	= universal gas constant ( $8.314 \text{ m}^3\cdot\text{kPa}\cdot\text{kmol}^{-1}\cdot\text{K}^{-1}$ )
$P$	= pressure (kPa)

## REFERENCES

1. *Global Polymer Industry 2012-2017: Trend, Profit, and Forecast Analysis*. 2012, Luncitel.
2. Karter, M.J., *Fire Loss in the United States*. 2013, NPFA.
3. van der Veen, I. and J. de Boer, *Phosphorus flame retardants: Properties, production, environmental occurrence, toxicity and analysis*. *Chemosphere*, 2012. **88**(10): p. 1119-1153.
4. Pavlidou, S. and C.D. Papaspyrides, *A review on polymer-layered silicate nanocomposites*. *Progress in Polymer Science*, 2008. **33**(12): p. 1119-1198.
5. Kashiwagi, T. et al., *Flammability properties of polymer nanocomposites with single-walled carbon nanotubes: effects of nanotube dispersion and concentration*. *Polymer*, 2005. **46**(2): p. 471-481.
6. Patel, P. et al., *Flammability properties of PEEK and carbon nanotube composites*. *Polymer Degradation and Stability*, 2012. **97**(12): p. 2492-2502.
7. Friederich, B. et al., *Tentative links between thermal diffusivity and fire-retardant properties in poly(methyl methacrylate)-metal oxide nanocomposites*. *Polymer Degradation and Stability*, 2010. **95**(7): p. 1183-1193.
8. Castrovinci, A. and G. Camino, *Fire-Retardant Mechanisms in Polymer Nano-Composite Materials*, in *Multifunctional Barriers for Flexible Structure*, S. Duquesne, C. Magniez, and G. Camino, Editors. 2007, Springer Berlin Heidelberg. p. 87-108.
9. Vigolo, B. et al., *Macroscopic Fibers and Ribbons of Oriented Carbon Nanotubes*. *Science*, 2000. **290**(5495): p. 1331-1334.

10. Kashiwagi, T. et al., *Thermal and flammability properties of polypropylene/carbon nanotube nanocomposites*. *Polymer*, 2004. **45**(12): p. 4227-4239.
11. Kashiwagi, T. et al., *Thermal Degradation and Flammability Properties of Poly(propylene)/Carbon Nanotube Composites*. *Macromolecular Rapid Communications*, 2002. **23**(13): p. 761-765.
12. Wu, Q. and B. Qu, *Synergistic effects of silicotungstic acid on intumescent flame-retardant polypropylene*. *Polymer Degradation and Stability*, 2001. **74**(2): p. 255-261.
13. Bourbigot, S. et al., *Zeolites: New Synergistic Agents for Intumescent Fire Retardant Thermoplastic Formulations—Criteria for the Choice of the Zeolite*. *Fire and Materials*, 1996. **20**(3): p. 145-154.
14. Matusinovic, Z. et al., *Polystyrene/molybdenum disulfide and poly(methyl methacrylate)/molybdenum disulfide nanocomposites with enhanced thermal stability*. *Polymer Degradation and Stability*, 2012. **97**(12): p. 2481-2486.
15. Chrissafis, K. and D. Bikiaris, *Can nanoparticles really enhance thermal stability of polymers? Part I: An overview on thermal decomposition of addition polymers*. *Thermochimica Acta*, 2011. **523**(1–2): p. 1-24.
16. Scharrel, B. and T.R. Hull, *Development of fire-retarded materials—Interpretation of cone calorimeter data*. *Fire and Materials*, 2007. **31**(5): p. 327-354.
17. Scharrel, B. and A. Weiß, *Temperature inside burning polymer specimens: Pyrolysis zone and shielding*. *Fire and Materials*, 2010. **34**(5): p. 217-235.
18. Laachachi, A. et al., *Use of oxide nanoparticles and organoclays to improve thermal stability and fire retardancy of poly(methyl methacrylate)*. *Polymer Degradation and Stability*, 2005. **89**(2): p. 344-352.
19. Katančić, Z. et al., *Study of flammability and thermal properties of high-impact polystyrene nanocomposites*. *Polymer Degradation and Stability*, 2011. **96**(12): p. 2104-2111.

20. Luche, J. et al., *Characterization of thermal properties and analysis of combustion behavior of PMMA in a cone calorimeter*. Fire Safety Journal, 2011. **46**(7): p. 451-461.
21. Shi, L. and M.Y.L. Chew, *Fire behaviors of polymers under autoignition conditions in a cone calorimeter*. Fire Safety Journal, 2013. **61**(0): p. 243-253.
22. Stoliarov, S.I. et al., *Prediction of the burning rates of charring polymers*. Combustion and Flame, 2010. **157**(11): p. 2024-2034.
23. Stoliarov, S.I. et al., *Prediction of the burning rates of charring polymers*. 2010, SRA International, Inc.: NJ.
24. Lyon, R.E. and S.I. Stoliarov, *Thermo-Kinetic model of burning for pyrolyzing materials*. in *Ninth International Symposium on fire Safety Science*. 2009.
25. Lautenberger, C. and C. Fernandez-Pello, *Generalized pyrolysis model for combustible solids*. Fire Safety Journal, 2009. **44**(6): p. 819-839.
26. Di Blasi, C., *Modeling and simulation of combustion processes of charring and non-charring solid fuels*. Progress in Energy and Combustion Science, 1993. **19**(1): p. 71-104.
27. Kashiwagi, T., *Polymer combustion and flammability - role of the condensed phase*. in *25th Combustion Institute Symposium (International) on Combustion*. 1994.
28. Fernandez-Pello, A.C., *The solid phase*, in: *Combustion Fundamentals of Fire*. 1995: Academic Press.
29. Lyon, R.E. and M.L. Janssens, *Polymer Flammability*. U.S. Department of Transportation, Federal Aviation Administration, DOT/FAA/AR-05/14, Final Report: April 15, 2005
30. Moghtaderi, B., *The state-of-the-art in pyrolysis modeling of lignocellulosic solid fuels*. Fire and Materials, 2006. **30**: p. 1-34.
31. Fernandez-Pello, A.C. and C. Lautenberger, *Pyrolysis modeling, thermal decomposition and transport processes in combustible solids*, in: *Transport phenomena in fires*. 2008: WIT Press.

32. Andrady, A.L. and M.A. Neal, *Applications and societal benefits of plastics*. Philosophical Transactions of the Royal Society, 2009. **364**(1526): p. 1977-1984.
33. Rabbi, F., *Systematic analysis of flammability reduction of polymer nanocomposites*. 2014, Oklahoma State University.
34. Cinausero, N. et al., *Synergistic effect between hydrophobic oxide nanoparticles and ammonium polyphosphate on fire properties of poly(methyl methacrylate) and polystyrene*. Polymer Degradation and Stability, 2011. **96**(8): p. 1445-1454.
35. Liu, M. et al., *Flame retardancy of poly(styrene-co-acrylonitrile) by the synergistic interaction between clay and phosphomolybdate hydrates*. Polymer Degradation and Stability, 2011. **96**(5): p. 1000-1008.
36. Laachachi, A. et al., *Fire retardant systems in poly(methyl methacrylate): Interactions between metal oxide nanoparticles and phosphinates*. Polymer Degradation and Stability, 2007. **92**(1): p. 61-69.
37. Laachachi, A. et al., *Effect of ZnO and organo-modified montmorillonite on thermal degradation of poly(methyl methacrylate) nanocomposites*. Polymer Degradation and Stability, 2009. **94**(4): p. 670-678.
38. Friederich, B. et al., *Investigation of fire-resistance mechanisms of the ternary system (APP/MPP/TiO<sub>2</sub>) in PMMA*. Polymer Degradation and Stability, 2012. **97**(11): p. 2154-2161.
39. Zhang, J. et al., *Experimental and numerical study of the effects of nanoparticles on pyrolysis of a polyamide 6 (PA6) nanocomposite in the cone calorimeter*. Combustion and Flame, 2009. **156**(11): p. 2056-2062.
40. Hopkins, Jr. D., *Predicting the ignition time and burning rate of thermoplastics in the cone calorimeter*, in *Department of Fire Protection Engineering*. 1995, University of Maryland.

41. Mouritz, A.P. and A.G. Gibson, *Fire reaction properties of composites* Fire properties of polymer composites materials, 2006. **Chapter 3**: p. 59-101.
42. Tsai, T.H. et al., *Experimental and Numerical study of autoignition and pilot ignition of PMMA plates in a cone calorimeter*. National Tsing Hua University.
43. Stoliarov, S.I. et al., *Prediction of the burning rates of non-charring polymers*. Combustion and Flame, 2009. **156**(5): p. 1068-1083.
44. Babrauskas, V., *Ten years of heat release research with the cone calorimeter*. 1993, National Institute of Standards and Technology.
45. Babrauskas, V. and W.H. Twilley, *User's guide for the Cone Calorimeter*. 2001, Fire Testing Technology Limited.
46. *Safety Data Sheet for Polyethylene*. 2014, Sigma-Aldrich.
47. Rhodes, B.T. and J.G. Quintiere, *Burning rate and flame heat flux for PMMA in a cone calorimeter*. Fire Safety Journal, 1996. **26**(3): p. 221-240.
48. Hopkins Jr., D. and J.G. Quintiere, *Material fire properties and predictions for thermoplastics*. Fire Safety Journal, 1996. **26**(3): p. 241-268.
49. Tewarson, A., *Generation of heat and chemical compounds in fires*. 3rd ed. Vol. chapter 4, section 3. 2002, Quincy, MA: The National Fire Protection Association Press.
50. Quintiere, J.G., *A semi-quantitative model for the burning of solid materials*. 1992, National Insitute of Standards and Technology.
51. Orwoll, R.A. and P.J. Flory, *Equation- of-state parameters for normal alkanes. Correlation with chain length*. Journal of the American Chemical Society, 1967. **89**(26): p. 6814-6822.
52. van Krevelen, D.W.and K. te Nijenhuis, *Properties of polymers, Their correlation with chemical structure; their numerical estimation and prediction from additive group contributions*. 4 ed. 2009: Elsevier.



53. Vasile, C. and M. Pascu, *Practical guide to polyethylene*. 2005: Rapra Technology Limited.
54. Spearpoint, M.J. and J.G. Quintiere, *Predicting the piloted ignition of wood in the cone calorimeter using an integral model — effect of species, grain orientation and heat flux*. Fire Safety Journal, 2001. **36**(4): p. 391-415.
55. Delichatsios, M.A. et al., *The use of time to ignition data for characterizing the thermal inertia and the minimum (critical) heat flux for ignition or pyrolysis*. Combustion and Flame, 1991. **84**(3-4): p. 323-332.
56. Babrauskas, V. and R.D. Peacock, *Heat release rate: The single most important variable in fire hazard*. Fire Safety Journal, 1992. **18**(3): p. 255-272.
57. Babrauskas, V., *Ignition Handbook*. 2003: Fire Sciences Publishers.
58. Janssens, M., *Measuring rate of heat release by oxygen consumption*. Fire Technology, 1991. **27**(3): p. 234-249.
59. Enright, P.A., *Heat release and combustion behaviour of upholstered furniture*. 1999, University of Canterbury.
60. Babrauskas, V. and G. Grayson, *Heat release in fires*. 1992, Essex, England: Elsevier Science Publishers Ltd.
61. International Organization of Standardization, *ISO 5660, Reaction to fire tests - heat release, smoke production and mass loss rate - Part 1 Heat release rate (cone calorimeter method)*. 2002.
62. Janssens, M., *SFPE Handbook of Fire Protection Engineering*. 2002: NFPA.
63. Thornton, W., *The relation of oxygen to the heat of combustion of organic compounds*. Philosophical magazine and journal of science, 1917. **33**: p. 196-203.
64. Huggett, C., *Estimation of rate of heat release by means of oxygen consumption measurements*. Fire and Materials, 1980. **4**(2): p. 61-65.

## APPENDICES

### Appendix A

Table 12 United States fire statistics

Year	Fires	Civilian Deaths	Civilian Injuries	Firefighter Deaths	Firefighter Injuries	Direct Property Damage (in Billions)	
						As Reported	In 2012 Dollars
1977	3,264,000	7,395	31,190	157	112,540	\$4.70	\$17.80
1978	2,817,500	7,710	29,825	174	101,100	\$4.50	\$15.80
1979	2,845,500	7,575	31,325	126	95,780	\$5.80	\$18.40
1980	2,988,000	6,505	30,200	138	98,070	\$6.30	\$17.60
1981	2,893,500	6,700	30,450	136	103,340	\$6.70	\$16.90
1982	2,538,000	6,020	30,525	128	98,150	\$6.40	\$15.20
1983	2,326,500	5,920	31,275	113	103,150	\$6.60	\$15.20
1984	2,343,000	5,240	28,125	119	102,300	\$6.70	\$14.80
1985	2,371,000	6,185	28,425	128	100,900	\$7.30	\$15.50
1986	2,271,500	5,850	26,825	119	96,450	\$6.70	\$14.00
1987	2,330,000	5,810	28,215	132	102,600	\$7.20	\$14.50
1988	2,436,500	6,215	30,800	136	102,900	\$8.40	\$16.30
1989	2,115,000	5,410	28,250	118	100,700	\$8.70	\$16.10
1990	2,019,000	5,195	28,600	108	100,300	\$7.80	\$13.70
1991	2,041,500	4,465	29,375	108	103,300	\$9.51	\$16.01
1992	1,964,500	4,730	28,700	75	97,700	\$8.30	\$13.60
1993	1,952,500	4,635	30,475	79	101,500	\$8.52	\$13.52
1994	2,054,500	4,275	27,250	106	95,400	\$8.20	\$12.70
1995	1,965,500	4,585	25,775	98	94,500	\$8.90	\$13.40
1996	1,975,000	4,990	25,550	96	87,150	\$9.40	\$13.80
1997	1,795,000	4,050	23,750	99	85,400	\$8.50	\$12.10
1998	1,755,500	4,035	23,100	91	87,500	\$8.60	\$12.10
1999	1,823,000	3,570	21,875	112	88,500	\$10.00	\$13.80
2000	1,708,000	4,045	22,350	103	84,550	\$11.20	\$14.90

Year	Fires	Civilian Deaths	Civilian Injuries	Firefighter Deaths	Firefighter Injuries	Direct Property Damage (in Billions)	
						As Reported	In 2012 Dollars
2001	1,734,500	61,963	211,004	4435	82,250	\$44.06	\$57.16
2002	1,687,500	3,380	18,425	98	80,800	\$10.30	\$13.10
2003	1,584,500	3,925	18,125	106	78,750	\$12.37	\$15.47
2004	1,550,500	3,900	17,875	104	75,840	\$9.80	\$11.90
2005	1,602,000	3,675	17,925	87	80,100	\$10.70	\$12.60
2006	1,642,500	3,245	16,400	89	83,400	\$11.30	\$12.90
2007	1,557,500	3,430	17,675	106	80,100	\$14.68	\$16.28
2008	1,451,500	3,320	16,705	105	79,700	\$15.59	\$16.69
2009	1,348,500	3,010	17,050	82	78,150	\$12.50	\$13.40
2010	1,331,500	3,120	17,720	73	71,875	\$11.60	\$12.20
2011	1,389,500	3,005	17,500	61	70,090	\$11.70	\$11.90
2012	1,375,000	2,855	16,500	64	69,400	\$12.40	\$12.40

Appendix B

Table 13 United States structure fire statistics

Year	Fires	Civilian Deaths	Civilian Injuries	Direct Property Damage (in Billions) <sup>1</sup>	
				As Reported	In 2012 Dollars
1977	1,098,000	6,505	26,310	\$4.10	\$15.50
1978	1,062,000	6,350	24,985	\$4.00	\$14.10
1979	1,036,500	5,970	24,850	\$5.00	\$15.80
1980	1,065,000	5,675	24,725	\$5.50	\$15.30
1981	1,027,500	5,760	25,700	\$6.00	\$15.10
1982	946,500	5,200	25,575	\$5.70	\$13.50
1983	868,500	5,090	26,150	\$5.80	\$13.30
1984	848,000	4,525	23,025	\$5.90	\$13.00
1985	859,500	5,265	23,350	\$6.40	\$13.60
1986	800,000	4,985	22,750	\$5.80	\$12.10
1987	758,000	4,880	23,815	\$6.20	\$12.50
1988	745,000	5,280	26,275	\$7.22	\$14.02
1989	688,000	4,655	24,025	\$7.53	\$13.93
1990	624,000	4,400	24,075	\$6.70	\$11.80
1991	640,500	3,765	24,975	\$8.34	\$14.04
1992	637,500	3,940	24,325	\$7.05	\$11.55
1993	621,500	3,980	26,550	\$7.46	\$11.86
1994	614,000	3,590	23,125	\$6.90	\$10.70
1995	573,500	39,857	21,725	\$7.60	\$11.40
1996	578,500	4,220	21,875	\$7.90	\$11.60
1997	552,000	3,510	20,375	\$7.10	\$10.10
1998	517,500	3,420	19,425	\$6.70	\$9.40
1999	523,000	3,040	18,525	\$8.50	\$11.70
2000	505,500	3,535	19,600	\$8.50	\$11.30
2001	521,500	3,220	17,225	\$8.90	\$11.50
2002	519,000	2,775	15,600	\$8.70	\$11.10
2003	519,500	33,859	15,600	\$8.71	\$10.91
2004	526,000	3,305	15,525	\$8.30	\$10.10
2005	511,000	3,105	15,325	\$9.20	\$10.80
2006	524,000	2,705	14,350	\$9.60	\$10.90
2007	530,500	3,000	15,350	\$10.61	\$11.71

				<b>Direct Property Damage (in Billions)<sup>1</sup></b>	
<b>Year</b>	<b>Fires</b>	<b>Civilian Deaths</b>	<b>Civilian Injuries</b>	<b>As Reported</b>	<b>In 2012 Dollars</b>
2008	515,000	2,900	14,960	\$12.41	\$13.21
2009	480,500	2,695	14,740	\$10.80	\$11.50
2010	482,000	2,755	15,420	\$9.70	\$10.20
2011	484,500	2,640	15,635	\$9.70	\$9.90
2012	480,500	2,470	14,700	\$9.80	\$9.80

## Appendix C

### Combined thermal analysis report for 40 – 45 – 50 - 55 kW·m<sup>-2</sup> (first set)

Report produced with the Fire Testing Technology ConeCalc software

page 1

## Cone Calorimeter Test Report

Laboratory name	FPST		
Operator	Roshan		
Sponsor			
Manufacturer			
Sample description	See individual reports		
Material name/ID	PE	Report name	See individual reports
Heat flux	See individual reports	Surface area	88.4 cm <sup>2</sup>
Orientation	Horizontal	Retainer frame used?	Yes

### Test averages

Test	t <sub>(ig)</sub> (s)	t <sub>(fo)</sub> (s)	t <sub>(end)</sub> (s)	HRR(peak) (kW/m <sup>2</sup> )	t <sub>peak</sub> (s)	THR (MJ/m <sup>2</sup> )	HRR(60) (kW/m <sup>2</sup> )	HRR(180) (kW/m <sup>2</sup> )	HRR(300) (kW/m <sup>2</sup> )
<b>Mean</b>	<b>53.3</b>	<b>250.5</b>	<b>341.3</b>	<b>605.55</b>	<b>161.3</b>	<b>102.66</b>	<b>315.03</b>	<b>455.22</b>	<b>256.72</b>
1	69	375	375	573.71	210	103.52	282.95	426.74	344.46
2	65	362	370	577.32	170	106.44	338.73	455.58	354.49
3	44		370	563.04	150	99.22	304.40	424.57	327.92
4	35	265	250	708.14	115	101.46	334.04	513.99	0.00

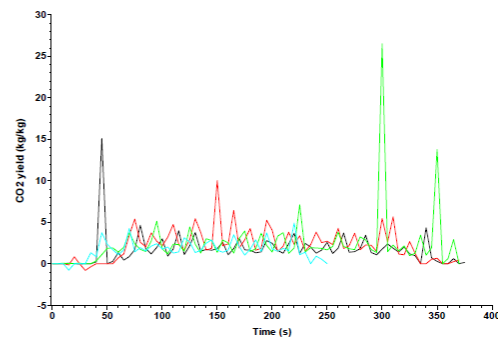
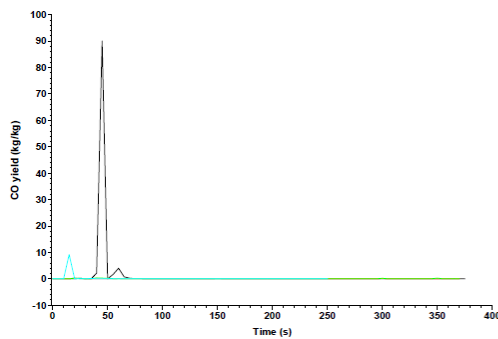
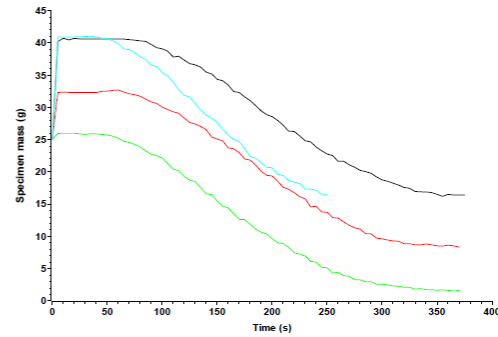
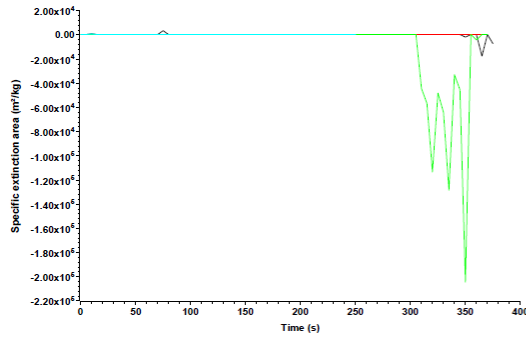
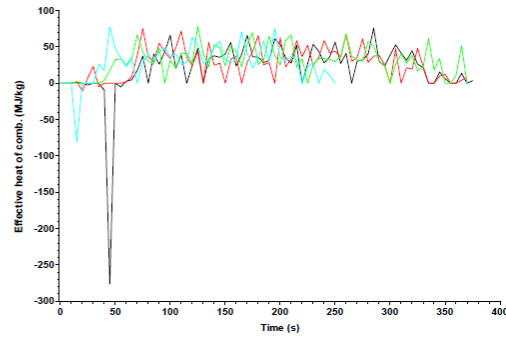
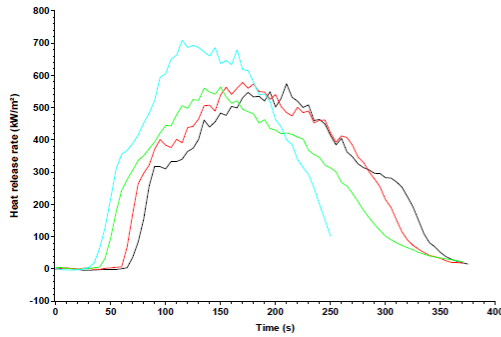
Test	Flux (kW/m <sup>2</sup> )	t (mm)	Area (cm <sup>2</sup> )	m(i) (g)	m(s) (g)	m(f) (g)	Δm (g/m <sup>2</sup> )	MLR(av) (g/s·m <sup>2</sup> )	$\dot{m}_{s,10-90}$ (g/s·m <sup>2</sup> )
<b>Mean</b>		<b>4.5</b>		<b>25.0</b>	<b>34.9</b>	<b>10.7</b>	<b>2739.8</b>	<b>9.75</b>	<b>12.90</b>
1	40	5	88.4	25.0	40.5	16.4	2732.0	8.94	11.50
2	45	5	88.4	25.0	32.4	8.3	2716.5	8.90	12.07
3	50	4	88.4	25.0	25.9	1.6	2742.1	8.40	12.19
4	55	4	88.4	25.0	41.0	16.5	2768.5	12.76	15.82

Test	THR(0-300) (MJ/m <sup>2</sup> )	THR(0-600) (MJ/m <sup>2</sup> )	THR(0-1200) (MJ/m <sup>2</sup> )	EHC(av) (MJ/kg)	SPR(av) (m <sup>2</sup> /s)	SEA(av) (m <sup>2</sup> /kg)	Fuel load (MJ/kg)	MARHE (kW/m <sup>2</sup> )
<b>Mean</b>	<b>72.54</b>	-	-	<b>37.52</b>	<b>0.0085</b>	<b>28.14</b>	<b>36.30</b>	<b>357.73</b>
1	93.86	-	-	37.98	0.0836	1059.75	36.61	313.86
2	101.62	-	-	39.18	0.0000	0.00	37.64	343.28
3	95.68	-	-	36.27	-0.1098	-1476.77	35.08	341.97
4	-	-	-	36.65	0.0603	529.58	35.88	431.83

Test	Date	Specimen #	Line colour	Filename
1	10/9/2014		—	C:\CC5\DATA\14090005.CSV
2	18/11/2014		—	C:\CC5\DATA\14110017.CSV
3	10/9/2014		—	C:\CC5\DATA\14090003.CSV
4	10/9/2014		—	C:\CC5\DATA\14090004.CSV

# Cone Calorimeter Test Report

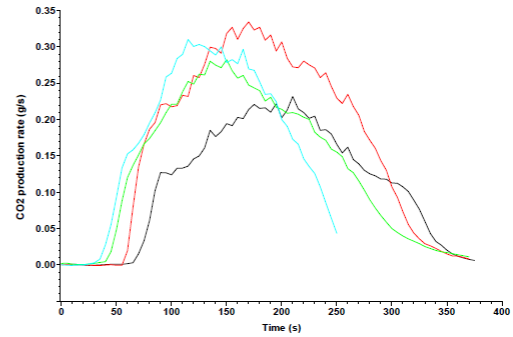
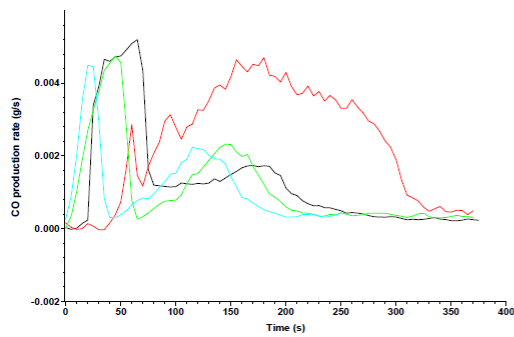
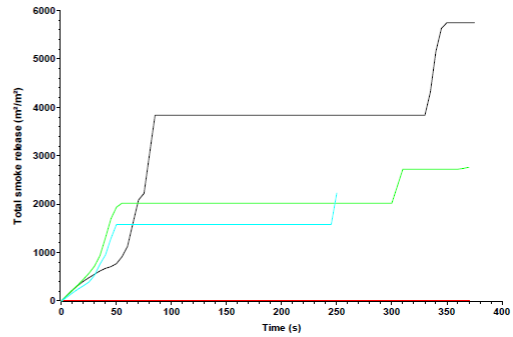
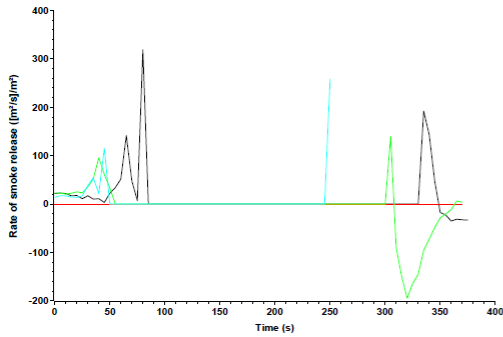
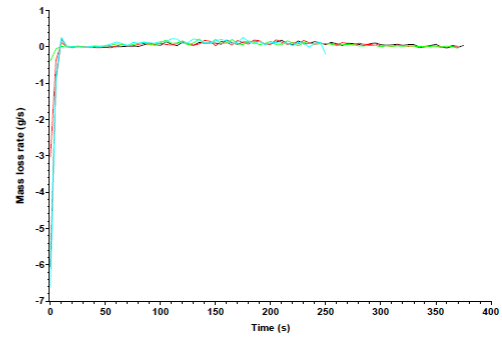
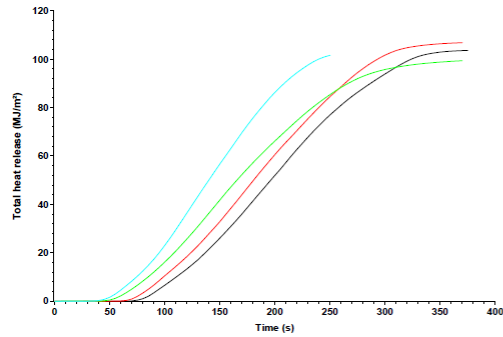
Laboratory name	FPST	Report name	See individual reports
Operator	Roshan	Surface area	88.4 cm <sup>2</sup>
Sponsor		Retainer frame used?	Yes
Manufacturer			
Sample description	See individual reports		
Material name/ID	PE		
Heat flux	See individual reports		
Orientation	Horizontal		



The test results relate to the behaviour of the test specimens of a product under the particular conditions of the test; they are not intended to be the sole criterion for assessing the potential fire hazard of the product in use.

# Cone Calorimeter Test Report

Laboratory name	FPST	Report name	See individual reports
Operator	Roshan	Surface area	88.4 cm <sup>2</sup>
Sponsor		Retainer frame used?	Yes
Manufacturer			
Sample description	See individual reports		
Material name/ID	PE		
Heat flux	See individual reports		
Orientation	Horizontal		

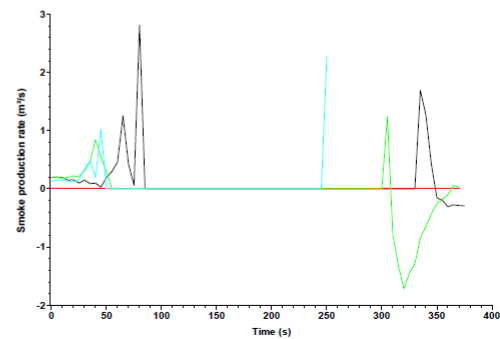
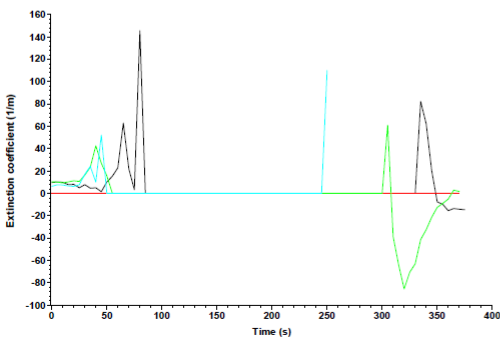
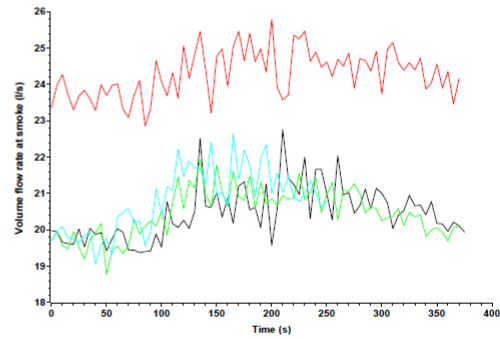
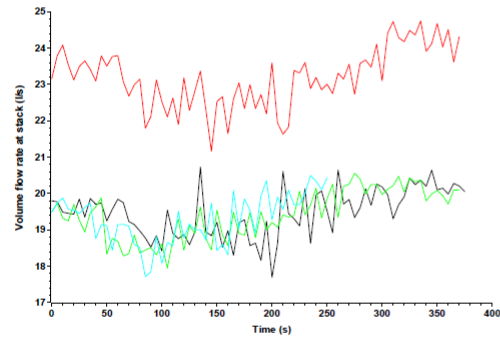
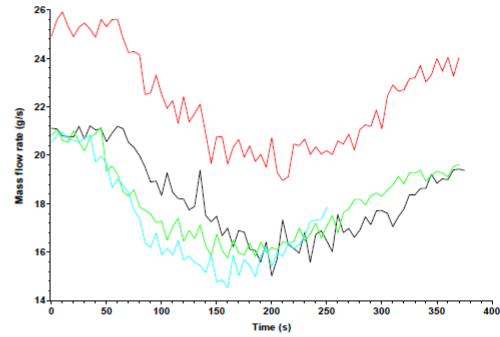
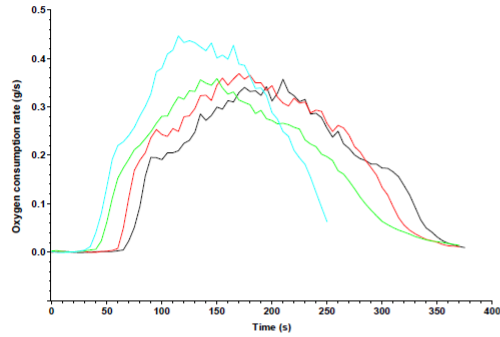


The test results relate to the behaviour of the test specimens of a product under the particular conditions of the test; they are not intended to be the sole criterion for assessing the potential fire hazard of the product in use.



# Cone Calorimeter Test Report

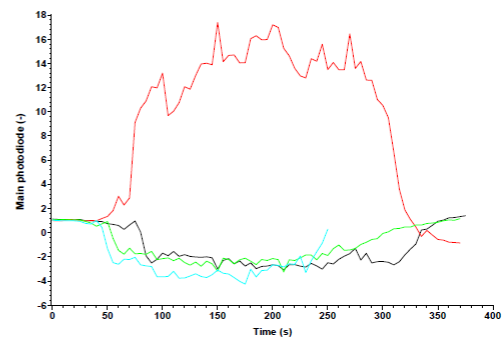
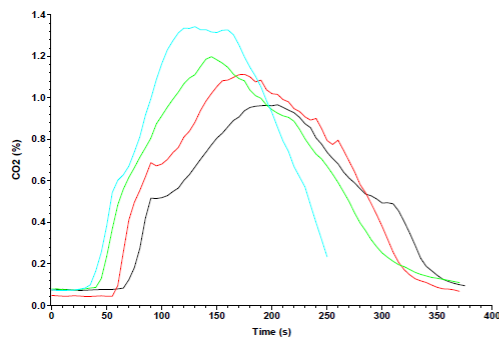
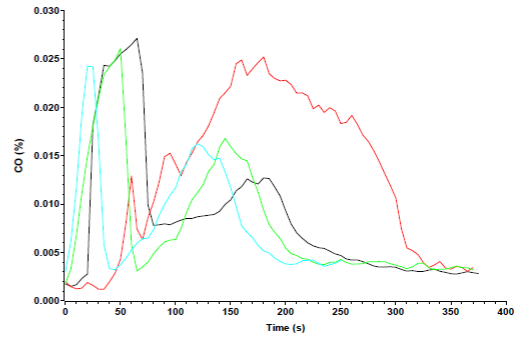
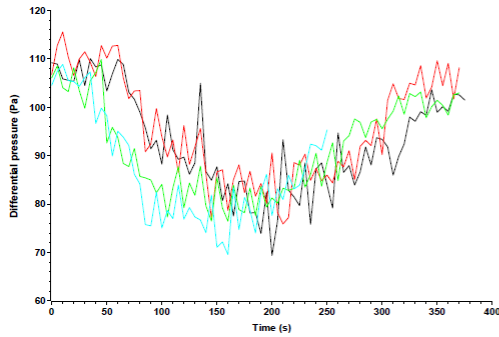
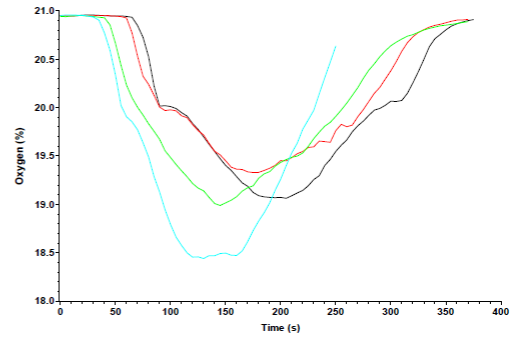
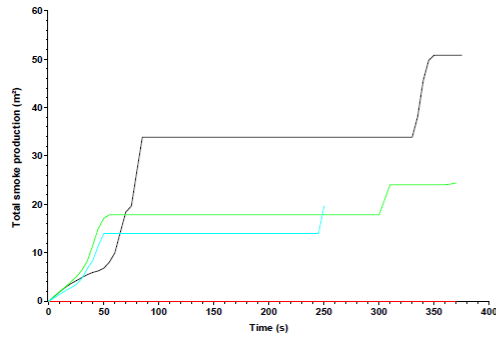
Laboratory name	FPST	Report name	See individual reports
Operator	Roshan	Surface area	88.4 cm <sup>2</sup>
Sponsor		Retainer frame used?	Yes
Manufacturer			
Sample description	See individual reports		
Material name/ID	PE		
Heat flux	See individual reports		
Orientation	Horizontal		



The test results relate to the behaviour of the test specimens of a product under the particular conditions of the test; they are not intended to be the sole criterion for assessing the potential fire hazard of the product in use.

# Cone Calorimeter Test Report

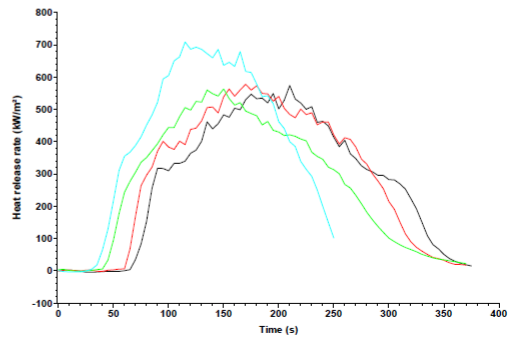
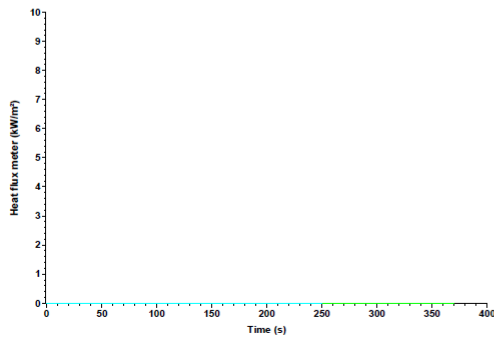
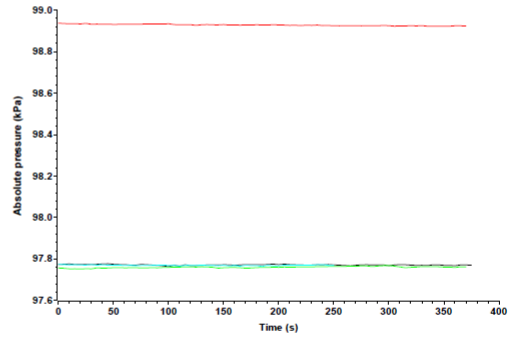
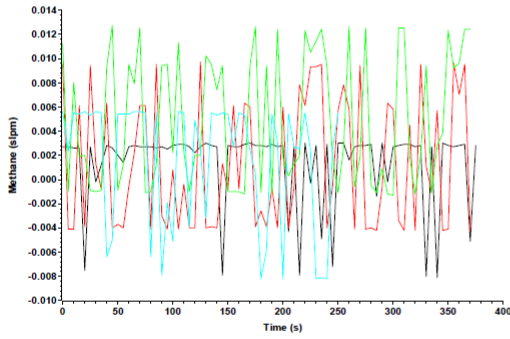
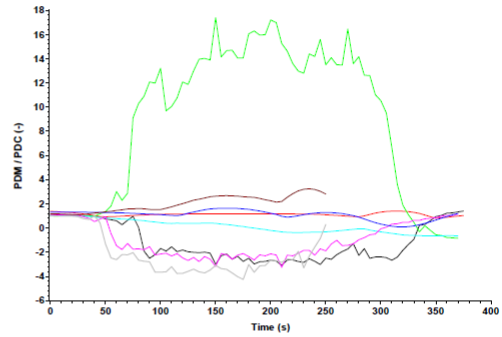
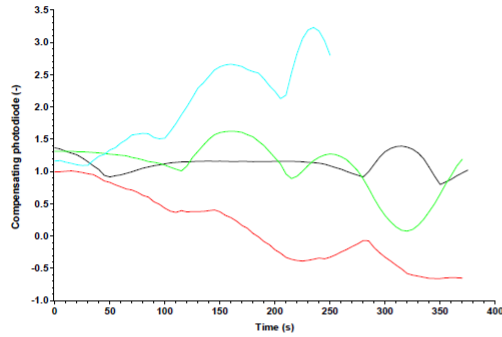
Laboratory name	FPST	Report name	See individual reports
Operator	Roshan	Surface area	88.4 cm <sup>2</sup>
Sponsor		Retainer frame used?	Yes
Manufacturer			
Sample description	See individual reports		
Material name/ID	PE		
Heat flux	See individual reports		
Orientation	Horizontal		



The test results relate to the behaviour of the test specimens of a product under the particular conditions of the test; they are not intended to be the sole criterion for assessing the potential fire hazard of the product in use.

# Cone Calorimeter Test Report

Laboratory name	FPST	Report name	See individual reports
Operator	Roshan	Surface area	88.4 cm <sup>2</sup>
Sponsor		Retainer frame used?	Yes
Manufacturer			
Sample description	See individual reports		
Material name/ID	PE		
Heat flux	See individual reports		
Orientation	Horizontal		



The test results relate to the behaviour of the test specimens of a product under the particular conditions of the test; they are not intended to be the sole criterion for assessing the potential fire hazard of the product in use.

## Appendix D

### Combined thermal analysis report for 40 – 45 – 50 - 55 kW·m<sup>-2</sup> (second set)

Report produced with the Fire Testing Technology ConeCalc software

page 1

## Cone Calorimeter Test Report

Laboratory name	FPST		
Operator	Roshan		
Sponsor			
Manufacturer			
Sample description	PE		
Material name/ID	PE	Report name	See individual reports
Heat flux	See individual reports	Surface area	88.4 cm <sup>2</sup>
Orientation	Horizontal	Retainer frame used?	Yes

### Test averages

Test	t(ig) (s)	t(fo) (s)	t(end) (s)	HRR(peak) (kW/m <sup>2</sup> )	tpeak (s)	THR (MJ/m <sup>2</sup> )	HRR(60) (kW/m <sup>2</sup> )	HRR(180) (kW/m <sup>2</sup> )	HRR(300) (kW/m <sup>2</sup> )
<b>Mean</b>	<b>56</b>	<b>323.5</b>	<b>326.3</b>	<b>724.45</b>	<b>148.8</b>	<b>113.83</b>	<b>351.72</b>	<b>529.99</b>	<b>81.52</b>
1	76	426	470	508.07	170	101.26	290.36	398.06	326.07
2	64	325	325	703.30	150	117.12	383.51	537.41	0.00
3	50	303	290	710.88	155	117.78	350.47	530.18	0.00
4	34	240	220	975.53	120	119.16	382.54	654.31	0.00

Test	Flux (kW/m <sup>2</sup> )	t (mm)	Area (cm <sup>2</sup> )	m(i) (g)	m(s) (g)	m(f) (g)	Δm (g/m <sup>2</sup> )	MLR(av) (g/s·m <sup>2</sup> )	$\dot{m}_{4,10-90}$ (g/s·m <sup>2</sup> )
<b>Mean</b>	<b>5</b>	<b>5</b>	<b>88.4</b>	<b>25.0</b>	<b>30.9</b>	<b>6.7</b>	<b>2738.3</b>	<b>10.90</b>	<b>14.09</b>
1	40	5	88.4	25.0	24.6	0.0	2781.3	7.05	11.13
2	45	5	88.4	25.0	24.8	1.3	2662.8	10.18	11.83
3	50	5	88.4	25.0	49.3	25.0	2749.2	11.43	14.19
4	55	5	88.4	25.0	25.0	0.6	2759.9	14.95	19.20

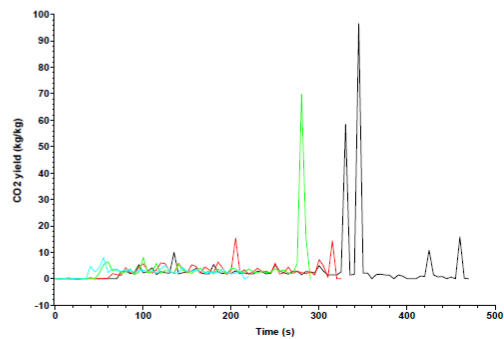
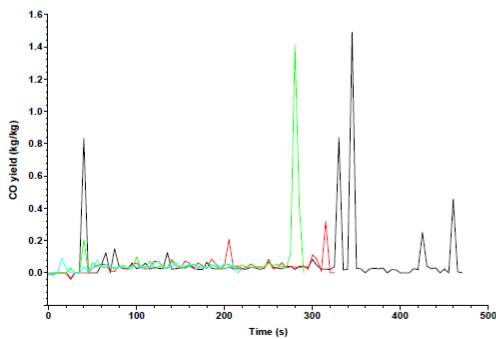
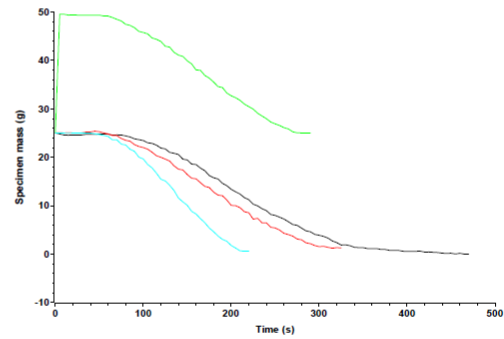
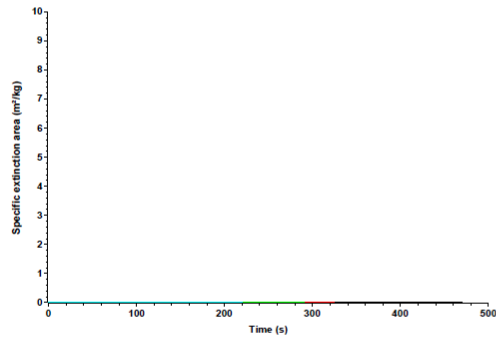
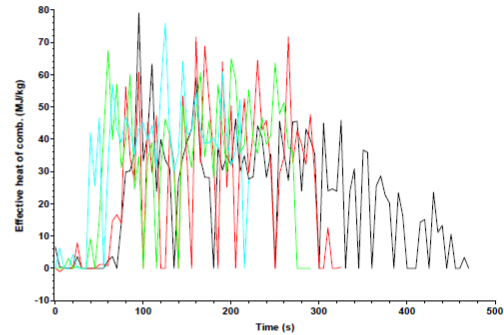
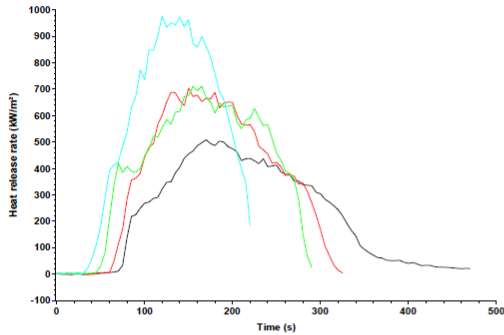
Test	THR(0-300) (MJ/m <sup>2</sup> )	THR(0-600) (MJ/m <sup>2</sup> )	THR(0-1200) (MJ/m <sup>2</sup> )	EHC(av) (MJ/kg)	SPR(av) (m <sup>2</sup> /s)	SEA(av) (m <sup>2</sup> /kg)	Fuel load (MJ/kg)	MARHE (kW/m <sup>2</sup> )
<b>Mean</b>	<b>-</b>	<b>-</b>	<b>-</b>	<b>41.78</b>	<b>0.0000</b>	<b>0.00</b>	<b>40.25</b>	<b>416.83</b>
1	86.08	-	-	36.54	0.0000	0.00	35.80	287.06
2	115.65	-	-	44.56	0.0000	0.00	41.41	396.69
3	-	-	-	42.84	0.0000	0.00	41.65	426.31
4	-	-	-	43.18	0.0000	0.00	42.14	557.25

Test	Date	Specimen #	Line colour	Filename
1	18/11/2014		—	C:\CC5\DATA\14110015.CSV
2	18/11/2014		—	C:\CC5\DATA\14110018.CSV
3	18/11/2014		—	C:\CC5\DATA\14110020.CSV
4	18/11/2014		—	C:\CC5\DATA\14110022.CSV

The test results relate to the behaviour of the test specimens of a product under the particular conditions of the test; they are not intended to be the sole criterion for assessing the potential fire hazard of the product in use.

# Cone Calorimeter Test Report

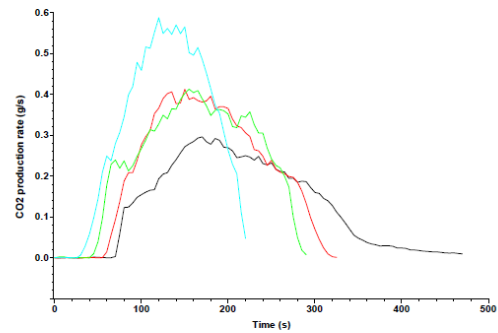
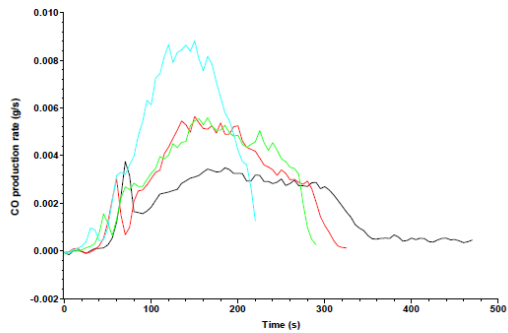
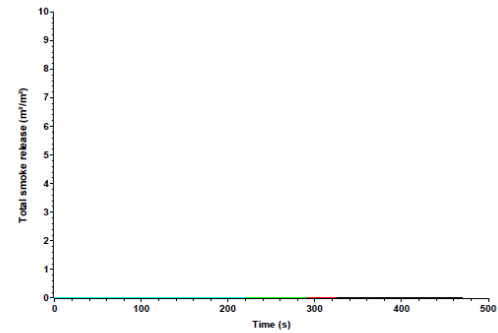
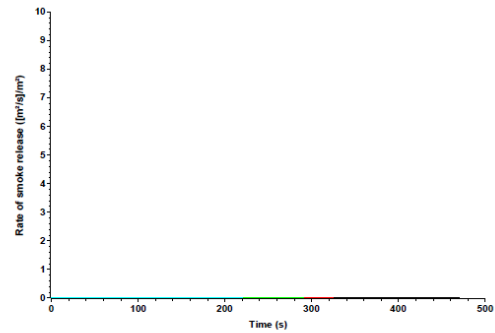
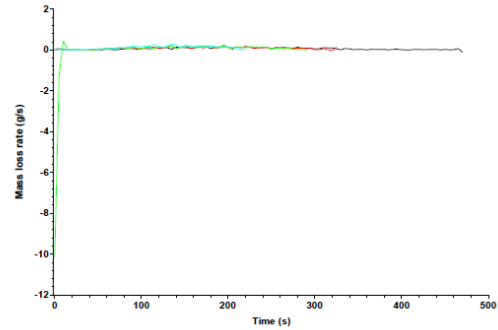
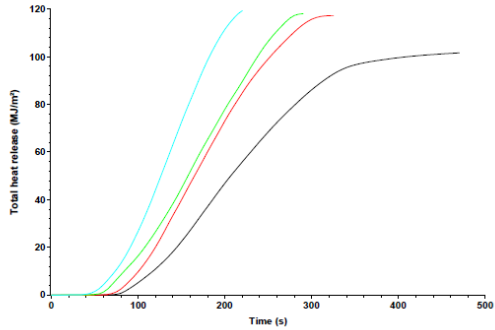
Laboratory name	FPST	Report name	See individual reports
Operator	Roshan	Surface area	88.4 cm <sup>2</sup>
Sponsor		Retainer frame used?	Yes
Manufacturer			
Sample description	PE		
Material name/ID	PE		
Heat flux	See individual reports		
Orientation	Horizontal		



The test results relate to the behaviour of the test specimens of a product under the particular conditions of the test; they are not intended to be the sole criterion for assessing the potential fire hazard of the product in use.

# Cone Calorimeter Test Report

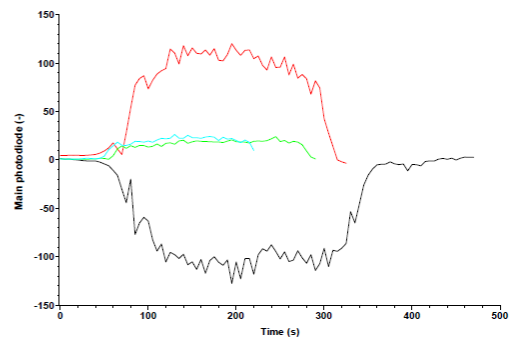
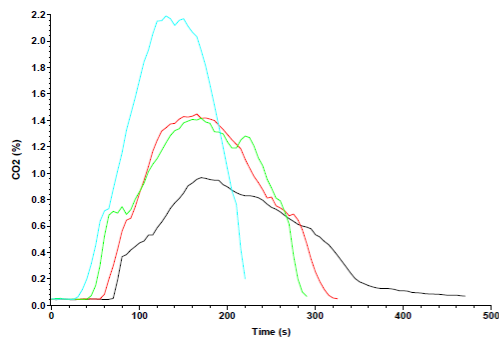
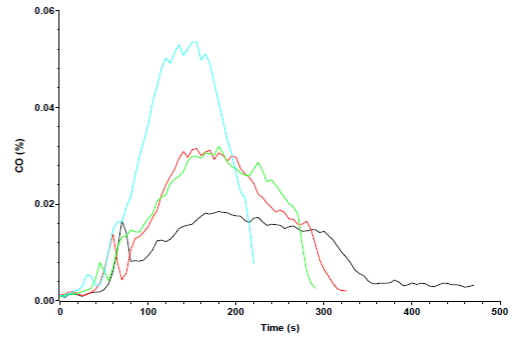
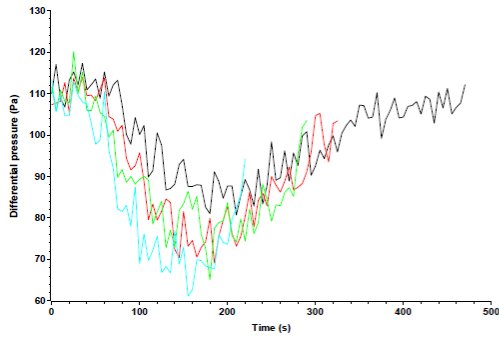
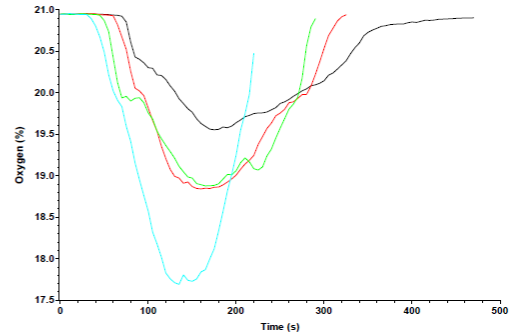
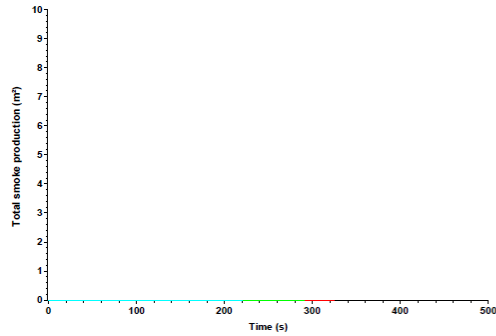
Laboratory name	FPST	Report name	See individual reports
Operator	Roshan	Surface area	88.4 cm <sup>2</sup>
Sponsor		Retainer frame used?	Yes
Manufacturer			
Sample description	PE		
Material name/ID	PE		
Heat flux	See individual reports		
Orientation	Horizontal		



The test results relate to the behaviour of the test specimens of a product under the particular conditions of the test; they are not intended to be the sole criterion for assessing the potential fire hazard of the product in use.

# Cone Calorimeter Test Report

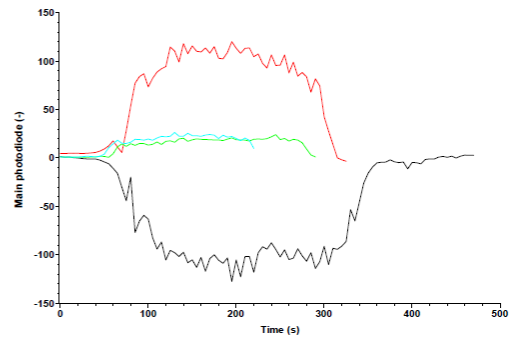
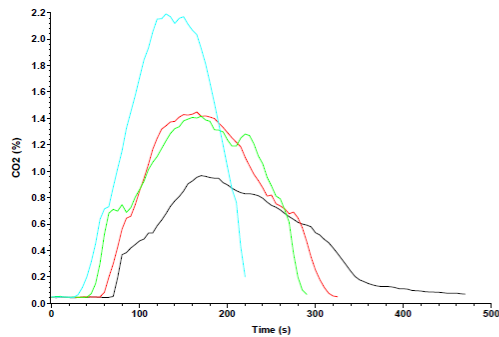
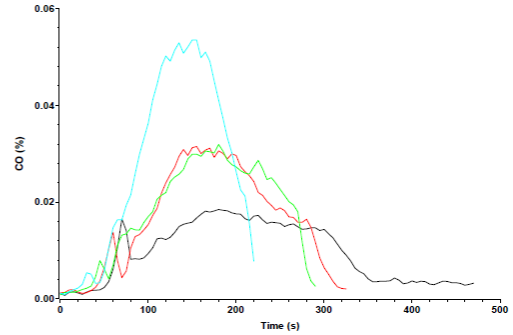
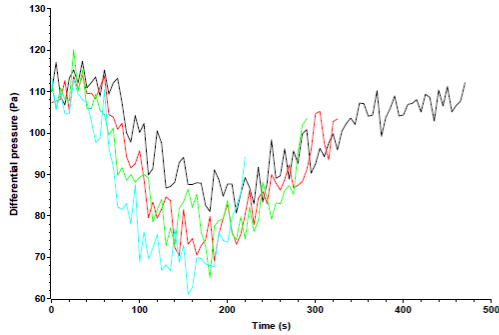
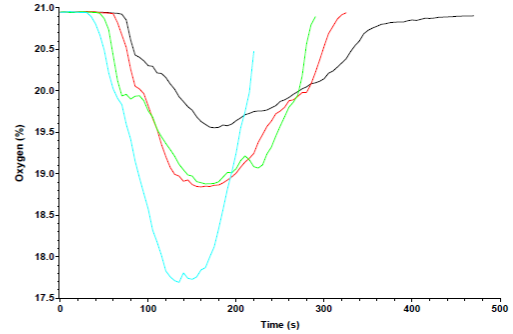
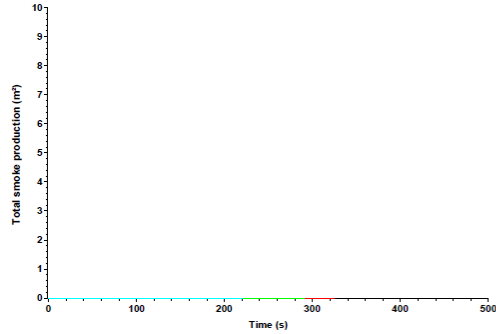
Laboratory name	FPST	Report name	See individual reports
Operator	Roshan	Surface area	88.4 cm <sup>2</sup>
Sponsor		Retainer frame used?	Yes
Manufacturer			
Sample description	PE		
Material name/ID	PE		
Heat flux	See individual reports		
Orientation	Horizontal		



The test results relate to the behaviour of the test specimens of a product under the particular conditions of the test; they are not intended to be the sole criterion for assessing the potential fire hazard of the product in use.

# Cone Calorimeter Test Report

Laboratory name	FPST	Report name	See individual reports
Operator	Roshan	Surface area	88.4 cm <sup>2</sup>
Sponsor		Retainer frame used?	Yes
Manufacturer			
Sample description	PE		
Material name/ID	PE		
Heat flux	See individual reports		
Orientation	Horizontal		

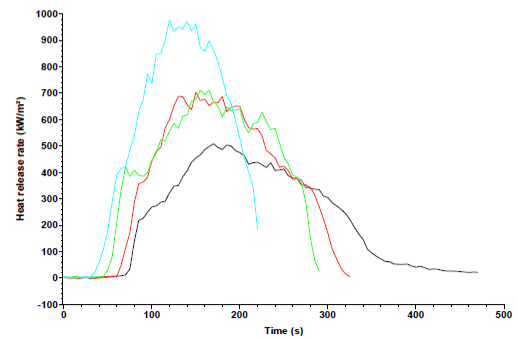
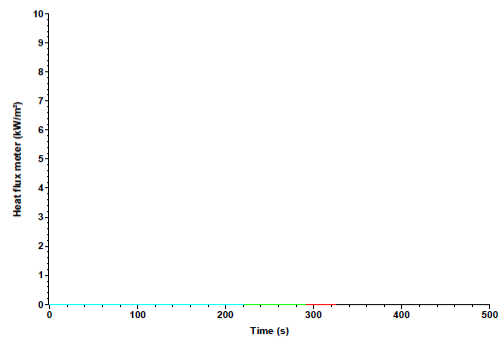
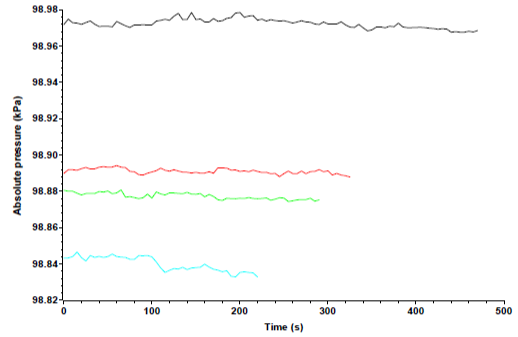
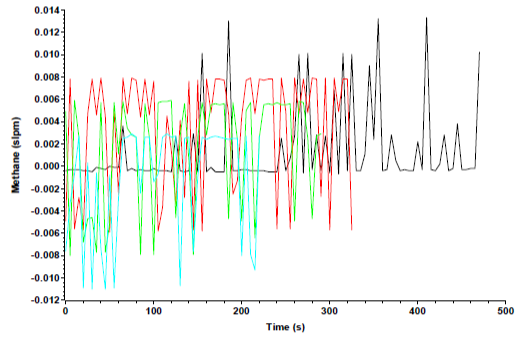
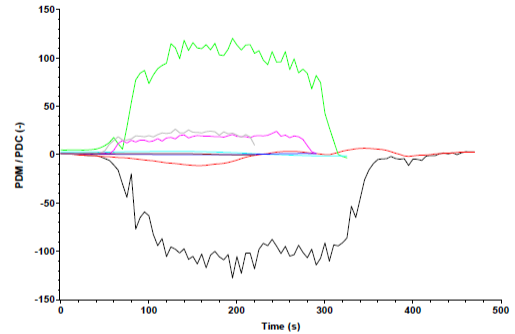
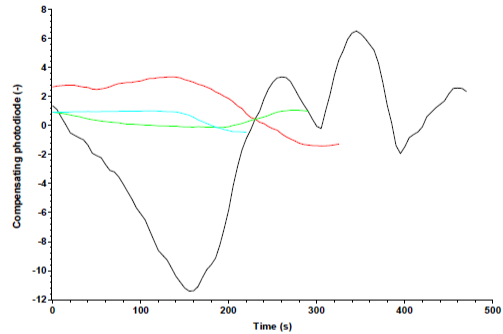


The test results relate to the behaviour of the test specimens of a product under the particular conditions of the test; they are not intended to be the sole criterion for assessing the potential fire hazard of the product in use.



# Cone Calorimeter Test Report

Laboratory name	FPST	Report name	See individual reports
Operator	Roshan	Surface area	88,4 cm <sup>2</sup>
Sponsor		Retainer frame used?	Yes
Manufacturer			
Sample description	PE		
Material name/ID	PE		
Heat flux	See individual reports		
Orientation	Horizontal		



The test results relate to the behaviour of the test specimens of a product under the particular conditions of the test; they are not intended to be the sole criterion for assessing the potential fire hazard of the product in use.

## Appendix E

### Combined thermal analysis report for 40 – 45 – 50 - 55 kW·m<sup>-2</sup> (third set)

Report produced with the Fire Testing Technology ConeCalc software

page 1

## Cone Calorimeter Test Report





Laboratory name	FPST		
Operator	Roshan		
Sponsor			
Manufacturer			
Sample description	PE		
Material name/ID	PE	Report name	See individual reports
Heat flux	See individual reports	Surface area	88.4 cm <sup>2</sup>
Orientation	Horizontal	Retainer frame used?	Yes

### Test averages

Test	t(ig) (s)	t(fo) (s)	t(end) (s)	HRR(peak) (kW/m <sup>2</sup> )	tpeak (s)	THR (MJ/m <sup>2</sup> )	HRR(60) (kW/m <sup>2</sup> )	HRR(180) (kW/m <sup>2</sup> )	HRR(300) (kW/m <sup>2</sup> )
<b>Mean</b>	<b>55.5</b>	<b>327.5</b>	<b>331.3</b>	<b>710.02</b>	<b>161.3</b>	<b>117.41</b>	<b>371.34</b>	<b>527.76</b>	<b>92.60</b>
1	72	463	505	500.69	185	118.51	299.38	400.68	370.41
2	62	294	285	724.54	215	116.79	369.12	556.70	0.00
3	51	312	305	649.35	130	117.42	374.73	519.39	0.00
4	37	241	230	965.50	115	116.92	442.13	634.27	0.00

Test	Flux (kW/m <sup>2</sup> )	t (mm)	Area (cm <sup>2</sup> )	m(i) (g)	m(s) (g)	m(f) (g)	Δm (g/m <sup>2</sup> )	MLR(av) (g/s·m <sup>2</sup> )	$\dot{m}_{t,10-90}$ (g/s·m <sup>2</sup> )
<b>Mean</b>		<b>5</b>		<b>25.0</b>	<b>37.2</b>	<b>12.6</b>	<b>2785.8</b>	<b>11.21</b>	<b>14.29</b>
1	40	5	88.4	25.0	24.7	0.1	2779.1	6.49	9.26
2	45	5	88.4	25.0	49.7	25.0	2788.6	12.67	15.39
3	50	5	88.4	25.0	49.8	25.0	2801.7	11.14	14.01
4	55	5	88.4	25.0	24.8	0.3	2774.0	14.53	18.49

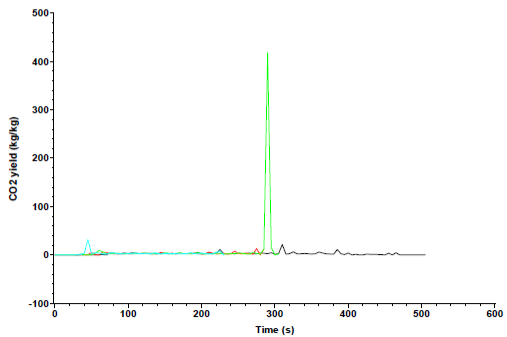
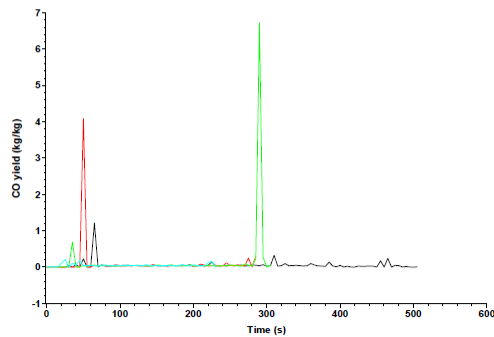
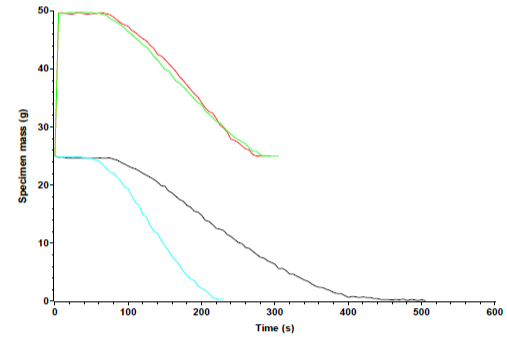
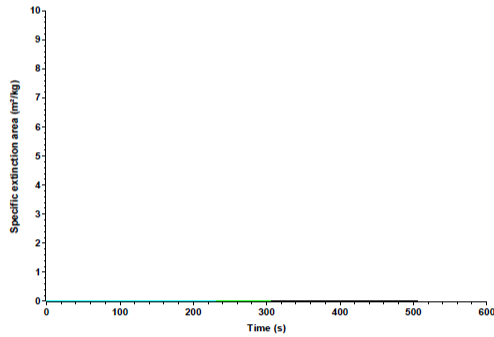
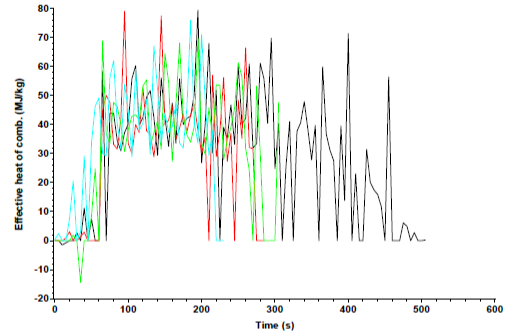
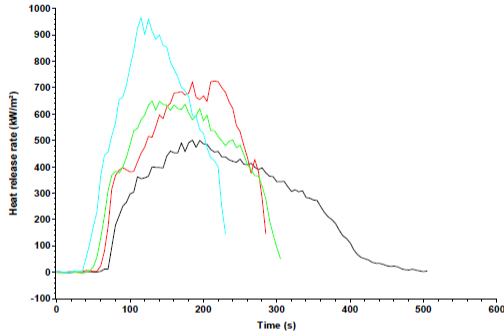
Test	THR(0-300) (MJ/m <sup>2</sup> )	THR(0-600) (MJ/m <sup>2</sup> )	THR(0-1200) (MJ/m <sup>2</sup> )	EHC(av) (MJ/kg)	SPR(av) (m <sup>2</sup> /s)	SEA(av) (m <sup>2</sup> /kg)	Fuel load (MJ/kg)	MARHE (kW/m <sup>2</sup> )
<b>Mean</b>	-	-	-	<b>42.20</b>	<b>0.0000</b>	<b>0.00</b>	<b>41.52</b>	<b>413.00</b>
1	89.99	-	-	42.53	0.0000	0.00	41.91	302.40
2	-	-	-	41.79	0.0000	0.00	41.30	416.29
3	117.16	-	-	42.16	0.0000	0.00	41.52	406.01
4	-	-	-	42.31	0.0000	0.00	41.34	527.28

Test	Date	Specimen #	Line colour	Filename
1	18/11/2014			C:\CC5\DATA\14110016.CSV
2	18/11/2014			C:\CC5\DATA\14110019.CSV
3	18/11/2014			C:\CC5\DATA\14110021.CSV
4	18/11/2014			C:\CC5\DATA\14110023.CSV

The test results relate to the behaviour of the test specimens of a product under the particular conditions of the test; they are not intended to be the sole criterion for assessing the potential fire hazard of the product in use.

# Cone Calorimeter Test Report

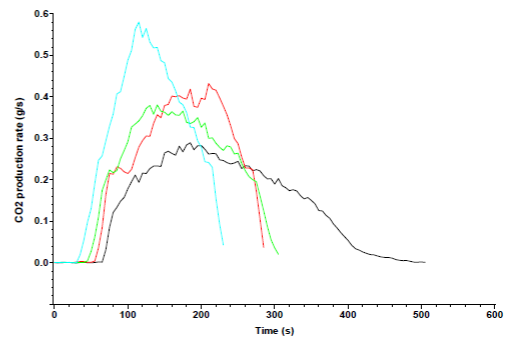
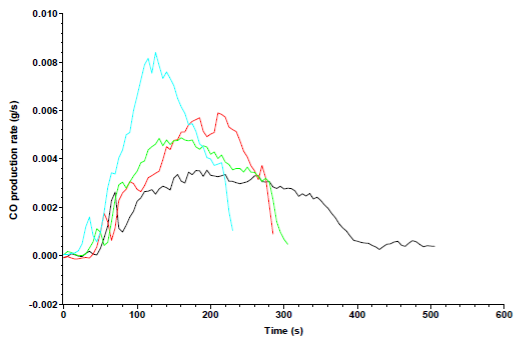
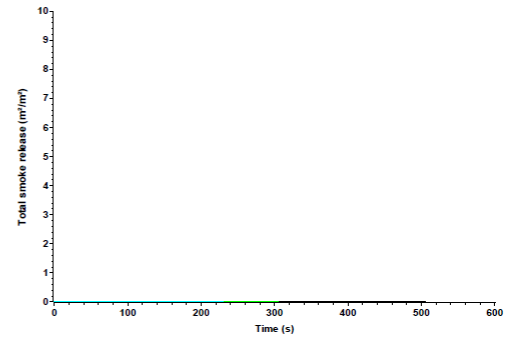
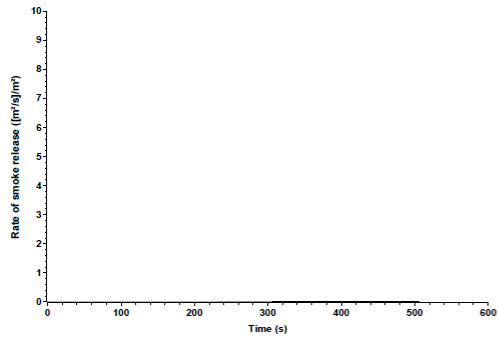
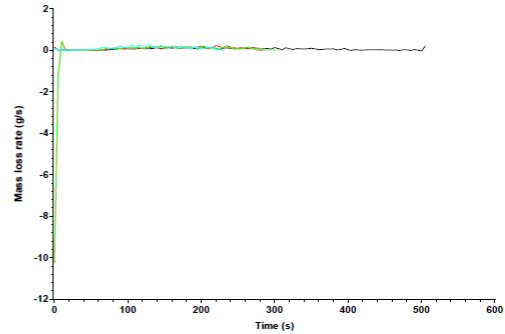
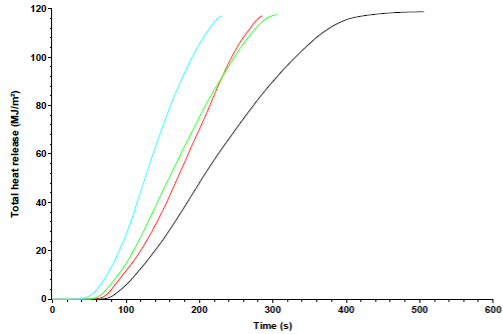
Laboratory name	FPST	Report name	See individual reports
Operator	Roshan	Surface area	88.4 cm <sup>2</sup>
Sponsor		Retainer frame used?	Yes
Manufacturer			
Sample description	PE		
Material name/ID	PE		
Heat flux	See individual reports		
Orientation	Horizontal		



The test results relate to the behaviour of the test specimens of a product under the particular conditions of the test; they are not intended to be the sole criterion for assessing the potential fire hazard of the product in use.

# Cone Calorimeter Test Report

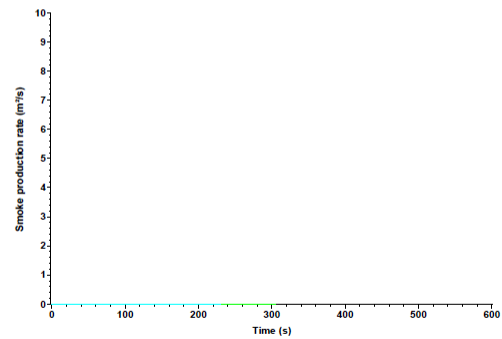
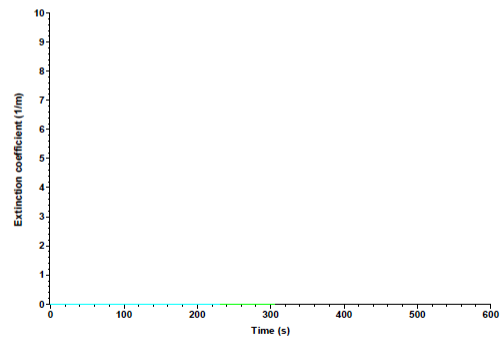
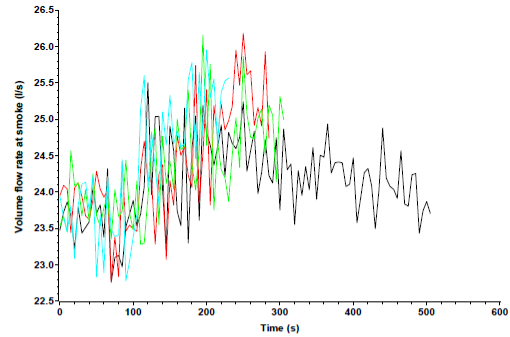
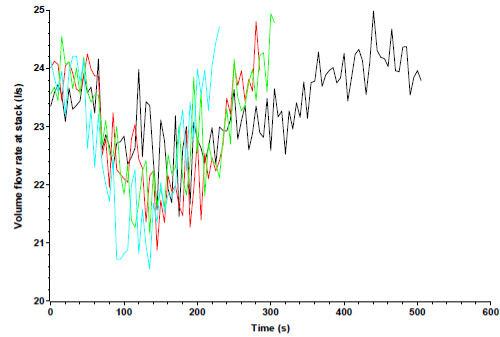
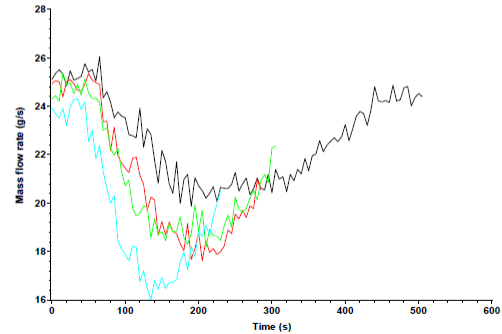
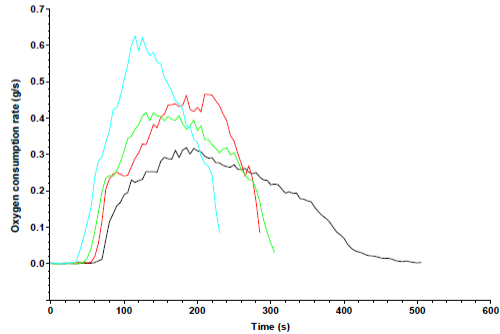
Laboratory name	FPST	Report name	See individual reports
Operator	Roshan	Surface area	88.4 cm <sup>2</sup>
Sponsor		Retainer frame used?	Yes
Manufacturer			
Sample description	PE		
Material name/ID	PE		
Heat flux	See individual reports		
Orientation	Horizontal		



The test results relate to the behaviour of the test specimens of a product under the particular conditions of the test; they are not intended to be the sole criterion for assessing the potential fire hazard of the product in use.

# Cone Calorimeter Test Report

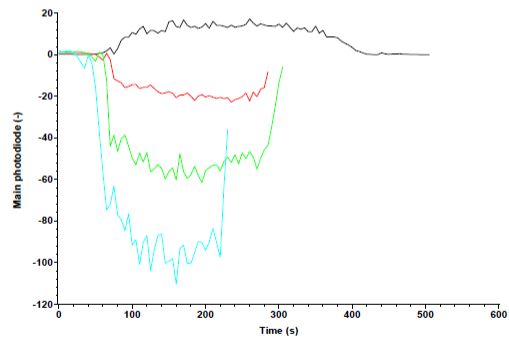
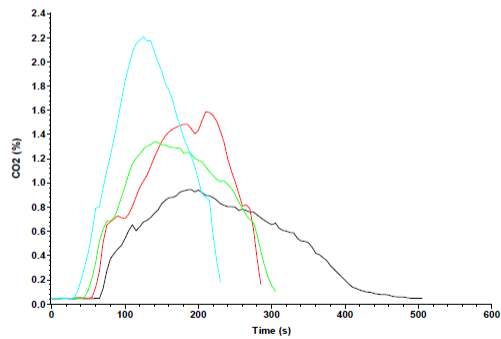
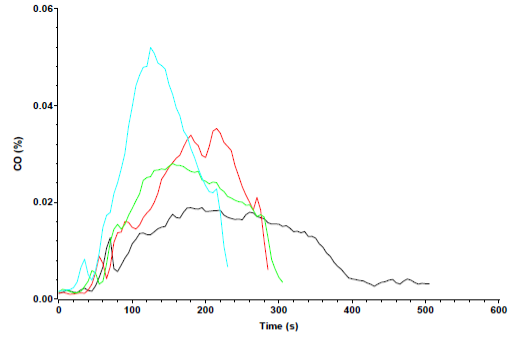
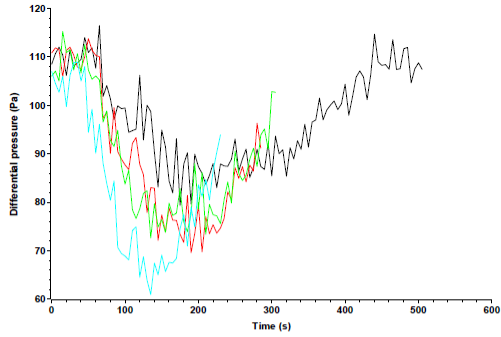
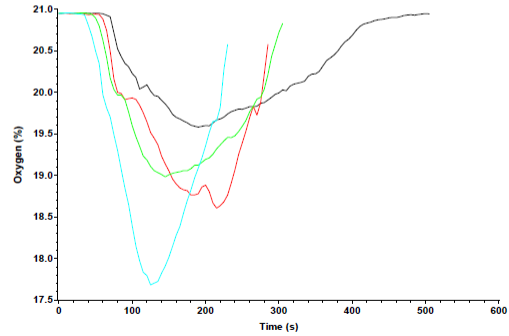
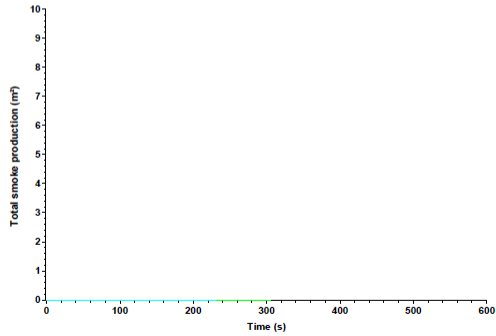
Laboratory name	FPST	Report name	See individual reports
Operator	Roshan	Surface area	88,4 cm <sup>2</sup>
Sponsor		Retainer frame used?	Yes
Manufacturer			
Sample description	PE		
Material name/ID	PE		
Heat flux	See individual reports		
Orientation	Horizontal		



The test results relate to the behaviour of the test specimens of a product under the particular conditions of the test; they are not intended to be the sole criterion for assessing the potential fire hazard of the product in use.

# Cone Calorimeter Test Report

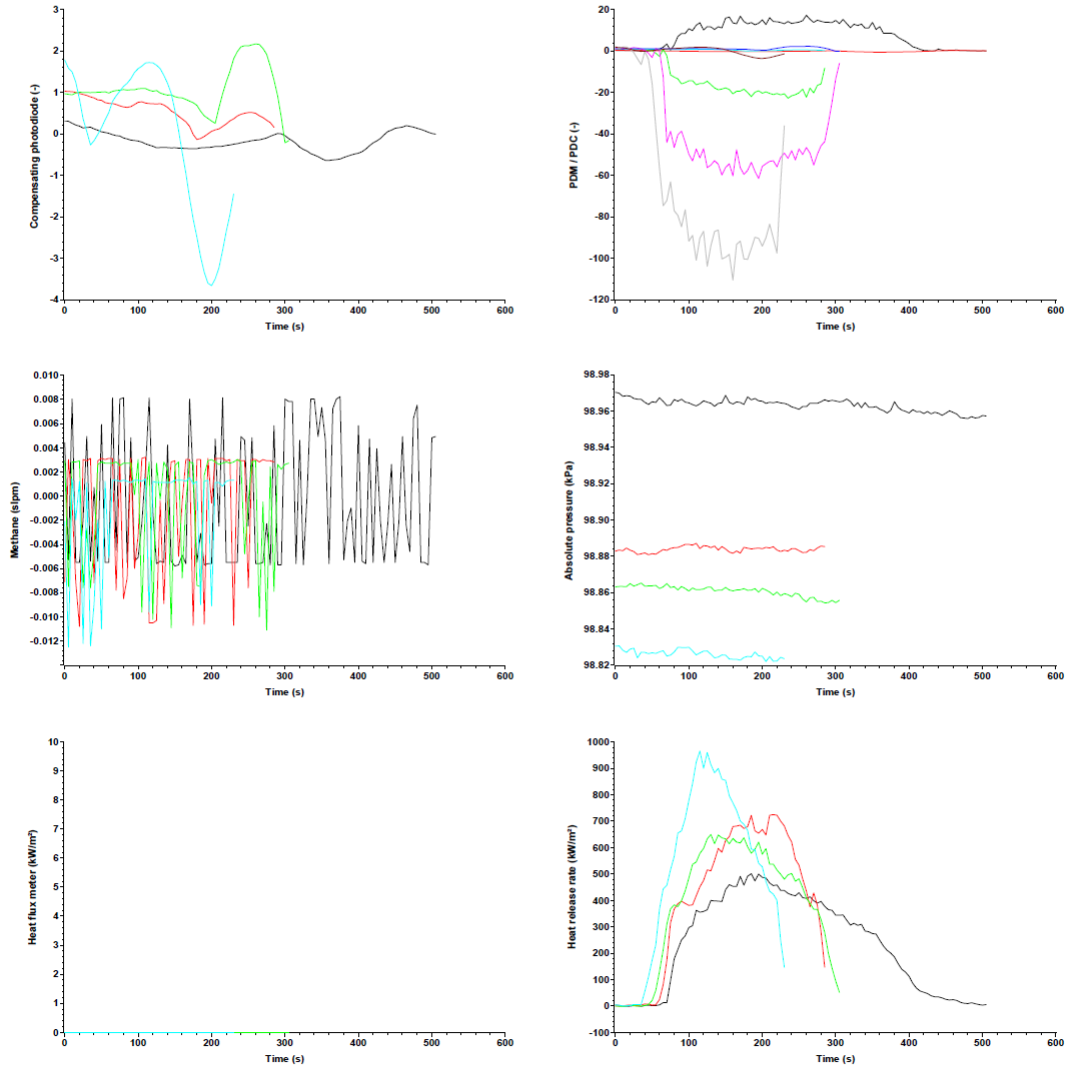
Laboratory name	FPST	Report name	See individual reports
Operator	Roshan	Surface area	88,4 cm <sup>2</sup>
Sponsor		Retainer frame used?	Yes
Manufacturer			
Sample description	PE		
Material name/ID	PE		
Heat flux	See individual reports		
Orientation	Horizontal		



The test results relate to the behaviour of the test specimens of a product under the particular conditions of the test; they are not intended to be the sole criterion for assessing the potential fire hazard of the product in use.

# Cone Calorimeter Test Report

Laboratory name	FPST	Report name	See individual reports
Operator	Roshan	Surface area	88.4 cm <sup>2</sup>
Sponsor		Retainer frame used?	Yes
Manufacturer			
Sample description	PE		
Material name/ID	PE		
Heat flux	See individual reports		
Orientation	Horizontal		



The test results relate to the behaviour of the test specimens of a product under the particular conditions of the test; they are not intended to be the sole criterion for assessing the potential fire hazard of the product in use.

## Appendix F

Cone calorimeter standard operating procedure from Fire Testing Technology Ltd.

- These steps are for the FTT Cone Calorimeter with Xentra gas analyzer (for oxygen, carbon dioxide and carbon monoxide), laser smoke system and operated in the “non-scrubbed” mode and the ConeCalc 5 software.
- The steps below are based on the assumption that the cone calorimeter has been shut down in the prescribed manner the previous day and that no problems were noted in any of the equipment. If the unexpected does occur, some troubleshooting and corrective action will be necessary.
- Note: Several calibrations are required each day prior to testing. These are integrated into section A of this Standard Operating Procedure (SOP).

The setup procedure can be split into the following routines

### F.1 Close cold trap tap

Remove the beaker from under the Cold Trap and close the Cold Trap tap. (This assumes that the cold trap tap has been left open as instructed in the Shutdown procedure – see Section C.)

### F.2 Turn system ON

- Turn on the computer and monitor (printer, if required).
- Ensure that the data logger is switch on and then start the software program by running the ConeCalc 5 icon on the desktop or in Start\Programs\FTT Applications
- Check that the power to all of the following is on (or turn each one on, in case they are not):
  - a) Analyzers must be on.
  - b) Laser (or Smoke) power must be on.



Note: The laser and analyzers takes several hours to warm up. They should be left on permanently.

- c) Cold Trap refrigerator must be on.
- d) Mass Loss Calorimeter Power must be on.
- e) Cone power must be on. Check that the set point temperature is 0°C. Use the ▼ button if necessary.
- f) Load Cell must be on.

Note: Overall main power should remain on permanently under normal conditions, except for repairs or long down periods (such as site shutdowns). This supplies power to the following devices: methane flowmeter, differential pressure transducer and oxygen analyzer.

### F.3 Check filters and drying agents

Check that the drying agent (drierite) is in good condition. Change if necessary. Check that the primary Balston filter and the secondary Hepa Vent are clean. Change if necessary.

### F.4 Set duct flow

- Check that the duct Fan, sample Pump and room extraction are switched off.
- In the software, select Calibrations|DPT & Flow. Ensure that the exhaust control is switched off (this closes the ports on the differential pressure transducer) and then press the Zero button. Then press OK to record the zero point of the DPT calibration.
- Switch the duct exhaust control on and switch the room extraction on. Enter 24 L·s<sup>-1</sup> as the required flow rate and press OK. Adjust the speed control to set the Volume Flow Rate to the required level (24 L·s<sup>-1</sup>). When 15 consecutive readings within 2 L·s<sup>-1</sup> of the required flow have been measured then the software will tell you that the flow is correctly set. Then press OK to return to the Calibrations panel.

## F.5 Calibrate smoke system

- a) Place the “smoke zero blank” between the laser and the compensating photodiode (next to the laser).
- b) Select the software routine: Calibrations|Smoke and then press the Zero button. (Check that the Calibrated Main and Compensating signals [PDM(-) and PDC(-)] are 0.000.)
- c) Remove the smoke zero blank and ensure that the blank slot and filter slot is covered.
- d) Press the Balance button to adjust the input values of each of the photodiodes to give a normalised ratio of 1.000 (this is in the PDC(-) and PDM(-) displays). If not then press the Balance button again.
- e) Then press the OK button.

[Additionally you may perform a secondary smoke system calibration as follows

- e1) Then press the Filter Calibration button.
- e2) Place the ND 0.3 filter in the main slot (at the front of the Cone, above the control panel) and ensure that this filter is selected using the radio buttons. Also check that the correct value of the filter is entered in the text box.
- e3) Then press Start. Wait 60 s for the data to be collected.
- e4) Check that the Optical Density Correction Factor is between 0.95 and 1.05. Then press OK. If not within these limits, then check that the filter is in position correctly and that the correct filter is selected in the software and that the same filter value is on the computer screen and repeat the routine again.
- e5) Remove the filter and turn the filter cover to stop any light hitting the photodiode.]

## F.6 Calibrate gas analyzers

- Turn on the sample pump and check for leaks or blockages. Ensure that the pressure to the analyzer is 5 psi on the gauge inside the rack (the flow to the oxygen analyzer should be 3 - 3.5 L·min<sup>-1</sup> and the flow to the CO/CO<sub>2</sub> analyzer should be 3 - 3.5 L·min<sup>-1</sup>). If leaks are present, locate the source of such leaks and correct the problem.
- We then calibrate the Oxygen and CO/CO<sub>2</sub> Analyzers. This will involve checking the zero, using nitrogen, and then setting the value at that for dry ambient air, namely 20.950% for the oxygen analyzer, and the span gas values for the CO and CO<sub>2</sub> analyzer.
  - a) With the lab extraction, fan and pump on, check that the volume flow rate is 24 l/s (use Status).
  - b) Make a note of the flow into the oxygen cell and the CO/CO<sub>2</sub> cell still with the pump on by moving the flags on the flowmeters to the position of the float.
  - c) Turn off the pump.
  - d) Select the software routine Calibrations → Gas Analyzers.
  - e) Turn on the nitrogen cylinder.
  - f) Turn the valve below the oxygen flowmeter to the Nitrogen position and the CO/CO<sub>2</sub> valve (below the CO/CO<sub>2</sub> flowmeter) to the Nitrogen position.
  - g) Adjust the nitrogen flow from the regulator on the bottle to obtain the same flow as mentioned in point b. This is very important.
  - h) Wait until the oxygen, CO and CO<sub>2</sub> readings stabilize at approximately 0.0%.

- i) Zero the CO on the analyzer, using the menu system (Menu|Calibrate|Password 4000|Manual Cal|▲|▲CO|Low Cal|0.0000%|Yes) When the CO reading has stabilized at 0.000% then press Quit twice.
- j) Then press ▼ and ▲ to select the CO2 channel. Select Low Cal and ensure the display says 0.000% and select Yes to perform the calibration. Then press Quit twice.
- k) Then press ▼ and ▲ to select the Oxygen channel. Select Low Cal and ensure the display says 0.000% and select Yes to perform the calibration. Then press Measure.
- l) In the gas analyzers transducer calibration panel press the Zero button in the Oxygen Cell section. After the routine has finished (the progress bar has reached the top) check that the Oxygen reads 0.000% on the computer screen.
- m) Then press the Zero buttons in the CO2 cell and CO cell sections. Check that the CO2 and CO both read 0.000% on the computer screen. Do NOT press the OK button.
- n) Turn off the nitrogen cylinder.
- o) Turn the oxygen analyzer valve to air or sample gas.
- p) Turn the CO/CO2 analyzer valve to CO/CO2 span gas.
- q) Turn on the calibration gas cylinder.
- r) Set the CO/CO2 flow rate to the value noted in *point b* by adjusting the gas cylinder valve.
- s) On the analyzer menu system select Menu|Calibrate|Password 4000|Manual Cal|CO|High Cal| then ensure that the value is that stated on the calibration gas bottle certificate. Then select Yes to perform the calibration of the CO cell. When the reading has stabilized, press Quit twice.

t) Then press ▼ and ▲ to select the CO<sub>2</sub> channel. Select High Cal and ensure the display shows the value is that stated on the calibration gas bottle certificate and select Yes to perform the calibration of the CO<sub>2</sub> cell. Then press Measure.

u) Check that the CO and CO<sub>2</sub> span values on the computer screen match those on the calibration gas bottle certificate (if not then edit the values). Then press the Span buttons for the CO<sub>2</sub> and CO cells. Check that the CO and CO<sub>2</sub> values are adjusted to the correct span concentrations.

v) Turn off the calibration gas supply at the gas cylinder.

w) Turn the CO/CO<sub>2</sub> analyzer valve to sample gas.

x) Turn on the sample pump.

y) Let the oxygen concentration stabilize for at least 5 minutes.

z) On the analyzer menu system select Menu|Calibrate|Password 4000|Manual Cal|Oxygen|High Cal| then ensure that the value is 20.95%. Then select Yes to perform the calibration. When the reading has stabilized press Measure.

aa) Then press the Span button in the oxygen section on the computer screen. Check that the oxygen value on the computer screen is 20.950%.

bb) Leave the sample pump on.

cc) Then press the OK button to accept all the gas analyzer calibrations. Then press Main to return to the Main panel.

#### F.7 Perform The C-Factor Calibration

- Perform a heat release system calibration with methane to determine the “C-factor”.

- a) In the software, select Status.
- b) Ensure that the sample pump is on and has been running for at least five minutes.
- c) Check that the following values are displayed:
  - i) Oxygen reads 20.950 %
  - ii) CO<sub>2</sub> reads ~0.04 %
  - iii) CO reads 0.00 %
  - iv) Volumetric flow at orifice reads 24 L·s<sup>-1</sup>.
- d) Press OK.
- e) Ensure that the methane bottle is turned off and that the Methane ball valve (on the Cone Calorimeter) is off. Then select Calibrations|Zero MFMs and press Zero in the methane mass flow meter section to zero the methane flow meter. (If a soot mass flow meter is also installed then you must also press Zero in the Soot Mass section). Check that the Methane (slpm) is 0.00.
- f) Then press OK.
- g) Select Calibrations|Gas Analyzers.
- h) On the analyzer check the oxygen concentration is 20.95%. If it is not 20.95% then reset the span by using the menu system: select Menu|Calibrate|Password 4000|Manual Cal|Oxygen|High Cal| then ensure that the value is 20.95%. Then select Yes to perform the calibration. When the reading has stabilised press Measure.
- i) Then press the Span button in the Oxygen Cell section on the computer screen.

j) Then press OK then Main.

k) If the CO is not within  $-0.002\%$  to  $0.002\%$  then set the zero ONLY ON THE ANALYZER. [Select Menu|Calibrate|Password 4000|Manual Cal|CO|Low Cal| then ensure that the value is  $0.000\%$  Then select Yes to perform the calibration. When the reading has stabilized press Measure.]

l) Place the burner in position under the cone, ensure the spark igniter is in the idle position and push the Ignition button on.

m) Turn the methane cylinder on.

n) Select the software option: C-factor, then Routine.

o) Enter the required information, including the atmospheric conditions (temperature, relative humidity and pressure). Then press OK.

p) Open the shutters under the Cone heater (if not already open).

q) Ensure that the methane valve is OFF and then select Yes to perform the pre-run calibrations.

r) Ensure that the methane is off and press Start to collect the baseline data.

s) When instructed to turn the methane on, place the igniter over the methane burner.

t) Turn the methane ball valve on half way.

u) When the methane ignites then turn the methane valve fully on. Then remove the igniter.

v) Adjust the methane flow to obtain approximately 5 kW (bottom left graph and display).

w) Allow the data collection part of the routine to complete and turn the methane off when instructed. (Do NOT adjust the methane flow valve or the pressure regulator on the bottle during the data collection phase (last 3 minutes of the routine).

x) The routine lasts for 6 minutes of burning – turn the gas off using the Methane On/Off valve when instructed and collect the after-test baseline data.

y) Then press the Stop button to finish the routine when instructed.

z) Turn the Pump off.

aa) Press Save to save the C-factor (and select which C-factor you wish to save). Make a note of the calibration factor and compare with previous values. The acceptable range for the instrument is 0.040 - 0.046. Measurements on two successive test days shall not differ by more than 0.002. Such differences indicate malfunctions which require rectification before testing is continued. (Typically a high C-factor results because of leaks or blockages, a very high C-factor means that the cold trap is still open, a low C-factor may be due to a leak in the methane line or a faulty mass flow meter.)

bb) Press the Exit button to return to the Main panel.

cc) Turn the Ignition off.

dd) Remove the methane burner.

#### F.8 Check the height of the cone

- Ensure that the cone height is 25 mm above the sample surface.
- Use a 23 mm spacer with the edge frame on the sample holder to ensure that the height is correct [or remove the edge frame and place a dummy specimen in place so that the surface is level with the inside of the edge frame, then use a 25 mm spacer].



## F.9 Set the heat flux

- To set the heat flux.
  - a) Ensure that the cooling water to the heat flux meter is flowing.
  - b) Open the shutters under the cone heater.
  - c) Place a non-combustible ceramic cover on the load cell platform.
  - d) Remove the red cap from the heat flux meter.

NOTE: NEVER TOUCH THE BLACK SURFACE.

- e) Place the heat flux meter under the Cone heater and ensure that it is 25 mm from the base of the cone heater. Use a 25 mm spacer to check this distance – take care to NOT touch the black surface. Remember that the cone may be HOT!!
- f) Select heat flux.
- g) Select the required heat flux from the drop down list and then set the temperature controller to give approximately the required heat flux. This is done by pressing the ▼ and ▲ buttons on the temperature controller.
- h) When the temperature has stabilized then look at the heat flux meter reading (Irradiance).
- i) Wait until the heat flux stabilizes before taking a reading. Adjust the temperature using the ▼ and ▲ buttons until the irradiance is at the required level (the Irradiance display will be green).
- j) When stable press the Save & Exit button.

k) Remove the flux meter and ensure that a backing block is placed on the load cell platform to protect the load cell from heat damage.

l) Check that the copper end of the heat flux meter is cold.

m) Place the red cap on the flux meter and put it in the clips behind the Fire Model.

#### F.10 Sample preparation and testing

- Before testing a set of materials check that the scale of the load cell output is appropriate for the mass of the specimen that will be tested.
- To set up the load cell output, firstly determine the maximum mass,  $m_{max}$ , of the samples you will be testing. Choose a range slightly higher than this largest mass. For example, if your samples weigh about 80g, select 100g as a full scale load. This value has to be entered into the Newport controller and into ConeCalc.
- To enter the value into the Newport controller (full details are in the Cone Calorimeter Users' Guide).

PUSH DISPLAY COMMENTS

MENU×17 OT.SC.OF

MIN READ 1

MAX/MIN 00000.0 READ 1 must be 00000.0

MENU OUTPT1

MAX/MIN 00.0000 OUTPT1 must be 00.0000

MENU READ 2

MAX/MIN  $m_{max}$  Enter maximum mass here (e.g. 00100.0)

## MENU OUTPT2

MAX/MIN 10.0000 OUTPT2 must be 10.0000

## MENU STOREDRESET2

- To enter the value into ConeCalc select Configure and then edit the Load cell transducer calibrations so that the four numbers match those entered into the Newport controller (i.e.  $0 - 10 \text{ V} = 0 - m_{\text{max}} \text{ g}$ ). Then press Accept. Then select Status. Tare the mass on the load cell and check that the Newport and computer screen both show zero. Then place a mass of the load cell and check that the mass displayed in the dialogue box is the same as that on the Newport (providing the Newport is indicating a mass below that entered above).
- Note that it is very important that the mass does not exceed the mass span value ( $m_{\text{max}}$ ) because the Newport controller will display the correct mass but the signal sent to the computer will “top out” (the signal will be greater than 10 V) and hence yield an incorrect mass. In such a case, all parameters involving mass calculations would be invalid.
- Collect the sample, from the controlled temperature/relative humidity cabinet, measure, and record the sample mass, thickness and the area of the top surface.
- Following are the steps to prepare the sample:
  - a) Wrap the sample in three to four layers of heavy-duty aluminium foil, shiny side towards the sample, covering the sides and bottom and leaving the testing surface exposed

Note: The fiber blanket must be dried by heating to  $150^{\circ}\text{C}$  for at least 3 hours and then placed in a desiccator containing silica gel to remove any water.

- b) Place sample in a clean horizontal specimen holder, which contains a fiber blanket.
- c) If needed, use the optional retainer frame and/or wire grid. If a different mounting procedure is to be used, as specified by the test sponsor, take the appropriate steps. Make a note of the mounting procedure used.
- d) Remove the specimen from the sample holder. Remove the cover on the load cell platform and place the empty holder (including edge frame if used) on the load cell. Allow the mass to stabilize and then press the Tare button on the Mass Loss Calorimeter Control Unit.
- e) Remove the sample holder from the load cell and replace the cover on the load cell platform. **DO NOT PRESS THE TARE BUTTON AGAIN.**
- f) Put the specimen in the holder and secure the edge frame to the specimen pan.
- Check the system one more time, as follows:
  - a) Ensure that there is sufficient drying agent in the column.
  - b) Check that the soot filters are clean.
  - c) Check that the laser system slots are covered.
  - d) Turn the sample Pump on.
  - e) Check that the flow rates to the oxygen and CO/CO<sub>2</sub> analyzers are the same as they were following the calibration of the analyzer.
  - f) Check that the volume flow rate through the duct is 24 L·s<sup>-1</sup>.
  - g) Check that the heater temperature is the same as the temperature noted at the time of the heat flux setting.

- h) Check the distance between the cone heater and the sample surface to confirm that it is set at 25 mm, using an identical empty specimen holder as a guide.
- i) Ensure that the pump has been running for 5 minutes. Then reset the span of the oxygen analyzer by using Calibrations|Gas Analyzers and then press Span in the oxygen cell section to set the oxygen concentration to 20.950%. Note that you may have to also adjust the span in the analyzer software.
- j) Ensure the spark electrode is in the idle position and then turn the spark Igniter on.
- Select Start Test and then enter the specimen information. Remember that your tests are performed “Non-scrubbed” and you must enter the correct laboratory conditions (temperature, relative humidity and atmospheric pressure).
  - Then press OK.
  - Then perform the pre-run calibrations by pressing the Yes button.
  - Testing:
    - a) Ensure that the shutters are open and do NOT put the specimen on the load cell.
    - b) Press Start Baseline and collect at least 60 s of data.
    - c) When instructed to insert the specimen, close the shutters.
    - d) Place the sample, held in the specimen holder (with the appropriate mounting method) on the load cell and allow the mass to stabilise.
    - e) Pull down the protection screens.
    - f) Move the spark igniter into position and ensure that the Igniter button is on.
    - g) Open the shutters under the Cone heater carefully and press button S on the handset.

- h) Record the time at which sustained ignition occurs by pressing button I on the handset and remove the spark igniter.
- i) Press button E on the handset to mark an event time. This time will be displayed in the Comments dialogue box after the end of the test where comments about the event can be entered.
- j) When the specimen stops flaming then press button F on the handset (this records the flameout time).
- k) Collect data for a further 2 minutes.
- l) Press the S key on the handset to stop the test or press the Stop button.
- m) If the specimen does not ignite within 10 minutes, terminate the test and discard the sample, unless the specimen is showing signs of heat evolution or unless specific alternative instructions have been received from test sponsor.
- n) Remove the specimen and place the ceramic cover on top of the load cell.
- o) To perform the next test go to step 2.
- p) Turn off the pump if you are not going to conduct any further tests for the next 10 minutes.

#### F.11 Shutdown procedure

- Adjust the Cone temperature to 0°C.
- Wait until the Cone heater temperature is below 250°C
- Turn the duct Fan off.
- Turn the room extraction off.
- Turn the following buttons OFF:

- a) Pump
- b) Cold Trap
- c) Load Cell
- d) Ignition
- e) Cone
- f) Power

Leave the Analyzers and Smoke buttons On all the time.

- Shut down the ConeCalc application and turn the computer off. Then turn the data logger off.
- Ensure that the gas bottles are off.
- Ensure that the cooling water is off.
- Place a beaker under the Cold Trap and open the Cold Trap tap to collect the water. Leave the tap open until the next time the instrument is used.

VITA

Roshan J. Patel

Candidate for the Degree of

Master of Science

Thesis: PREDICTION OF PROPERTIES AND MODELING FIRE BEHAVIOR  
OF POLYETHYLENE USING CONE CALORIMETER

Major Field: Chemical Engineering

Biographical:

Education:

Completed the requirements for the Master of Science in Chemical Engineering at Oklahoma State University, Stillwater, Oklahoma in December, 2014.

Completed the requirements for the Bachelor of Chemical Engineering at the Maharaja Sayajirao University of Baroda, Vadodara, Gujarat, India in 2011.

Experience:

Graduate Teaching Assistant with Chemical Engineering Department at Oklahoma State University (August 2013 – December 2014)

Graduate research Associate with Fire Protection & Safety Technology Department at Oklahoma State University (January – May 2014)

Graduate Teaching Assistant with Fire Protection & Safety Technology Department at Oklahoma State University (August – December 2014)

Process Engineer with Linde Engineering India Pvt. Ltd., India (July 2011 – July 2013)

Professional Memberships:

Society of Petroleum Engineers (since 2013)

General Secretary, Chemical Engineering Graduate Student Association (since 2014)